



ALMA MATER STUDIORUM  
UNIVERSITA' DI BOLOGNA

DEPARTMENT OF CIVIL, CHEMICAL,  
ENVIRONMENTAL AND MATERIALS ENGINEERING  
- DICAM -  
FACULTY OF ENGINEERING

PhD PROGRAM:  
"MATERIALS ENGINEERING"  
*Cycle XXV*  
ING-IND/22

## **Zirconia in Dentistry**

PhD THESIS OF:

**Dott. Carlo Monaco**

Promoter:

**Prof. Ing. Giorgio Timellini**

Co-Promoter:

**Dott. Ing. Arturo Salomoni**

Co-Promoter:

**Prof. Roberto Scotti**

---



**To my wife Francesca  
that smiles through the eyes of the  
sweet Camilla and the radiant Ludovico**



“It would be possible to describe everything scientifically, but it would make no sense; it would be without meaning, as if you described a Beethoven symphony as a variation of wave pressure.”

**Albert Einstein**



## CONTENTS

Chapter 1: Properties of the zirconia	9
Chapter 2: Microstructural changes produced by abrading Y-TZP in pre-sintered and sintered conditions.	25
Chapter 3: Microstructural study of microwave sintered zirconia for dental applications	45
Chapter 4: Bonding effectiveness of zirconia after different sandblasting procedures.	63
Chapter 5: Adhesion mechanisms at the interfaces between Y-TZP and veneering ceramics.	83
Chapter 6: Marginal adaptation, gap width, and fracture strength of teeth restored with different all-ceramic vs metal ceramic crown systems: an in vitro study.	105
Chapter 7: Marginal and internal fitting of zirconia-based single crowns made after intraoral digital impression.	125
Chapter 8: Clinical evaluation of 1132 zirconia-based single crowns: a retrospective cohort study from the AIOP Clinical Research Group.	145
Chapter 9: Conclusions and recommendations	163



***CHAPTER 1***

**Properties of the zirconia**

## 1.1 Introduction

Rapid improvements of the all-ceramic restorations, combined with the use of computer-aided design (CAD)/computer-aided manufacturing (CAM), has made the digital dentistry increasingly popular over the past decade. CAD/CAM systems have been continuously developed and upgraded in prosthetic dentistry in association with zirconium oxide, used primarily for the restoration of single crowns and fixed partial dentures (FPDs) in both the anterior and posterior regions. Zirconium oxide-based materials, especially yttria-tetragonal zirconia polycrystals (Y-TZP), were recently introduced for prosthetic rehabilitations as a core material for single crowns, conventional and resin-bonded fixed partial dentures (FPDs) [1], and, in dental implantology, as abutments or implants [2]. The raw materials of the zirconia are the minerals zircon ( $ZrSiO_4$ ) and baddelyite ( $\beta-ZrO_2$ ), whose mines are located in South Africa, Australia and USA. Zirconia was discovered by the German chemist Martin Heinrich Klaproth in 1789. The term zirconium refers to the metal, while zirconia ceramic (“zirconia”) refers to zirconia-dioxide-ceramic ( $ZrO_2$ ) [Figure 1].

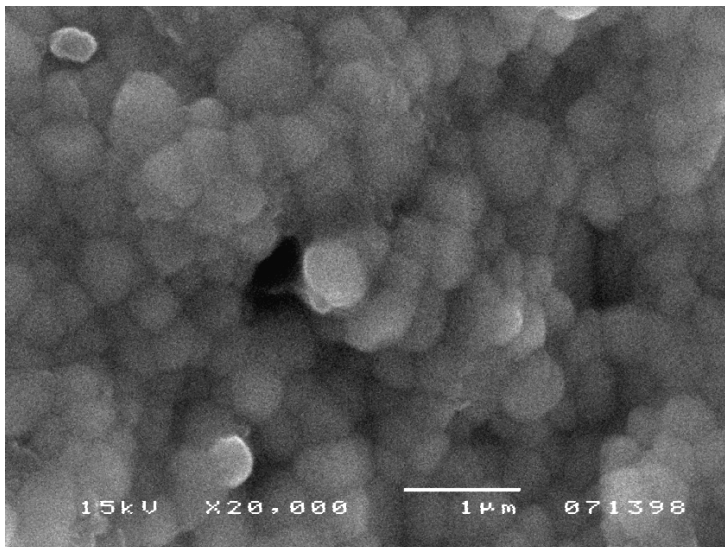


**Figure 1.** Surface of the zirconia: grain size at 20.000 magnification.

## 1.2 Properties

Zirconia takes up a peculiar place amongst oxide ceramics due to its excellent mechanical properties. This condition is due to the huge amount of the research that has been performed since the discovery of the transformation toughening capabilities of this material. The different

stages of polymorph zirconia are temperature dependent: at ambient pressure, unalloyed zirconia can assume three crystallographic forms. At room temperature and upon heating up to 1170°C, the symmetry is monoclinic (P21/c). The structure is tetragonal (P42/nmc) between 1170 and 2370°C and cubic (Fm $\bar{3}$ m) above 2370°C and up to the melting point [3] [4]. The transformation from the tetragonal (t) phase to the monoclinic (m) phase upon cooling is accompanied by a substantial increase in volume (~4.5%), sufficient to lead to catastrophic failure [5]. The ceramic shows a hysteretic martensitic t  $\rightarrow$  m transformation during heating and cooling. This transformation is reversible and begins at ~950 °C on cooling. Alloying pure zirconia with stabilizing oxides such as CaO, MgO, Y<sub>2</sub>O<sub>3</sub> or CeO<sub>2</sub> allows the retention of the tetragonal structure at room temperature and therefore the control of the stress-induced. Zirconia has a high temperature stability and melting point (2680°C), high hardness (1200-1350 HVN), high thermal expansion (>10 x 10<sup>-6</sup> 1/K), low thermal conductivity (<1 W/mK) and a good thermo-shock resistance ( $\Delta T=400-500^\circ\text{C}$ ) [6] [Figure 2].

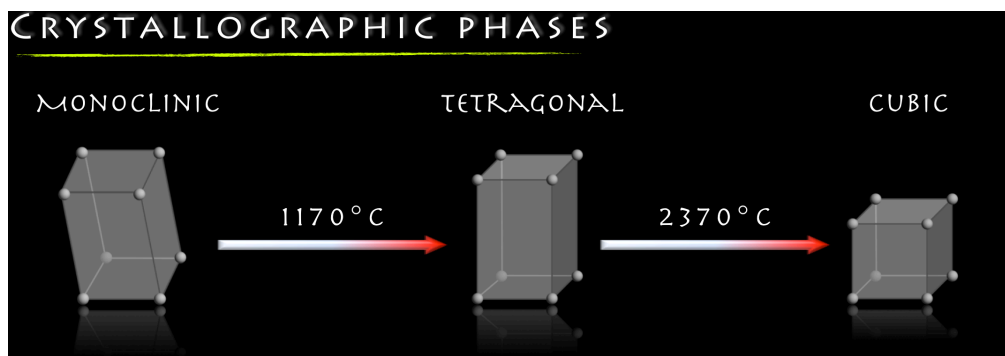


**Figure 2.** Crystallographic and relative temperature of the three zirconia phases.

### 1.3 Transformation toughening

However, the metastability of tetragonal zirconia could increase the susceptibility to aging because some stress-generating surface treatments such as grinding or sandblasting can trigger the t $\rightarrow$ m transformation with volume increase and formation of compressive stresses on the surface, thereby modifying the phase integrity though increasing the flexural strength [7]. The increase of volume determines a local stop of the crack propagation. This process is called “transformation toughening”, with the resistance against crack propagation that increases with the length of the crack [8] [Figure 3-4-5].

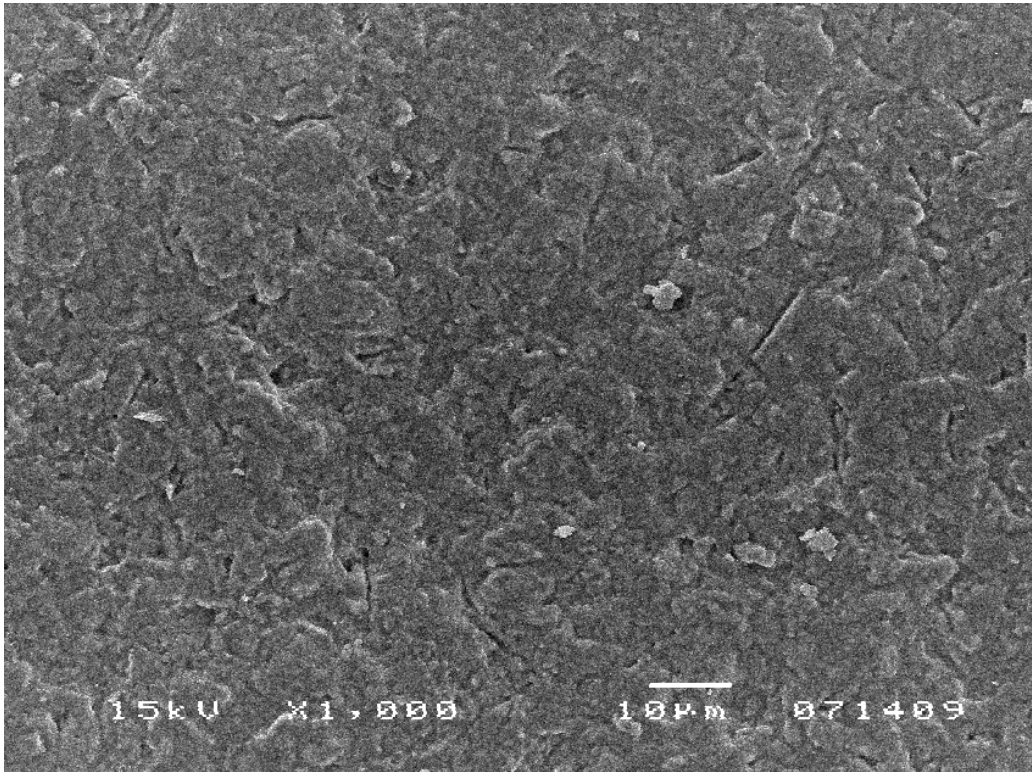


**Figure 3.** Microcracks due to the sandblasting treatment.

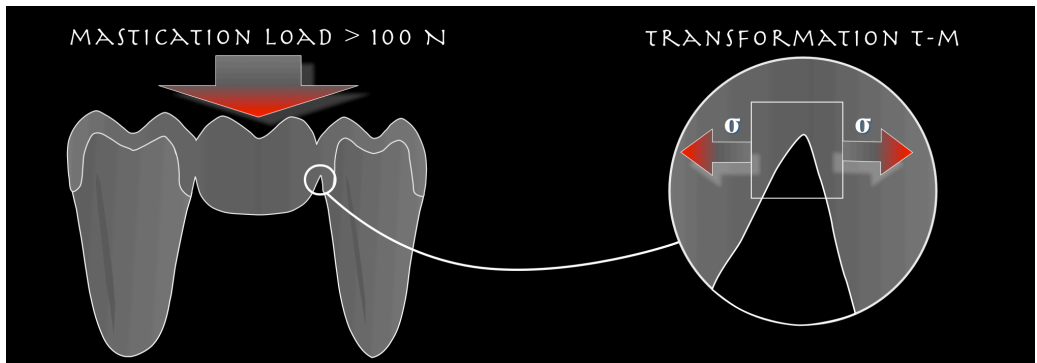


**Figure 4.** Tensile area in a fixed partial denture during chewing cycles.

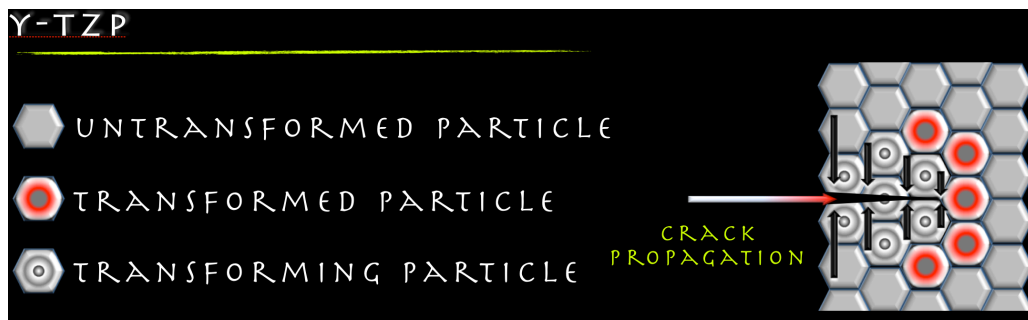


**Figure 5.** Representation of the transformation toughening.

Only three types of zirconia systems are used in dentistry although currently there are many systems of zirconia available on the market . The first is yttrium cation-doped tetragonal zirconia polycrystals (3Y-TZP), the second is magnesium cation-doped partially stabilized zirconia (Mg-PSZ) and finally the zirconia-toughened alumina (ZTA). The partly stabilized zirconia (PSZ) is stabilized with magnesia and in addition to the cubic phase, a transformable tetragonal phase is available. Its microstructure at room temperature is mostly cubic with portions of monoclinic and tetragonal phases. While the Tetragonal Zirconia Polycrystals (TZP) have a ultra-fine, nanometre-scaled structure that allows the transformation during cooling from the cubic to the tetragonal phase, but not to the monoclinic phase. [10]

### 1.4 Low temperature degradation (LTD)

One of the aging process is well-described in the literature and is called "low temperature degradation" (LTD) of the zirconia. This is a phenomenon due to the presence of water [10] [11] [12]. The consequences of this aging process are determine the degradation of the zirconia surface with the grain pullout and subsequently microcracking of the structure. This phenomena represent an strength degradation [Figure 6-7].

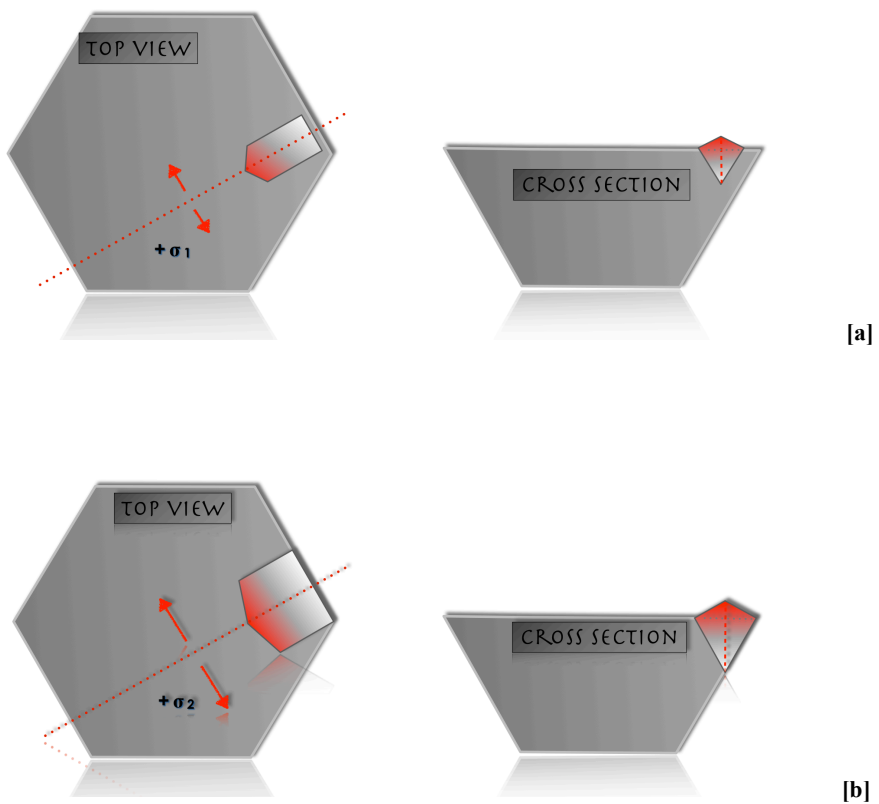


**Figure 6.** The t-m transformation starts [a] from the surface of the sample and then proceeds inward [b].

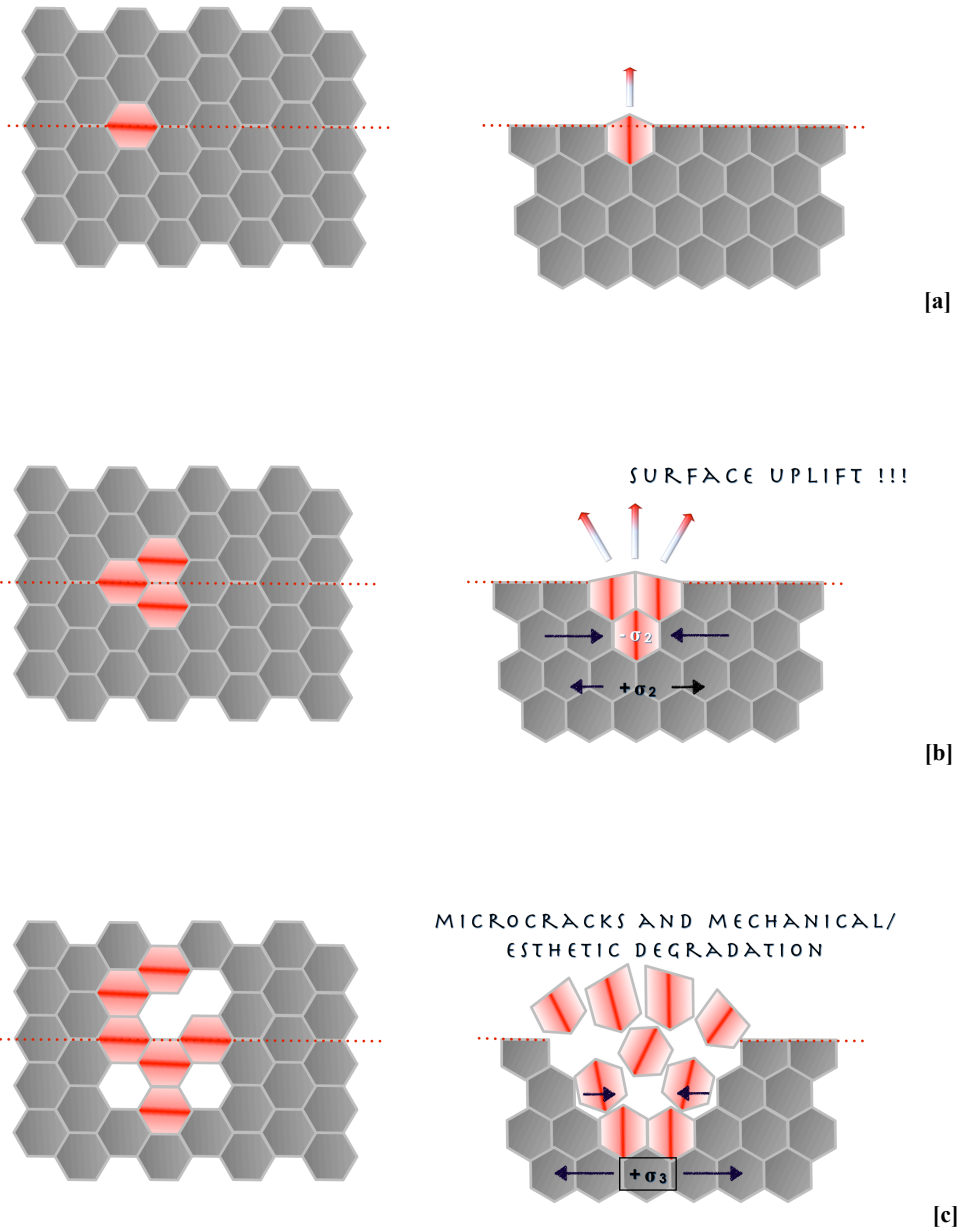


**Figure 7.** The phase transformation determines [a] the increase of the grain volume with the subsequent uplift of the surface [b]. The presence of the water rapidly causes microcracks and esthetic degradation of the zirconia surface [c].

Three are the hypotheses of the low temperature degradation. The first speculate that there is the the diffusion of water species (here OH-) into the lattice via oxygen vacancies and (b) resulting change of lattice parameters [13] [Figure 8].

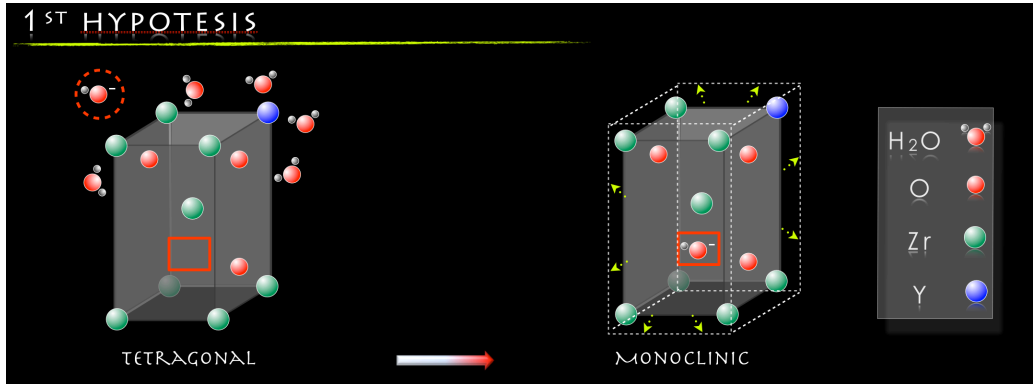


**Figure 8.** Diffusion of the OH- into the regular lattice arrangement of the particles (molecule of the water in the dashed circle that migrate in the red rectangle).

The second hypothesis claim that  $H_2O$  reacts with  $Y_2O_3$  to form clusters rich in  $Y(OH)_3$  [14][Figure 9].

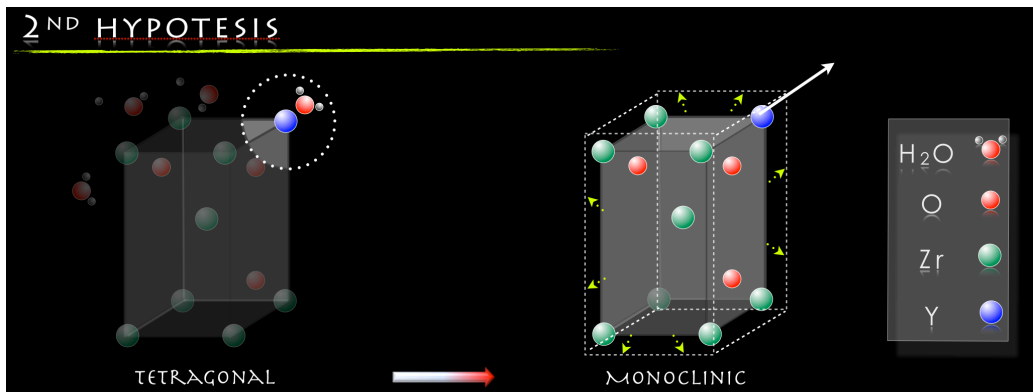


**Figure 9.**  $Y_2O_3$  and  $H_2O$  reacts together.

The last hypothesis sustain that the water vapor attacks the Zr-O bond, breaking it and leading to a stress accumulation due to movement of -OH. This in turn generates lattice defects acting as nucleating agents for the subsequent T-M transformation [15] [Figure 10].

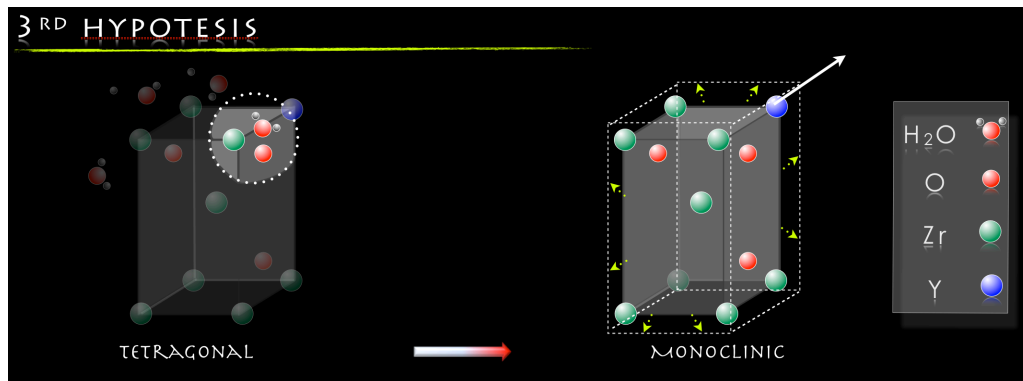


**Figure 10.** Rupture of the Ze-O bond due to the water vapor.

### 1.5 Mechanical Properties

Zirconia-based materials have higher strength, fracture toughness [16] in comparison to the feldspatic ceramics [17]. The failure mechanism of the zirconia, like others ceramic materials, is due to sub-critical crack-growth. The metal-oxide bonds which were destroyed when the stress is present near the tip of the initial crack with a water-assisted mechanism [18]. Cyclic loading during the biting or chewing simulation can slowly cause the degradation of the toughening mechanisms [19] determine the fracture of the zirconia framework because a toughened material could be more susceptible to rupture. The cracks can originate inside of the zirconia framework or close to the ceramic veneer interface and propagate to the interface [20].

### 1.6 Configuration

The zirconia in dentistry is milled in pre-sintered stage. This configuration is a soft, chalk-like stage that is called “green” stage. During the sintering process, the material shrinks and reduces the volume shrinkage of about 20-25%. It’s very important to know the exact volume shrinkage information for the individual zirconia blank blocks in order to optimize the fitting of the restoration. The zirconia is called hipped (hot iso-static pressed) when the material is

industrially sintered, and then is CAD-milled at its final high strength. Hipped zirconia has a constant grading and thus a more homogeneous quality. As expected, milling time and wear of the milling tools is higher in comparison to the pre-sintered variants. The zirconia for dental applications, zirconia is stabilized at room temperature with the addition of 3 mol% yttria. This configurations reach high strength (800-1200 MPa) good fracture toughness (6-15 MPa x m<sup>1/2</sup>).

### **1.7 Fabrication process**

The fabrication of the framework or the monolithic zirconia requires rapid prototyping procedures such as milling with a computer aided design and manufacturing (CAD/CAM) [21]. The different manufacturers use milling-machines directly in the dental laboratories or centralized production center. The process starts with optically digitizing the clinical abutment with an intraoral camera or with 3D-scanning devices using gypsum models or wax models. Afterwards the substructure is designed on the computer (CAD) and the core is anatomically shaped to support the ceramic veneering material. In the last few year is increased the use of zirconia as monolithic restoration. This approach is been possible because now the burs can mill the anatomic occlusal design with fissures.

The properties of the zirconia substructures could depend by the manufacturing process. The use of insufficient preparations, or frameworks with imprecise dimensions / thickness could reduce the integrity of zirconia restorations. The design of the core, when it is a simple cap or an occlusal supporting design, has a strong influence on the lifetime of the veneering [22-23] [Figure 11].



**Figure 11.** The zirconia frameworks don't support the ceramic material even in the Fixed partial denture that in the single crown. In this clinical case the risk of chipping or delamination is higher.

The zirconia framework has to support completely the veneering ceramic material in order to avoid chipping or delamination of the aesthetic porcelain [Figure 12].

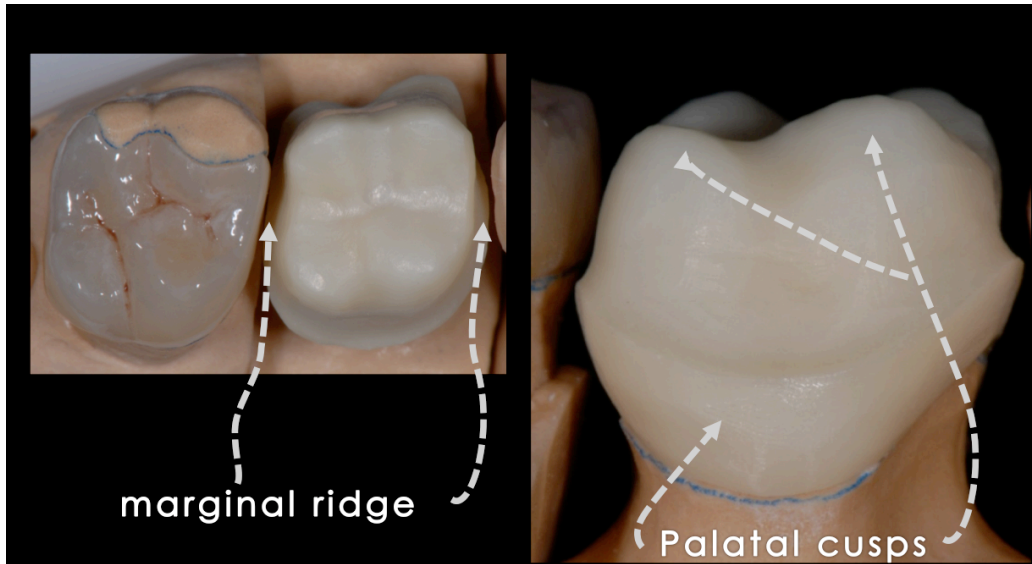


**Figure 12.** The zirconia framework support the ceramic material even in the marginal ridge that under the palatal cusps. In this case the risk of chipping or delamination is lower.

The dimensions and design of FPDs, especially in the connector areas in posterior and in anterior fixed partial dentures, is important to increase the clinical life of the all-ceramic restoration. The volume of the connector area in anterior and posterior FPDs must be minimum of  $3 \times 3 \text{mm}^2$  [24-25].



**Figure 13.** In anterior fixed partial dentures the zirconia framework could support the ceramic material in the marginal ridge and have sufficient volume of the connector areas.

For the quality of the marginal fit, besides the well-known clinical parameters, the CAD/CAM fabrication process may play a decisive role. Different milling devices, milling strategies, and software capabilities may contribute to the results even more than the different types of ceramic materials. Based on the assumption that the clinically acceptable marginal fit extends to  $200 \mu\text{m}$ , CAD/CAM fabricated restorations with values between  $64\text{-}83 \mu\text{m}$  and  $245 \mu\text{m}$  [26-28] are in most cases good to acceptable. The results for the marginal fit are in the range of porcelain-fused-to-metal (PFM) restorations or pressed-ceramics and vary widely depending on the abilities of the dental technician.

### **1.8 Content of this thesis**

The above factors emphasize the scope of this thesis for further investigations on zirconia, the improvement of all-ceramic zirconia restorations, and especially the interaction of zirconia

and veneering and its influence on the performance of the whole restoration.

The introduction, chapter 1, gave a literature overview on zirconia ceramics.

In chapter 2, the objective of the study was to evaluate the effect of abrading before and after sintering using alumina-based abrasives on the surface of yttria-tetragonal zirconia polycrystals. Particular attention was paid to the amount of surface stress-assisted phase transformation (tetragonal→monoclinic) and the presence of microcracks.

Chapter 3 is based on the idea that the conventional sintering techniques for zirconia based materials, which are commonly used in dental reconstruction, may not provide a uniform heating, with consequent generation of microstructural flaws in the final component. As a consequence of the sintering system, using microwave heating, may represent a viable alternative. The purpose of the study was to compare the dimensional variations and physical and microstructural characteristics of commercial zirconia (Y-TZP), used as a dental restoration material, sintered in conventional and microwave furnaces.

Chapter 4 described the effect of sandblasting before and after sintering on the surface roughness of zirconia and the microtensile bond strength of a pressable veneering ceramic to zirconia.

Chapter 5 analyzed the interface between zirconia and ceramic materials using two different methods of veneering. Alternative veneering in the press-technique was compared to conventional layering methods. Moreover was described the interface between before and after sandblasting treatment.

Chapter 6 compared the fracture resistance of various available systems for posterior restorations. The study evaluated marginal adaptation before and after thermomechanical loading, gap width and fracture strength of all-ceramic single crowns, as compared to porcelain-fused-to-metal (PFM).

The last two chapters 7 and 8 are clinical evaluation of the behaviour of the zirconia restorations. Chapter 7 evaluated the accuracy of single all-ceramic zirconia crowns resulting

from digital intraoral impressions with active wavefront sampling technology by measuring the marginal and internal fits of the crowns, moreover chapter 8 recorded the survival of the and zirconia restorations on single crowns, FPD and on implants.

## 1.9 References

- [1] Denry I, Kelly JR. State of art of zirconia for dental applications. *Dental Materials* 2008; **24**: 299 – 307.
- [2] Hisbergues M, Vendeville S, Vendeville P. Zirconia: established facts and perspectives for a biomaterial in dental implantology. *Journal of Biomedical Material Research* 2009; Part B: Appl Biomater **88B**: 519 - 29.
- [3] Garvie RC, Hannink RH, Pascoe RT. Ceramic steel? *Nature* 1975;**258**:703–4.
- [4] Subbarao EC. Zirconia-an overview. In: Heuer AH, Hobbs LW, editors. Science and technology of zirconia. Columbus, OH: The American Ceramic Society; 1981. p. 1–24.
- [5] Kisi E, Howard C. Crystal structures of zirconia phases and their interrelation. *Key Eng Mater* 1998;**153/154**:1–35.
- [6] Badwal SPS, Zirconia-based solid electrolytes: microstructure, stability and ionic conductivity. *Solid state Ionics* 1992; **52**: 23-32.
- [7] Deville S, Chevalier J, Gremillard L. Influence of surface finish and residual stresses on the ageing sensitivity of biomedical grade zirconia. *Biomaterials* 2006;**27**:2186–92.
- [8] Fischer H, Rentzsch W, Marx R. R-curve behavior of dental ceramic materials. *J Dent Res* 2002;**81**:547-51.
- [9] Hannink RHJ, Kelly PM, Muddle BC. Transformation toughening in zirconia-containing ceramics. *J Am Ceram Soc* 2000;**83**:461–87.
- [10] Sato T, Shimada M. Crystalline phase-change in yttria-partially-stabilized zirconia by low-

temperature annealing. *J Am Ceram Soc* 1984;**67**:C212–3.

[11] Lange FF, Dunlop GL, Davis BI. Degradation during aging of transformation-toughened ZrO<sub>2</sub>–Y<sub>2</sub>O<sub>3</sub> materials at 250 °C. *J Am Ceram Soc* 1986;**69**:237–40.

[12] Chevalier J, Cales B, Drouin JM. Low-temperature aging of Y-TZP ceramics. *J Am Ceram Soc* 1999;**82**:2150–4.

[13] Chevalier J, Gremillard L. The Tetragonal-Monoclinic Transformation in Zirconia. *J Am Ceram Soc* 2009;**92**:1901-20.

[14] Lange FF, et al. Degradation during aging of transformation toughened ZrO<sub>2</sub>-Y<sub>2</sub>O<sub>3</sub>. *J Am Ceram Soc* 1986;**69**:1-4.

[15] Yoshimura M, Noma T, Kawabata K, Somiya S. Role of water on the degradation process of T-TZP. *J Mater Sci Lett* 1987;**6**:465-7.

[16] De Aza AH, Chevalier J, Fantozzi G, Schehl M, Torrecillas R. Crack growth resistance of alumina, zirconia and zirconia toughened alumina ceramics for joint prostheses. *Biomater* 2002;**23**(3):937-45.

[17] Guazzato M, Albakry M, Ringer SP, Swain MV. Strength, fracture toughness and microstructure of a selection of all-ceramic materials. Part II. Zirconia-based dental ceramics. *Dent Mater* 2004;**20**:449-56.

[17] Michalske TA, Freiman SW. A molecular mechanism for stress-corrosion in vitreous silica. *J Am Cer Soc* 1983;**66**:284-288.

[19] Studart A, Filser F, Kocher P, Lüthy H, Gauckler LJ. Cyclic fatigue in water of veneer framework composites for all-ceramic dental bridges. *Dent Mater* 2007;**23**:177-85.

[20] Chevalier J, Olagnon C, Fantozzi G. Subcritical crack propagation in 3Y-TZP ceramics: static and cyclic fatigue. *J Am Cer Soc* 1999;**82**:3129-3138.

[21] Otzel C, Clasen R. Preparation of zirconia dental crowns via electrophoretic deposition. *J Mat Sci* 2006;**41**:8130-37.

[22] de Jager N, Pallav P, Feilzer AJ. The influence of design parameters on the FEA determined stress distribution in CAD-CAM produced all-ceramic dental crowns. *Dent Mater*

2005;**21**:242-51.

[23] de Jager N, de Kler M, van der Zel JM. The influence of different core material on the FEA-determined stress distribution in dental crowns. *Dent Mater* 2006;**22**:234-42.

[24] Proos KA, Swain MV, Ironside J, Steven GP. Influence of margin design and taper abutment angle on a restored crown of a first premolar using finite element analysis. *Inter J Prosthodont* 2003;**16**:442-9.

[25] Kou W, Kou S, Liu H, Sjogren G. Numerical modelling of the fracture process in a threeunit all-ceramic fixed partial denture. *Dent Mater* 2007;**23**:1042-49.

[26] Reich S, Wichmann M, Nkenke E, Proeschel P. Clinical fit of all-ceramic three-unit fixed partial dentures, generated with three different CAD/CAM systems. *Eur J Oral Sci* 2005;**113**:174-179.

[27] Coli P, Karlsson S. Precision of CAD/CAM technique for the production of zirconium dioxide copings. *Int J Prosthodont* 2004;**17**:577-580.

[28] Naert I, Van der Donck A, Beckers L. Precision of fit and clinical evaluation of allceramic full restorations followed between 0.5 and 5 years. *J Oral Rehabil* 2005;**32**:51-57.

**CHAPTER 2**

**Microstructural changes produced by abrading Y-TZP in pre-sintered and sintered conditions.**

## **2.1 Abstract**

**Objective:** To evaluate the effect of abrading before and after sintering using alumina-based abrasives on the surface of yttria-tetragonal zirconia polycrystals. Particular attention was paid to the amount of surface stress-assisted phase transformation (tetragonal→monoclinic) and the presence of microcracks. **Methods:** Pre-sintered zirconia ceramic specimens (ZirCAD; Ivoclar Vivadent) were first surface-ground flat with #600-800-1000-grit SiC paper. They were then surface-treated with different grain size abrasives before and after the sintering step. Samples that underwent no surface treatment were used as controls. For each condition, eight specimens were prepared. The physical/mechanical characteristics of zirconia material were determined by measuring density, porosity, grain size, hardness, and fracture toughness. The effects of surface treatments were assessed by surface roughness measurements, quantitative X-ray diffraction analysis, and scanning electron microscopy. **Results:** With increased dimensions of the abrasive particles, the abraded surfaces of zirconia specimens exhibited a widespread system of microcracks and an increased monoclinic zirconia quantity. These structural changes likely affect the aging of the material during its clinical service.

## 2.2 Introduction

In recent years, the use of ceramic restorations has increased due to their superior aesthetic appearance, biocompatibility, and absence of metal [1]. Zirconium oxide-based materials, especially yttria-tetragonal zirconia polycrystals (Y-TZP), were recently introduced for prosthetic rehabilitations as a core material for single crowns, conventional and resin-bonded fixed partial dentures (FPDs) [2], and, in dental implantology, as abutments or implants [3]. The combination of Y-TZP and computer-aided design/computer-aided manufacture (CAD/CAM) systems is a new approach that reduces the number of steps in prosthetic manufacturing and eliminates the variables introduced by the manual procedures of the dental technician. Y-TZP exhibits exceptional physical and mechanical properties, such as high flexural strength, fracture toughness, hardness, wear and corrosion resistance in acidic and basic ambient conditions, translucency [4], colour stability, greater effectiveness of diagnostic radiographs [5] [6], and high biocompatibility. Moreover, the polycrystalline structure, which lacks a glass matrix, makes zirconia ceramic more resistant to hydrofluoric acid etching and, as a consequence, resistant to chemical roughening [7]. For this reason, different approaches have been used to enhance the bond between the zirconia and resin cements, such as coating methods [8], a selective infiltration-etching technique [9], phosphate ester monomer, 10-methacryloyloxydecyl dihydrogen phosphate (MDP)-based materials [10] and, above all, surface roughening by airborne-particle abrasion.

To enhance the bonding between zirconia frameworks and veneering porcelain, surface roughness is increased with variable-grained alumina-based abrasives and/or the use of interlayers in current practice. Furthermore, despite the use of CAD/CAM, the final steps, involving strong mechanical action on zirconia components, must be still performed by dental technicians [11] [12]. By favouring the tetragonal to monoclinic phase transformation, the stresses induced by this kind of operation cause surface compressive stresses with an increased fracture toughness, low temperature degradation (LTD) [13], and crack formation. This affects the flexural strength of zirconia components, in line with the damage induced [14] [15]. Furthermore, the high kinetic energy of the impacting abrasive particles may chemically contaminate the surface during machining [16] [17]. This phenomenon may have a positive effect on bond strength at the interface between zirconia and the veneering ceramic.

The aim of this investigation was to evaluate the effect of abrading the surface of zirconia

ceramics (Y-TZP) before and after sintering with alumina-based abrasives with varying grit. Particular attention was paid to the development of surface stress–assisted phase transformation (tetragonal→monoclinic) and microcracking. X-ray diffraction (XRD) and scanning electron microscopy (SEM) analyses were used to detect changes in surface morphology.

### **2.3 Materials and methods**

The starting material was a 3 mol% yttria-doped zirconia (ZirCAD C15L; Ivoclar Vivadent, Schaan, Liechtenstein) in the form of pre-sintered blocks. Specimens were cut using a low-speed diamond disc (MDS100; Norton, USA) in a special device to obtain blocks of zirconia that were 7.2 mm in height, 9.2 mm in width, and 9.2 mm in length. To ensure identical initial roughness, surface treatment with a #600-800-1000-grit SiC polishing paper was performed on all specimens. For each treatment eight specimens were prepared. The samples were randomly divided in seven groups. The control group (group A) was not sandblasted. Three groups (B-C-D) were abraded in the pre-sintered condition and then sintered in a dedicated machine (Sintramat; Ivoclar Vivadent), following the manufacturer’s instructions. Three other groups (E-F-G) were before subjected to the same thermal treatment and then surface abraded.

Abrasion of the surfaces of pre-sintered and sintered zirconia samples was performed using a Rocatec system (3M ESPE). The abrasive particles were ejected for 10 seconds at a pressure of two bars, with a nozzle–specimen distance of 15 mm. Three abrasives were used; two were alumina with average particle sizes of 50 and 110  $\mu\text{m}$ , and the third was silica-coated alumina with an average particle size of 30  $\mu\text{m}$ . Samples B to D were abraded in the pre-sintered condition with these abrasive particles, and samples E to G were abraded after sintering using the same particles (Table I).

The density and porosity of pre-sintered and sintered zirconia samples were determined following the 1993 standard of EN 623-2 [18]. The phase fraction amounts of zirconia were evaluated by XRD using a diffractometer (PW 3830; Philips, The Netherlands), with  $\text{CuK}\alpha$  radiation (0.02° step-scan, 10 s per step). Zirconia diffraction peaks were deconvoluted using a Lorentz function to obtain the integral breadth. The monoclinic phase fraction of the zirconia was calculated using the Garvie and Nicholson method [19]:

where  $I_{t(111)}$  and  $I_{m(111)}$  represent the integrated intensity of the tetragonal  $t(111)$  and monoclinic  $m(111)$  respectively and  $\overline{m(111)}$  the peaks.

Hardness and fracture toughness ( $K_{IC}$ ) of the material were determined by the Vickers indentation technique. Ten valid impressions were obtained using a semi-automatic hardness tester (model 3212; Zwick, Germany), and the mirror finish surface of the specimens was measured under an applied load of 196.2 N at room temperature in an air atmosphere with a relative humidity of ~50%.  $K_{IC}$  was calculated by the Palmqvist formula [20] [21]:

$$K_{IC} = 0.0319 (P d^{-1} l^{0.5}),$$

where  $P$  is the indentation load,  $d$  is the diagonal of the impression, and  $l$  is the length of the crack arising from the corner of the impression.

Surface microstructure was observed under a scanning electron microscope (EVO 40; Zeiss Corporation, Germany) equipped with an energy-dispersive X-ray analyser (EDS; Inca; Oxford Instruments, UK). The average grain size of the zirconia was determined using SEM observations of the fractured surface of each pre-sintered sample and the polished surface of each sintered sample after thermal etching. SEM images of randomly selected areas were analysed with computer software (Qwin Imaging System; Leica), and average values were obtained using a base of at least 150 grains.

The average roughness values ( $R_a$ ) of treated surfaces were measured for all samples after sinterization treatment using a roughness meter (Hommel tester T2000; Germany) according to the test method recommended by the EN 623-4 standard [22].

## 2.4 Results and discussion

The physicochemical characteristics of pre-sintered and sintered zirconia samples are shown in Table II. Sintered samples reached the theoretical density, with a dense microstructure characterised by the presence of small grains (average size, 0.44  $\mu\text{m}$ ). In addition, the thermal cycle used completely transformed the monoclinic zirconia that remained in the pre-sintered sample in the tetragonal phase.

Average roughness values ( $R_a$ ) are reported in Table I. The surfaces of all abraded groups were rougher than that of the control (A).  $R_a$  values of samples B to D, which were abraded in the pre-sintered condition, were higher than those of samples E to G, which were abraded after the final sintering step. Surface roughness, as expressed by  $R_a$ , increased with the size of the impacting particles in all treated groups.

The proportion of the monoclinic phase on the treated surfaces of sintered zirconia samples is shown in Table I. The surfaces of control samples and samples B–D consisted of 100% tetragonal phase; no diffraction peak of the monoclinic phase was detected. Thus, in these samples, the sintering step allowed complete phase transformation of the monoclinic phase that existed in the pre-sintered condition.

In contrast, abrasion of the sintered zirconia surface produced detectable monoclinic peaks with a marked m(111) preference. The tetragonal to monoclinic phase transformation induced by the impact of abrasive particles with average dimensions of 50 and 30  $\mu\text{m}$  (groups F and G) was similar (10% and 8%, respectively). A further increase in monoclinic proportion (to 14%) resulted from abrading with particles with an average diameter of 110  $\mu\text{m}$  (group E).

Mechanical stress, in this case erosion by hard ceramic particles, induces phase transformation of the metastable tetragonal phase into the monoclinic phase and is associated with an increase in volume ( $\sim 4\%$ ) and shear strain ( $\sim 7\%$ ) [23]. This may result in both a compressive residual stress on the surface and a widespread crack network if the intrinsic strength of the material is overcome. Thus, in addition to the presence of stress-induced tetragonal to monoclinic phase transformation, analysis of zirconia peaks in XRD patterns (Fig. 1) allowed the identification of a hump at the left shoulder of the tetragonal (111) peak of the sandblasted surfaces. The size of this peak increased with the abrasive grain size used in the surface treatments. This phenomenon, observed by various authors [24] after cutting or surface grinding TZP ceramics, is correlated with the presence of lattice distortion [25] [26] induced by strong mechanical action. Residual stresses can also be detected by analysing the ratio of the intensity peaks ( $I_{(002)t}/I_{(200)m}$ ; Fig. 2 and Table I).

This ratio was increased after abrasion of sintered samples (samples E–G) and was highest when the largest (110  $\mu\text{m}$ ) abrasive particles were used. This intensity change has been attributed to the ferroelasticity of Y-TZP ceramics [27]. Strong mechanical stresses can induce a permanent strain in zirconia due to a hysteresis loop between the strain and the applied stress (in this case abrasion), which results in the failure to induce tetragonal to monoclinic phase transformation. Instead, an interchange of the a and c axes occurs, as indicated by the altered relative intensity of the diffraction peaks. This can cause an additional increase in the fracture toughness of the sample because the application of tensile stress, as found at the tip of an advancing crack, can cause domain reorientation and the absorption of fracture energy without

phase transformation.

Evidence of the presence of residual stresses in samples that were abraded after sintering indicates that the abrasion processes performed here introduced various levels of compressive stresses to the surfaces of the zirconia samples. This finding was supported by the morphological SEM analysis. The sintered surfaces of control samples were rough, but cracks were absent (Fig. 3). In contrast, the zirconia surface of sample G exhibited some small cracks after abrasion with 30- $\mu\text{m}$  abrasive particles, which were probably caused by stress-induced phase transformation. Furthermore, very small particles adhered to the surface in some areas (Fig. 4). EDS analyses revealed the presence of silicon and aluminium residues of the impacting abrasive particles.

The use of 50- $\mu\text{m}$  alumina particles (sample F) caused more marked deformation. The impact of an alumina particle (Fig. 5) ploughed and plastically deformed the zirconia surface. Microanalyses detected aluminium at the base of the impact area, testifying to a strong reaction between zirconia and the alumina abrasive particle due to the energy of the impact.

The use of larger (average diameter 110  $\mu\text{m}$ , sample E) abrasive particles resulted in further enhanced surface abrasive phenomena (Fig. 6a). The impact area of plastically deformed zirconia was larger and exhibited deep ploughing. Several cracks formed when the intrinsic strength of the material was overcome, and the branching of the cracks caused the detachment of surface sheets in tetragonal to monoclinic phase transformation (Fig. 6b).

Samples B–D, which were abraded in the pre-sintered state (Fig. 7a), did not exhibit such plastic deformation. Their surfaces were very rough and valleys and scratches were present, although they were not as deep and sharp as those in samples E–G. Average roughness measurements showed that the use of larger abrasive particles caused the formation of longer and deeper scratches. Chemical contamination due to the co-sintering of particles containing silicon and/or aluminium onto zirconia surfaces was also detected (Fig. 7b).

Our data suggest that the abrasion of pre-sintered zirconia specimens (samples B to D) resulted in the formation of a highly rough surface after the final firing step. The resulting material was exclusively zirconia in the tetragonal phase and was free from residual stresses, but contained some contaminants (silicon and aluminium) due to the embedding of the harder abrasive particles in the pre-sintered (softer) zirconia after impact.

The abrasion of sintered samples (E to G) caused a lower surface roughness due to the increased hardness of sintered zirconia, and a meaningful tetragonal to monoclinic phase transformation. The proportion of the monoclinic phase was correlated directly with abrasive particle diameter, and thus with impact energy. Several surface cracks were caused by the high stress developed during abrasion and by the tetragonal to monoclinic phase transformation. These cracks negatively affect the mechanical behaviour of the component. In particular, they could cause: *i*) decreased reliability due to the increased number and dimension of flaws, and *ii*) decreased toughness due to the lower proportion of available tetragonal phase. On the other hand, analysis of the XRD spectra showed a lattice distortion of the tetragonal phase, as evidenced by the increase in (002) peak intensity and simultaneous decrease in that of the (200) peak. This phenomenon represents an index of the development of surface residual stresses that can be considered a positive attribute because the domain reorientation caused by stresses at the tip of an advancing crack represents an additional energy-absorbing mechanism and serves to increase fracture toughness [20].

While surface cracks [15] increase the kinetic aging of zirconia components at low temperatures, the role of residual stresses [16] has not been well studied. However, these phenomena play a key role in phase transformation and thus likely have some effect on the aging of the material. These structural changes likely affect the aging of the material during its clinical service [28] [29].

## 2.5 Conclusions

This study evaluated the effects of different abrasive procedures on the surfaces of pre-sintered and sintered zirconia. The abrasive techniques we employed are currently used to increase adhesion between zirconia and luting cement. The results can be summarized as follows:

1. Abrasion of pre-sintered zirconia specimens resulted in rougher surfaces, and the monoclinic phase associated with the abrasion was completely transformed to the tetragonal state during the subsequent sintering step;
2. Abrasion of sintered zirconia specimens resulted in surfaces with a lower roughness, a monoclinic phase, and compressive surface residual stresses, the degree of which was associated with the abrasive grain size;
3. The phases and microstructural changes induced by abrasion may markedly impact clinical performance, i.e. by increasing the rate of aging.

## 2.6 Tables

**Table I** – Surface treatments.

Samples	Surface condition before abrasion	Abrasive grain size ( $\mu\text{m}$ )	Nozzle–zirconia surface distance (cm)	Surface roughness, Ra ( $\mu\text{m}$ ) <sup>§</sup>	Monoclinic (%) <sup>§</sup>	$I_{(002)t}/I_{(200)t}$ <sup>#</sup>
A	--	--	--	$0.35 \pm 0.16$	0	0.6
B	pre-sintered	110*	1.5	$3.44 \pm 0.44$	0	-
C	pre-sintered	50*	1.5	$2.33 \pm 0.46$	0	-
D	pre-sintered	30**	1.5	$1.22 \pm 0.22$	0	-
E	sintered	110*	1.5	$0.60 \pm 0.04$	14	4.2
F	sintered	50*	1.5	$0.48 \pm 0.04$	10	1.5
G	sintered	30**	1.5	$0.41 \pm 0.03$	8	1.6

\*Al<sub>2</sub>O<sub>3</sub>; \*\*SiO<sub>2</sub>-coated Al<sub>2</sub>O<sub>3</sub> § Values determined after sintering. # Ratio of the intensity peaks.

**Table II** - Physicomechanical characteristics of pre-sintered and sintered zirconia samples.

Characteristic	Pre-sintered	Sintered
Bulk density, g cm <sup>-3</sup>	3.11	6.05
Porosity, %	48.0	0.0
Grain size, $\mu\text{m}$	0.20	0.45
Phase composition	97% tetragonal 3% monoclinic	100% tetragonal
HV <sub>19.62</sub> , GPa	--	12.0
K <sub>IC</sub> , MPa m <sup>0.5</sup>	--	6.9

2.7 Figures

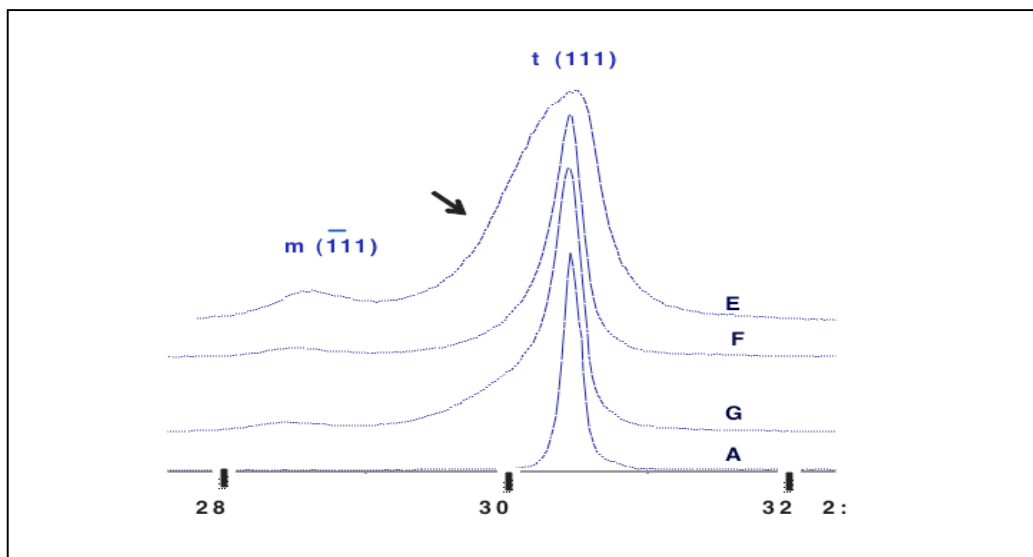


**Figure 1** – X-ray diffraction patterns of the control sample (A) and samples E–G, the surfaces of which were treated with 110-, 50-, and 30- $\mu$ m abrasive particles, respectively, after firing. Arrow indicates the hump.

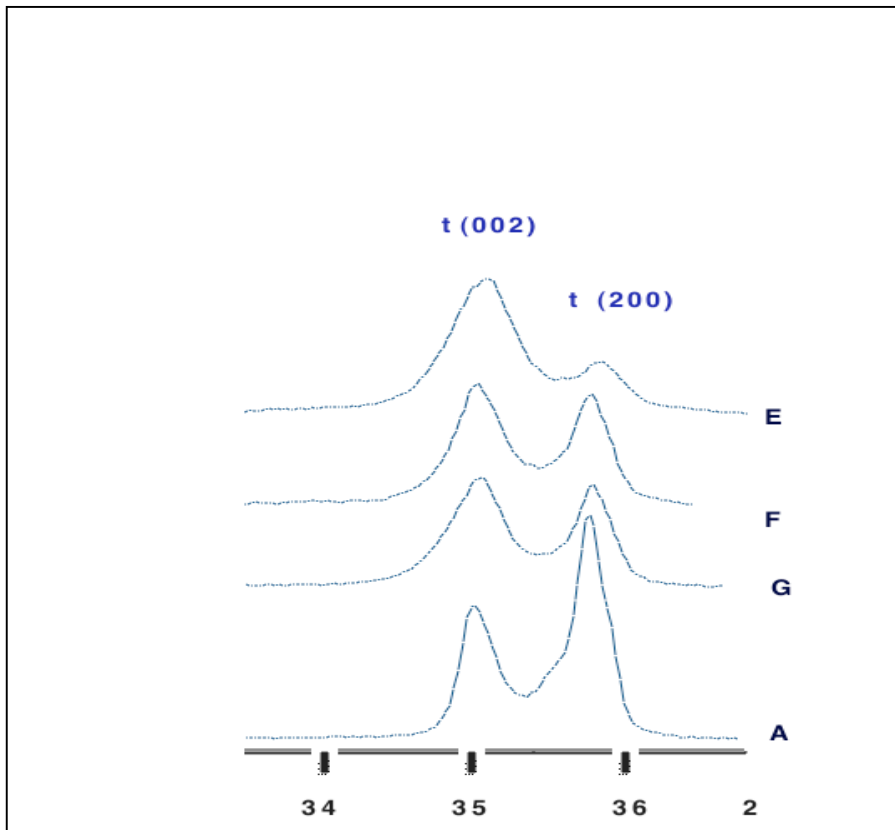


**Figure 2** – X-ray diffraction patterns of the control sample (A) and samples E–G, the surfaces of which were treated with 110-, 50-, and 30- $\mu\text{m}$  abrasive particles, respectively, after firing.

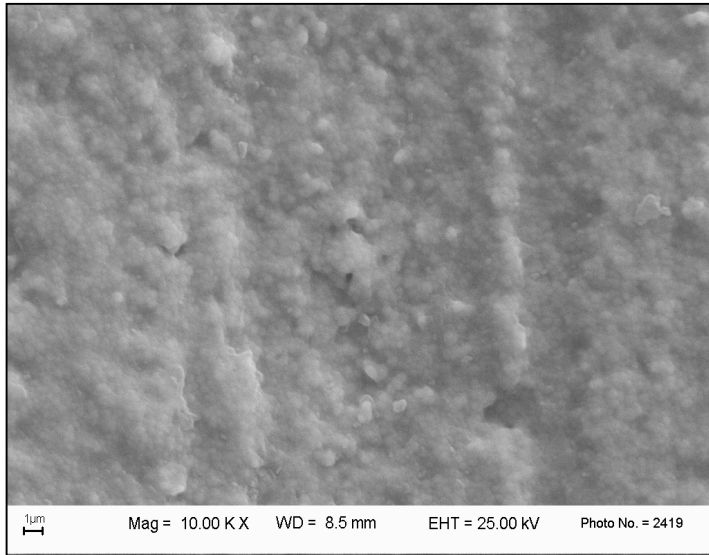


**Figure 3** – Scanning electron micrograph of the sintered surface of sample A without cracks.

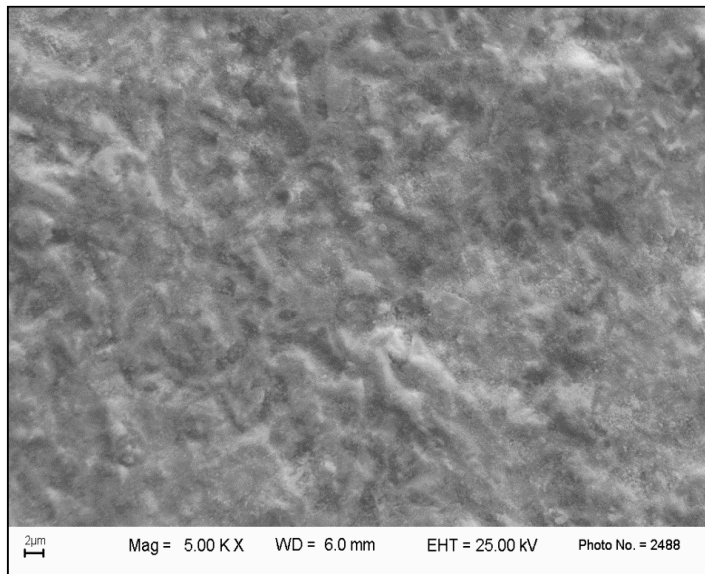


**Figure 4** – SEM-SE micrograph of the surface of Sample G, the small agglomerated particles contain silicon.

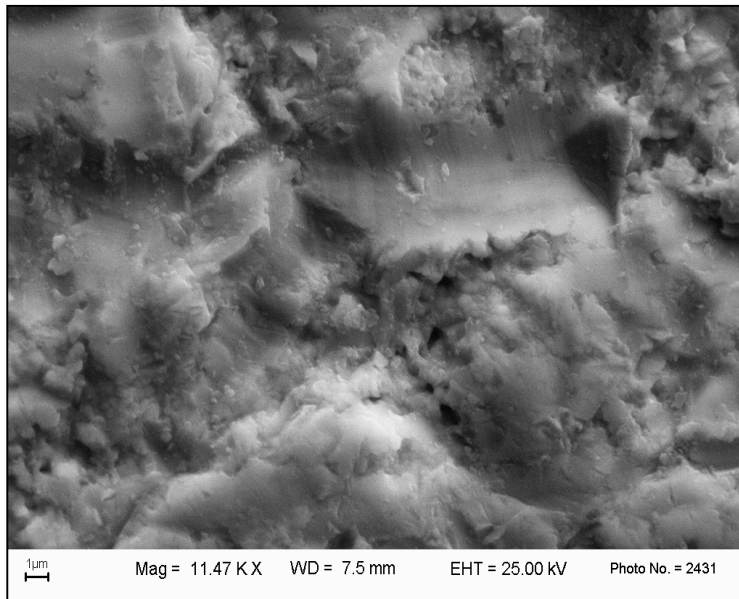


**Figure 5** – Scanning electron micrograph of the surface of sample F. The smooth area was ploughed by 50µm alumina abrasive particle.

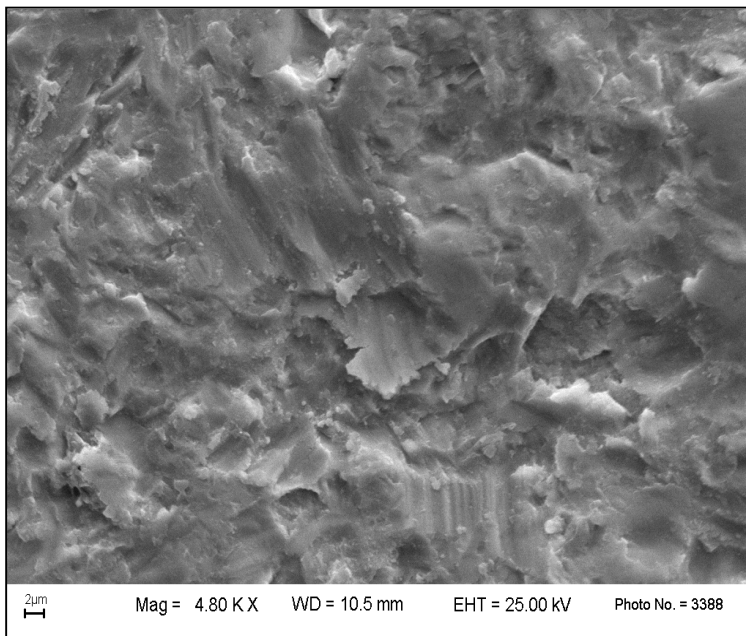


**Figure 6a.** SEM image of the abrasive phenomena after the use of 110µm alumina particles on the surface of sample E.

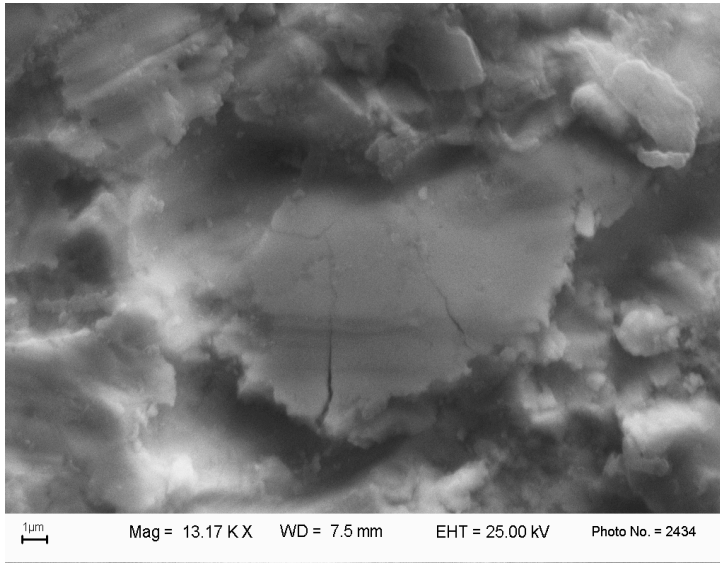


**Figure 6b.** Magnified image of the central area of the Fig. 6a. The surfaces showed several cracks and the detachment of the surface sheets with tetragonal to monoclinic transformation.

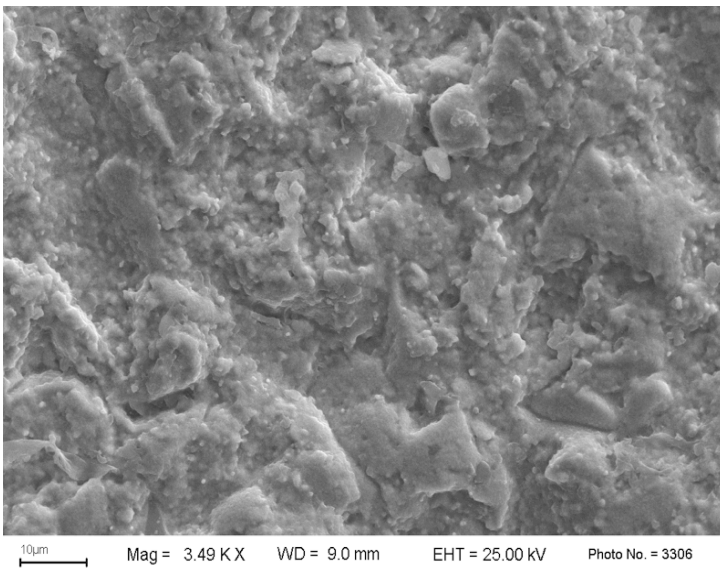


**Figure 7a.** Scanning electron micrographs of the surface of sample B. The surface did not exhibit plastic deformation although valleys and scratches were present.

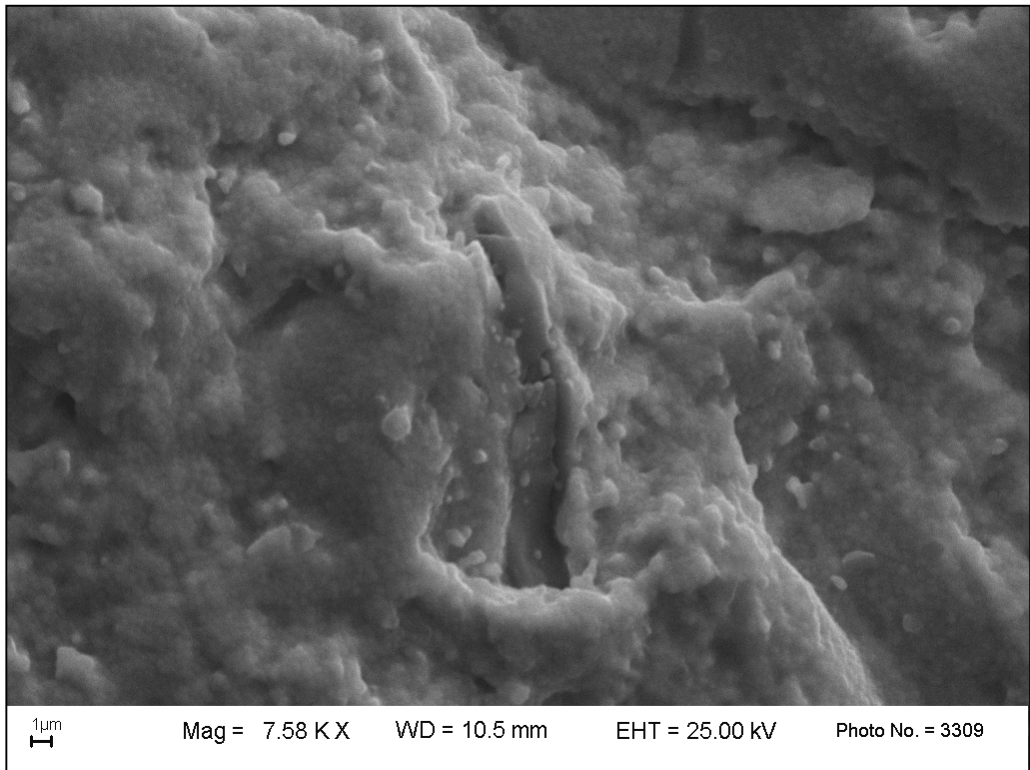


**Figure 7b.** Central magnification of the fig. 7a showed an elongated particle containing aluminium embedded in the zirconia matrix.

## 2.8 References

- [1] Stevenson B, Ibbetson R. The effect of the substructure on the colour of samples/restorations veneered with ceramic: A literature review. *Journal of Dentistry* 2010; **38**: 361-368.
- [2] Denry I, Kelly JR. State of art of zirconia for dental applications. *Dental Materials* 2008; **24**: 299 – 307.
- [3] Hisbergues M, Vendeville S, Vendeville P. Zirconia: established facts and perspectives for a biomaterial in dental implantology. *Journal of Biomedical Material Research* 2009; Part B: Appl Biomater **88B**: 519 - 29.
- [4] Vagkopoulou T, Koutayas SO, Koidis P, Strub JR. Zirconia in dentistry: part 1. Discovering the nature of an upcoming bioceramic. *European Journal of Esthetic Dentistry* 2009; **4**: 2 - 23.
- [5] Blatz MB. Long-term clinical success of all-ceramic posterior restorations. *Quintessence International* 2002; **33**: 415 - 426.
- [6] Raigrodski AJ. Contemporary materials and technologies for all-ceramic fixed partial dentures: a review of the literature. *Journal of Prosthetic Dentistry* 2004; **92**: 557 - 62.
- [7] Piconi C, Maccauro G. Zirconia as a ceramic biomaterial. *Biomaterials* 1999; **20**: 1 - 25.
- [8] Kitayama S, Nikaido T, Takahashi R, Zhu L, Ikeda M, Foxton RM, Sadr A, Tagami J. Effect of primer treatment on bonding of resin cements to zirconia ceramic. *Dental Materials* 2010; **26**: 426 - 32.
- [9] Aboushelib MN, Kleverlaan CJ, Feilzer AJ. Selective infiltration-etching technique for a strong and durable bond of resin cements to zirconia-based materials. *Journal of Prosthetic Dentistry* 2007; **97**: 379 - 388.
- [10] Blatz MB, Sadan A, Martin J, Lang B. In vitro evaluation of shear bond strengths of resin to densely sintered high-purity zirconium-oxide ceramic after long-term storage and thermal cycling. *Journal of Prosthetic Dentistry* 2004; **91**: 356 - 62.
- [11] Deville S, Chevalier J, Gremillard L. Influence of surface finish and residual stresses on the aging sensitivity of biomedical grade zirconia, *Biomaterials* 2006; **27**: 2186 - 92.
- [12] Bonfante EA, Sailer I, Silva NR, Thompson VP, Rekow ED, Coelho PG. Failure modes of Y-TZP crowns at different cusp inclines. *Journal of Dentistry* 2010; **38**: 707-712.
- [13] Bonfante EA, Coelho PG, Guess PC, Thompson VP, Silva NR. Fatigue and damage accumulation of veneer porcelain pressed on Y-TZP. *Journal of Dentistry* 2010; **38**: 318-324.
- [14] Guazzato M, Quach L, Albakry M, Swain MV. Influence of surface and heat treatments on the flexural strength of Y-TZP dental ceramic *Journal of Dentistry* 2005; **33**: 9 - 18.

- [15] Guazzato M, Albakry M, Ringer SP, Swain MV. Strength, fracture toughness and microstructure of a selection of all-ceramic materials. Part II. Zirconia-based dental ceramics. *Dental Materials* 2004; **20**: 449 - 56.
- [16] Rateick RG Jr, Karasek KR, Cunningham AJ, Goretta KC, Routbort JL. Solid-particle erosion of tungsten carbide/cobalt cermet and hardened 440C stainless steel-A comparison. *Wear* 2006; **7**: 773 - 78.
- [17] de Arellano-Lopez AR, Martinez-Fernandez J, Varela-Feria FM, Orlova TS, Goretta KC, Gutierrez-Mora F, Chen N, Routbort JL. Erosion and strength degradation of biomorphic SiC. *Journal of the European Ceramic Society* 2004; **24**: 861 - 70.
- [18] European Standard EN 623-2, Advanced technical ceramics - monolithic ceramics - general and textural properties - Part 2: Determination of density and porosity, 1993.
- [19] Garvie RC, Nicholson PS. Phase analysis in Zirconia systems. *Journal of American Ceramic Society* 1984; **67**: 119 - 21.
- [20] Ponton CB, Rawlings RD. Vickers indentation fracture toughness test—Part 1: Review of literature and formulation of standardised indentation toughness equation. *Materials Science and Technology* 1989; **5**: 865 - 72.
- [21] Ponton CB, Rawlings RD. Vickers indentation fracture toughness test—Part 2: Application and critical evaluation of standardised indentation toughness equations. *Materials Science and Technology* 1989; **5**: 961–76.
- [22] European Standard EN 623-4, Advanced technical ceramics - monolithic ceramics-general and textural properties - Part 4: Determination of surface roughness, 1993.
- [23] Swain MV. Limitation of maximum strength of zirconia-toughened ceramics by transformation toughening increment. *Journal of American Ceramic Society* 1985; **68**: C97 - C99.
- [24] Kosmač T, Oblak C, Jevnikar P, Funduk, N, Marion L. The effect of surface grinding and sandblasting on flexural strength and reliability of Y-TZP zirconia ceramic. *Dental Materials* 1999; **15**: 426 - 33.
- [25] Chang JH, Hsuan CL, Wei HT. Effect of abrasive grinding on the strength of Y-TZP. *Journal of European Ceramic Society*: 2009; **29**: 2665 - 669.
- [26] Kondoh J. Origin of the hump on the left shoulder of the X-ray diffraction peaks observed in Y<sub>2</sub>O<sub>3</sub>-fully and partially stabilized ZrO<sub>2</sub>. *Journal of Alloys and Compounds*: 2004; **375**: 270 - 82.
- [27] Virkar AV, Matsumoto RLK. Ferroelastic Domain Switching as a Toughening Mechanism in Tetragonal Zirconia. *Journal of American Ceramic Society*: 1986; **69**: C224 - C226.

[28] Abou Tara M, Eschbach S, Wolfart S, Kern M. Zirconia ceramic inlay-retained fixed dental prostheses - first clinical results with a new design. *Journal of Dentistry* 2011; **39**: 208-211.

[29] Harder S, Wolfart S, Eschbach S, Kern M. Eight-year outcome of posterior inlay-retained all-ceramic fixed dental prostheses. *Journal of Dentistry* 2010; **38**: 875-881.



***CHAPTER 3***

**Microstructural study of microwave sintered zirconia for dental applications.**

### **3.1 Abstract**

**Statement of problem.** Conventional sintering techniques for zirconia based materials, which are commonly used in dental reconstruction, may not provide a uniform heating, with consequent generation of microstructural flaws in the final component. A sintering system, using microwave heating, may represent a viable alternative.

**Purpose.** The purpose of this study was to compare the dimensional variations and physical and microstructural characteristics of commercial zirconia (Y-TZP), used as a dental restoration material, sintered in conventional and microwave furnaces.

**Material and Methods.** Microwave sintering tests were conducted using a commercial CEM-MAS 7000 multimode applicator (2.45-GHz, 950 W nominal power) and on a TE10n single mode applicator, connected to a 2.45GHz TM030 microwave generator (0.5–3-kW output power), under various experimental conditions. The same material was sintered in an electric heating furnace for comparison. A physical-mineralogical-microstructural characterization was carried out to evaluate the level of densification and the presence of flaws in the sintered specimens.

**Results.** Use of the microwave systems allowed reducing the length of the sintering cycle to a few minutes, compared to several hours necessary with a traditional heating system. Additionally, the maximum temperature, used to reach the required density, decreased from values 1450-1480°C with the electric furnace to 1200°C in the microwave furnace.

**Conclusions.** Microwave heating systems have specific advantages in terms of energy efficiency, process simplicity, and equipment maintenance and operator costs.

**Clinical implications:** The reduced of the sintering time could allow the introduction of zirconia in the chair-side treatments, if used as a monolithic material.

### 3.2 Introduction

A well-known review on zirconia for dental applications [1] noted that as in the last 20 years, the diffusion of metal-free restorations in the dental practice has increased considerably due to the growing demand for highly esthetic and natural-appearing components. In particular, bioceramics [2] are particularly suitable for use in prosthodontics as possible metal substitutes because of their combination of several excellent properties, including wear resistance, excellent esthetical appearance, superior mechanical properties and high biocompatibility.

Particular attention has been paid to yttria tetragonal zirconia polycrystalline materials (Y-TZPs), which have been used as a framework materials for dental crowns and fixed partial dentures (FDPs), because their esthetical appearance is very similar to that of natural teeth and their mechanical characteristics are good, indeed, the highest ever reported for any dental ceramic [3]. Both the chemistry and the processing of these materials allow obtaining a fully dense polycrystalline zirconia, in its tetragonal phase, with a homogeneous distribution of submicron zirconia grains, giving a translucent aspect, that meets the requirements for natural teeth-looking restorations<sup>2</sup>. Furthermore, its particular mechanical behavior, characterized by high fracture toughness and flexural strength, is essentially caused by a stress-induced phase transformation, from a tetragonal (t) phase to monoclinic (m) phase, which increases its crack-propagation resistance [4].

This combination of features also allows Y-TZP to be particularly suitable for use with CAD/CAM systems [5]. Thus, Y-TZP blocks, in a pre-sintered condition, are quickly converted into dental restoration components that need a final firing step, necessary both to reach a higher density and to eliminate any stress induced by the strong surface working actions.

The final sintering is currently performed using electrically heated ovens, and, following the thermal cycles typically indicated by the manufacturer, is characterized by the reaching of maximum temperatures in the range 1350-1550°C, at which the ceramic components remain for almost 60 min. Furthermore, because the cooling step must be rather slow, to prevent cracking of ceramic components, a total sintering cycle can take 6-10 h.

One possible method of shortening the thermal cycle and lowering the maximum temperature is the use of microwave irradiation in place of the conventional electrical heating sources. Microwave irradiation, also known as dielectric heating, as applied to the sintering of advanced ceramic components, has recently become an important topic of scientific research [6], [7], [8], [9]. In particular, regarding the microwave sintering of zirconia, significant advantages in terms of higher density at lower heat work for cubic zirconia ceramics have been found [10]. The sintering behavior of nano Y-TZP by using hybrid conventional-microwave heating sintering

allowed obtaining greater than 99% dense ceramics with an average grain size < 100 nm [11], but also near theoretical density values for 3-YTZP using a multimode microwave sintering furnace at 2.45 GHz [12]. Further improvements in the physical and mechanical properties of  $Y_2O_3$ - $ZrO_2$  ceramics through the use of nanopowders and utilization of microwave sintering have been achieved [13].

The results of these studies underlined that, compared with conventional sintering, the use of microwaves provides to obtain several advantages, such as rapid and volumetric heating, lower heating temperatures, enhancements in densification, grain growth limitations and cost savings. In conventional sintering, heat is transferred from the radiant elements of the furnace to the surface of the ceramic component, by reaching the core of the component through conduction mechanisms. In microwave sintering, the heat is produced as a consequence of the interaction between the ceramic sample and the electromagnetic waves and involves the entire sample volume; in this way, the heating is more rapid and uniform [14].

The extent of the energy transfer, from the electromagnetic field to the matter, depends strongly on the dielectric properties of the sample, on the temperature, and on the radiation frequency [15], [16], [17], [18]. Most of advanced ceramics, such as  $Al_2O_3$  and  $ZrO_2$ , have low microwave absorption capacities at room temperature and an increased absorption capacities at higher temperatures. Thus, to improve microwave coupling and to enhance sintering efficiency, it is important to raise the initial temperature of the material to the critical value it starts to absorb more effectively. For this purpose, silicon carbide susceptors, that are strongly microwave absorbing materials, are commonly used because they absorb microwave energy and subsequently transfer it in the form of heat to the material via conduction. This approach is often referred to in the literature as hybrid microwave heating.

When samples are heated in an electric furnace or a microwave furnace, two methods can be used to control the temperature: 1) intermittent powering of the magnetron at a fixed power output (on/off control method or time-control method), or 2) continuous powering of the magnetron with a variable power output (power-control method). The first method involves the use of the magnetron at its highest output power as typically programmed in domestic ovens, while the second one is commonly used in industrial processes, where continuous adjustments of output power are necessary to follow the desired heating profile. It has been pointed out that there is no difference between the two methods in terms of grain growth or sample densification level, but the power-control method gives more precise control of temperature *versus* the on/off control method [19].

The aim of the present work was to assess the possibility of applying the hybrid microwave

sintering to a Y-TZP pre-sintered material, used for dental applications. Two different microwave methods, multimode and single mode, were used for the tests, both of which were fed with continuous variable power to better control the process temperature. Results indicate that the density of the microwave-fired samples depended strongly on the different firing changes, which, once optimized, allowed generation of highly dense zirconia samples with a firing time of only a few minutes.

### 3.3 Materials and methods

A 3% Y-TZP pre-sintered commercial material (Biotech Srl, Milano, Italy), suitable for shaping using CAD-CAM technology, was used for the sintering tests. From the commercial supplies, provided in the form of cylinders, rectangular specimens, of about 20x10x14 mm, were cut with an electric high-precision saw (Isomet 1000 Precision Saw, Buehler Ltd, Düsseldorf, Germany) and subjected to three heat heating treatments: conventional, multimode, and single-mode microwave sintering.

Conventional sintering was conducted in an electric furnace by using the following sintering cycle: 12°C/min up to 300°C, 5°C/min up to the maximum temperature, holding time 60 min, natural cooling. Two different maximum temperatures were used: 1450 and 1480°C. These sintering cycles required ~ 10 h at either maximum temperature.

Microwave sintering was performed, with a commercial CEM-MAS 7000 multimode applicator (CEM Corporation, Matthews, NC) at 2.45 GHz (950 W of nominal power) and on a TE10n single mode applicator (0.5–3-kW output power), connected to a 2.45-GHz TM030 microwave generator (Alter Power System, Long Beach CA). The multimode applicator can generate lower field density *versus* the single mode applicator; this was the reason for comparing the two systems. Additionally, a single-mode process can be designed or adjusted to stay in tune with the load to ensure that the sample is in the region of high microwave intensity. Because microwave sintering causes very rapid temperature increases in tested samples, the resulting thermal shock could be able to destroy the zirconia specimens. For this reason, several trials, with different arrangements using SiC susceptors or a refractory crucible, were conducted to choose the optimum operating conditions, allowing us to obtain sintered specimens with no cracks. In this study, the following sintering conditions were used. For the multimode applicator, a fiber insulating housing was placed inside the microwave chamber. Temperature measurements were made possible by using a k-type thermocouple inserted into the multimode cavity and placed in direct contact with the specimen. Each sample was located inside a cordierite crucible full of alumina powder. The general scheme of the experimental set-up is

shown in Figure 1. For the experiments conducted in the single-mode applicator, each sample was located inside a SiC crucible full of alumina powder (Fig. 2a). The crucible was positioned inside a refractory support (Fig. 2a) and then placed in the microwave chamber (Fig. 2b). Temperature was detected, in contact with the sample, using an optical fiber and transformed to a temperature signal. Manual adjustment to keep the sample in the maximum of electric field intensity was made during the whole heating cycle by means of a shorting plunger, which was positioned at the end of the single-mode applicator.

The relative density and apparent porosity of each sample were measured, before and after conventional or microwave sintering, following the European Standard EN 623-2 (1993) [20]. The degree of shrinkage after the firing was calculated, and the thickness of each rectangular specimen was measured using a digital micrometer before and after sintering. To avoid errors due to possible distortion of the specimens, the resulting values were the means of three measurements made at different parts of the bars.

The phase fraction amounts of zirconia, in the pre-sintered and sintered conditions, were evaluated by X-ray diffraction (XRD), using a diffractometer (Philips PW 3830; Koninklijke; the Netherland), with Cu  $K\alpha$  radiation ( $0.02^\circ$  step-scan, 10 s per step). Zirconia diffraction peaks were deconvoluted by using a Lorentz function in order to obtain the integral breadth. The monoclinic phase fraction of the zirconia was calculated as follows [21]:

$$X_m = \frac{I_m(111) + I_m(11\bar{1})}{I_m(111) + I_m(11\bar{1}) + I_t(111)}$$

where  $I_t$  and  $I_m$  are the integrated intensities of the tetragonal  $t(111)$ , and monoclinic  $m(111)$ , and  $m(11\bar{1})$  peaks.

The microstructures of the zirconia specimens, before and after the sintering step were determined by analyzing gold sputter-coated fresh fractured and sintered surfaces using a scanning electron microscope (EVO 40; Carl Zeiss Microscopy GmbH, Oberkochen, Germany) equipped with an EDS system (Inca Energy 250; Oxford Analytical Instruments, Uedem, Germany).

### **3.4 Results**

The results of the physical-mineralogical characterization of the tested material, in the as-received pre-sintered condition, are reported in Table 1. Even though it had a rather compact

microstructure, with a density consistent with other commercial materials of the same class, SEM analysis performed on the bulk of the samples showed some microcracks, usually connected with fragments of agglomerates originating from the starting powder, not completely destroyed by the processing operations (Fig. 3). The zirconia grains, with an equiaxed geometry, are rather fine, with a diameter of  $\sim 80\text{nm}$ , confirming that the pre-sintering heating cycle did not allow grain growth. The crystalline structure was present at 4 wt% of zirconia in the monoclinic phase, while after each of the different sintering cycles, only the tetragonal phase was detected.

In Table 2, the values of density, apparent porosity, and shrinkage of the samples, sintered under the different conditions, are presented.

Samples B1 and B2, sintered with the two conventional cycles in the electrical furnace, reached rather high values of density,  $> 99\%$  TD, with similar values of shrinkage. The use of the lower temperature,  $1450^\circ\text{C}$ , provided a good level of compactness, even if some small flaws, pre-existing in the pre-sintered specimen, were still present, as evidenced by the SEM analysis (Fig. 4a). With the increase in the maximum sintering temperature, to  $1480^\circ\text{C}$ , an almost total elimination of the flaws was observed, although the higher temperature caused an increase in grain size dimension (Fig. 4b).

Samples B3 and B4 were microwave-sintered in the system CEM-MAS 7000 multimode applicator by using two different cycle lengths, both reaching the maximum temperature of  $1200^\circ\text{C}$ . The shortest one, with a total length of 6 min, caused only a partial sintering of the specimens; the apparent porosity was rather high, 5.20%, with a density that reached 92.1% TD. Increasing of the time, to 25 min, did improve the final shrinkage, but did not increase meaningfully change the density, which reached only 95.6%TD with an apparent porosity of 1.03%. The microstructural analysis showed the presence of very small pores, distributed rather homogeneously among the submicron zirconia grains (Fig. 5). They were likely responsible for the poor level of density.

Samples B5 and B6, microwave-sintered with the TE10n single mode applicator, reached two maximum temperatures,  $1100$  and  $1200^\circ\text{C}$ , with sintering cycle lengths of few minutes, 4 and 6 minutes. The temperature of  $1100^\circ\text{C}$ , samples B5, did not allow to reach acceptable level of density and shrinkage. Its microstructure is characterized by the presence of rather homogeneous distribution of small pores, but also microcracks, already present in the presintered samples, and agglomerates of microporosity, linked to the presence of fragments of the original powder agglomerates, are recognizable (Fig. 6a). This sintering condition allows to rapidly densify the zirconia, in the areas where the particles are rather well close, but it is not able

to eliminate the larger flaws, that probably would need higher temperature and time.

The same sintering time, 4 minutes, but at 1200°C, sample B6, allows to meaningfully increase the density, even if there is still a certain amount of open porosity, its apparent porosity is in fact 0.80wt%. From the microstructural analysis, together with very small isolated pores, some open porosity is still evident (Fig. 6b), while no appreciable growth of zirconia grains is visible. With the use of a longer time, 6 minutes, always at 1200°C, the zirconia sample, B7, reached the maximum density value, for the microwaves sintering, comparable with the ones reached with the longer conventional heating treatments.

### **3.5 Discussion**

The results of this study underline as it is possible to reach high level of densification and shrinkage by using the single mode microwaves sintering, in the conditions related to samples B7, 6 minutes at 1200°C. While the open porosity of the specimens is not practically ever existing, the shrinkage is slightly lower in comparison with samples B1 and B2, conventionally heated. All that can be better understood by examining their microstructural features. From Fig. 6c, corresponding to a cross-section of B7, it is evident as, at the border near the external surface, the material is perfectly compact, without any pores, while in the bulk some small close porosities are still present, responsible of the reduced shrinkage (Fig. 6d).

It is to underline as reduced grain growth was observed for all the microwaves sintered samples, in comparison with the ones conventionally sintered, also when the lowest temperature, 1450°C, was adopted. This aspect is of particular importance for ceramic materials, because the presence, of coarse grains size distribution or also of few grains characterized by exaggerated grain growth, is strongly deleterious for the mechanical characteristics of a structural component. In these conditions, microwave sintering allows to obtain specimens with a more uniform microstructure, by confirming the volumetric heating phenomenon.

The elemental EDX microanalysis performed on the external surfaces of the specimens, differently microwaves sintered, did not find any extraneous element, only zirconium, oxygen and yttrium were detected. That means as no contamination phenomena from the alumina powder used to eliminate thermal shock phenomena happened.

The results of the present study allow to foresee very interesting possibility in a larger use of microwave sintering, even if several implementations are still necessary to provide larger furnace chamber and easier temperature control systems. Further works, regarding these aspects, is in progress.

### 3.6 Conclusions

A microwaves sintering study of zirconia material was performed adopting two different systems to avoid thermal shock cracks in the specimens.

The results obtained from the present work allow to draw the following conclusions:

1. By optimizing the microwaves sintering conditions, it is possible to obtain rather dense specimens strongly reducing both the maximum sintering temperature and the total thermal cycle length, passing from several hundreds of minutes at 1450°C to few minutes at 1200°C.
1. The less drastic sintering conditions, in terms of reduced temperature and thermal cycle length, allowed obtaining a limited grain growth, able to improve the mechanical characteristics of the sintered zirconia components.
3. The dielectric heating method produces specific advantages in terms of energy efficiency, process simplicity, saving costs of equipment maintenance and operator.

### 3.7 Tables

**Table 1** - Physical-mineralogical characteristics of the pre-sintered material

Density (g/cm <sup>3</sup> )	Porosity (%)	<i>t</i> phase (wt%)	<i>m</i> phase (wt%)	Grain size (nm)
3.04	49.62	96	4	80

**Table 2** - Physical characteristics of the tested samples, after the different sintering conditions.

Sample	Sintering temperature (°C)	Thermal cycle length (min)	Density (g/cm <sup>3</sup> )	Apparent porosity (vol.%)	Shrinkage (%)
Conventional sintering					
B1	1450	600	6.06	0.01	21.77
B2	1480	600	6.06	0.01	21.70
Multi mode microwaves sintering					
B3	1200	6	5.60	5.20	18.90
B4	1200	25	5.82	1.03	21.52
Single mode microwaves sintering					
B5	1100	4	5.05	14.52	16.71
B6	1200	4	5.98	0.80	21.49
B7	1200	6	6.01	0.01	21.32

3.8 Figures

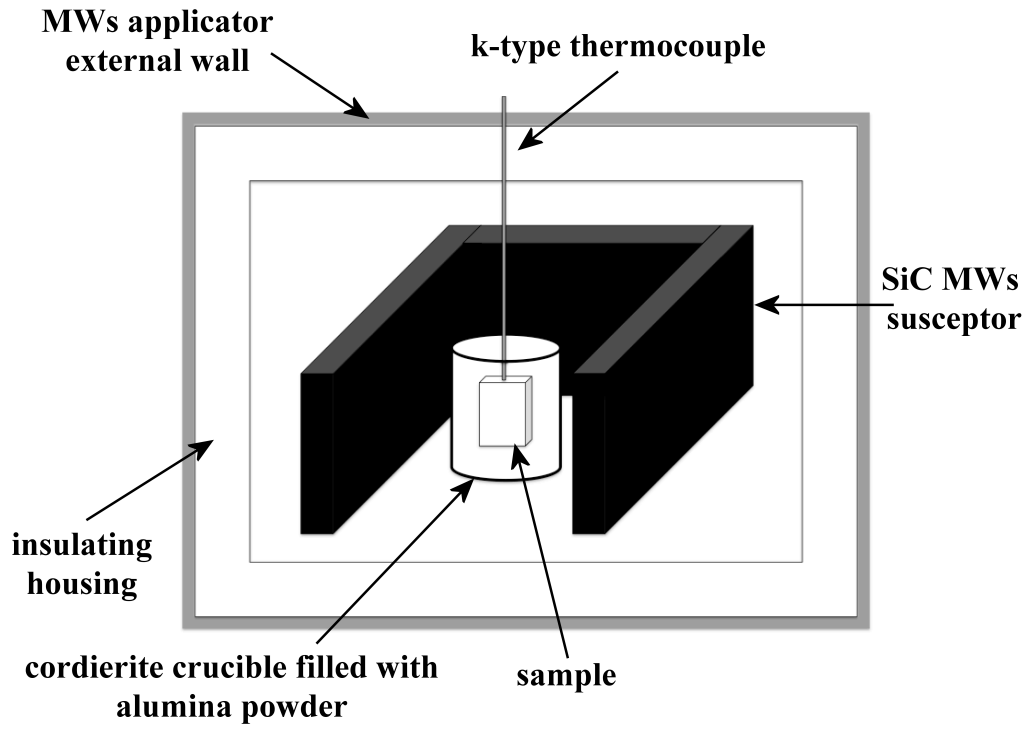
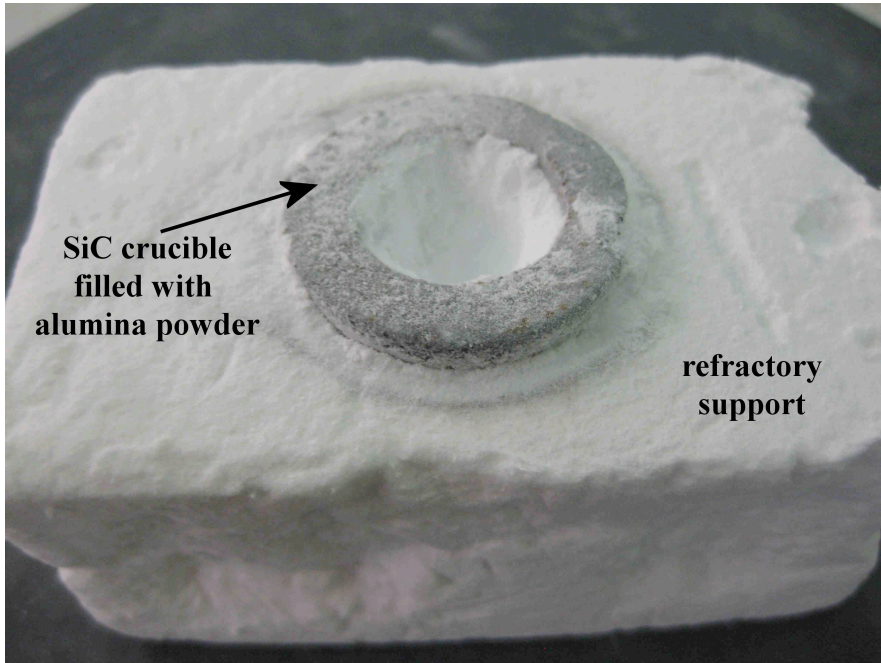
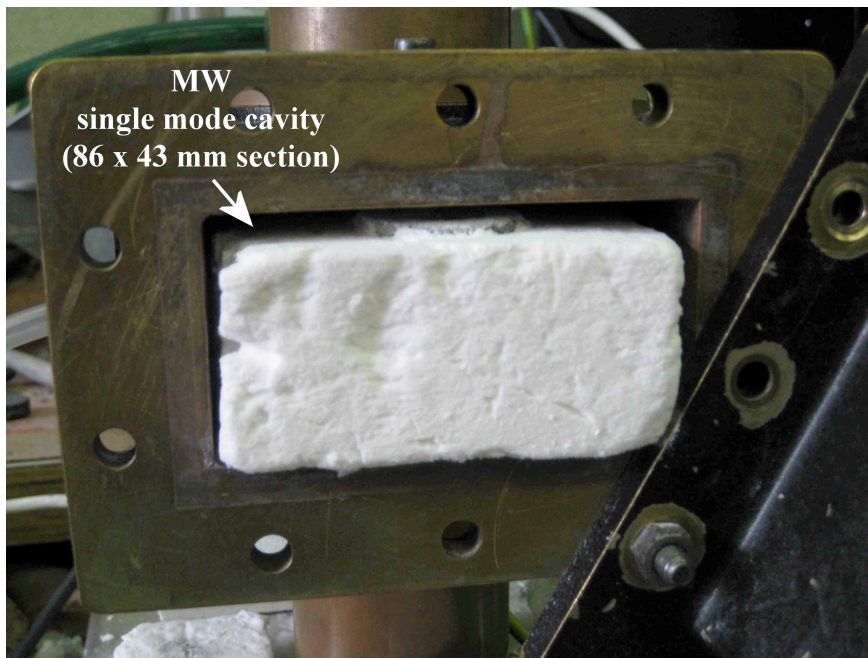


Fig. 1. Sample arrangement inside the microwave multi mode applicator.



**Fig. 2a.** Sample arrangement used in the microwave single mode applicator; a) SiC crucible filled with alumina powder inserted into a refractory support.



**Fig. 2b.** Refractory support positioned inside the single mode cavity.

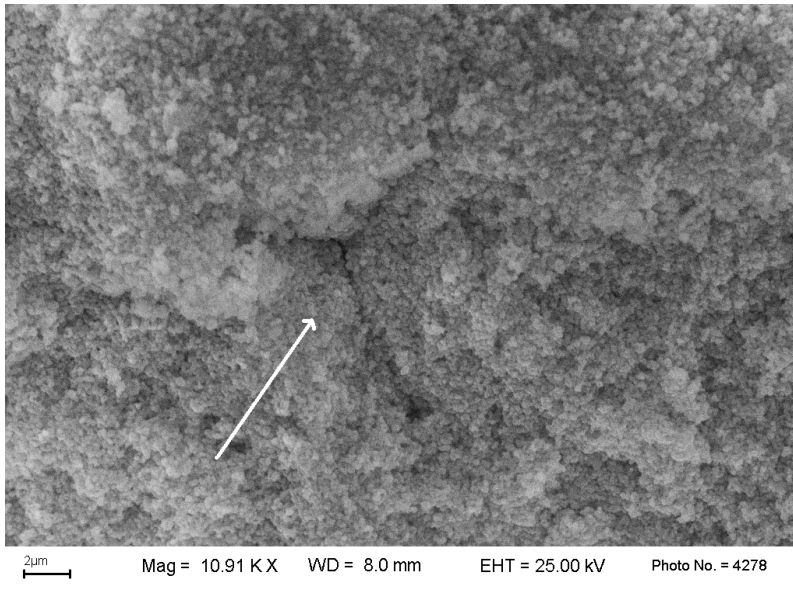


**Fig. 3.** SEM -SEI micrograph of the fracture surface of the tested material, in the pre-sintered condition. An evident microcrack, surrounding rests of agglomerates of the starting powder, is arrowed.

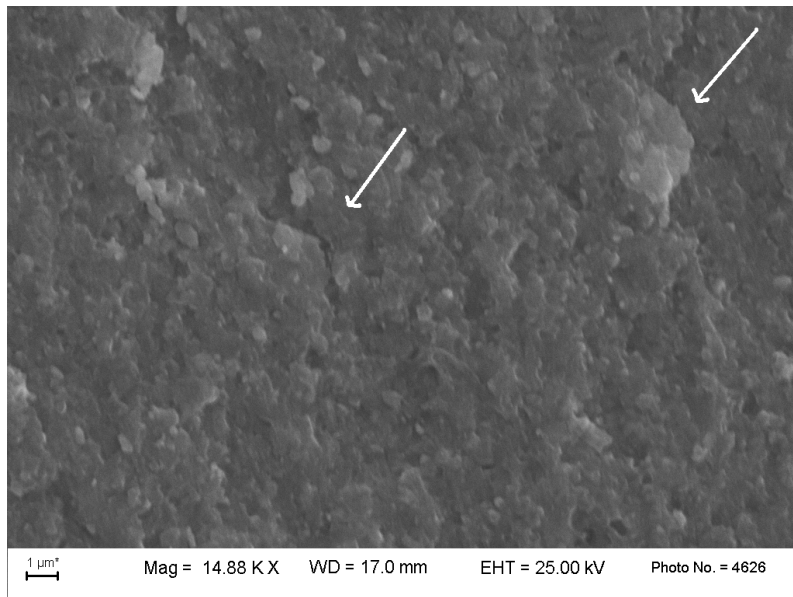


**Fig. 4a.** SEM-SEI micrograph of the fracture surface of sample B1, conventional sintering 1450°C/1h. Microflaws are arrowed.

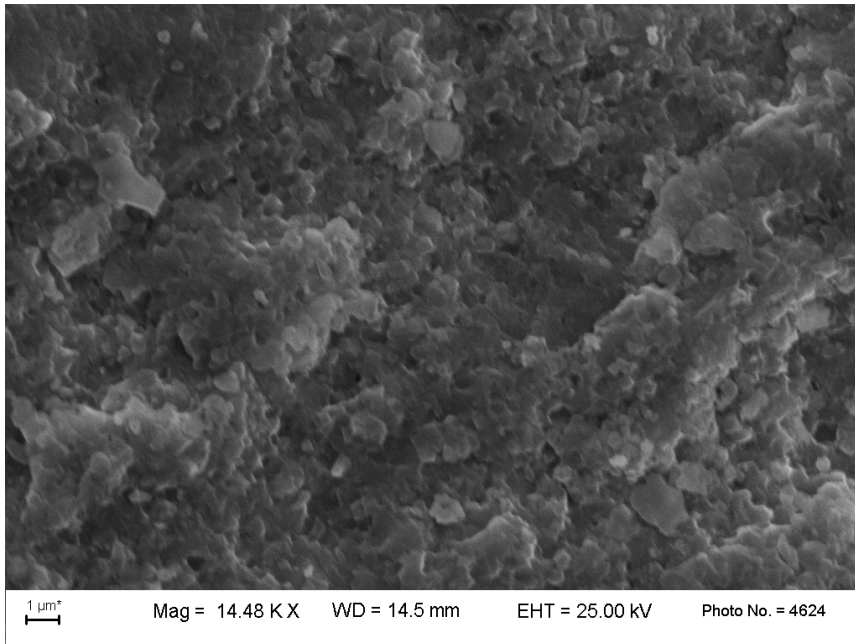


**Fig. 4b.** SEM -SEI micrograph of the fracture surface of sample B2, conventional sintering 1480°C/1h.

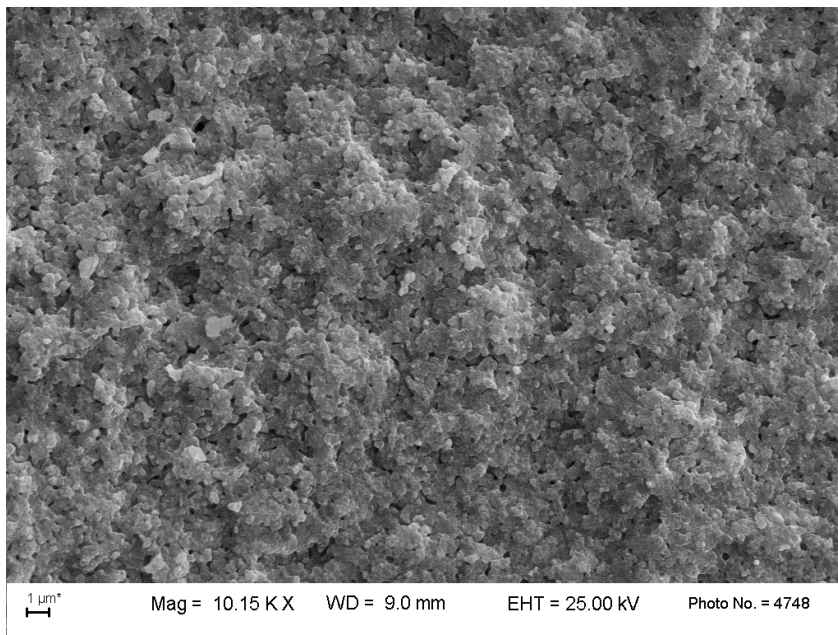


**Fig. 5.** SEM -SEI micrograph of the fracture surface of sample B4, multimode microwaves sintered, maximum temperature 1200°C, total length of the thermal cycle 25 minutes.

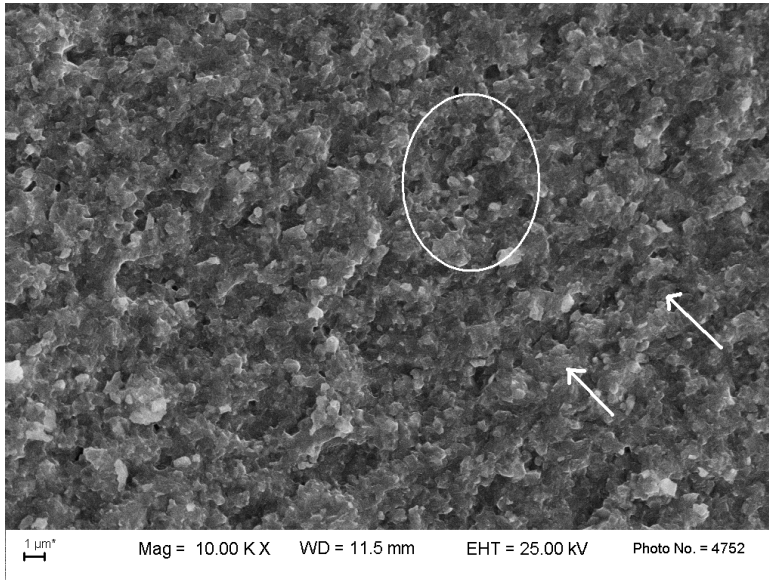


**Fig. 6a.** SEM - SEI micrograph of the fracture surface of sample B5, single mode microwaves sintered, maximum temperature 1100°C, total length of the thermal cycle 4 minutes. A microcrack is arrowed, an agglomerates of pores is circled.

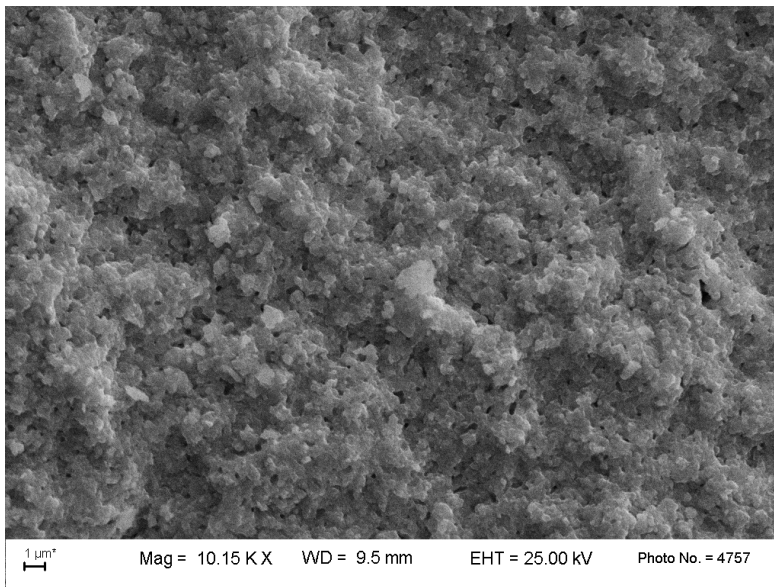


**Fig. 6b.** SEM - SEI micrograph of the fracture surface of sample B6, single mode microwaves sintered, maximum temperature 1200°C, total length of the thermal cycle 4 minutes.

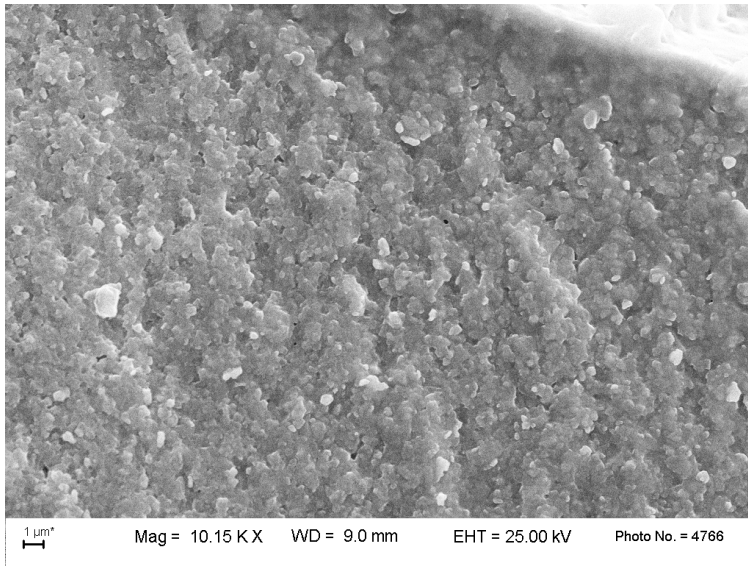


**Fig. 6c.** SEM - SEI micrograph of the fracture surface of sample B7, single mode microwaves sintered, maximum temperature 1200°C, total length of the thermal cycle 6 minutes. The external surface is at the topbright of the micrograph.

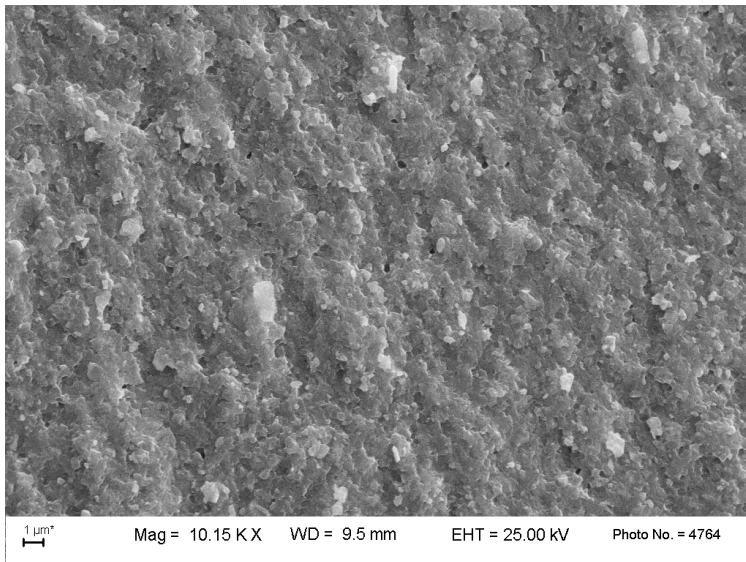


**Fig. 6d.** Small close porosities are responsible of the reduced shrinkage.

### 3.9 References

- [1] Denry I, Kelly JR. State of the art of zirconia for dental applications. *Dent Mater* 2008; **24**:299 - 307.
- [2] Chevalier J, Gremillard L. Ceramics for medical applications: A picture for the next 20 years. *J Eur Ceram Soc* 2009; **29**:1245 - 55.
- [3] Kelly JR, Denry I. Stabilized zirconia as a structural ceramic: An overview. *Dent Mater* 2008; **24**:289 - 98.
- [4] Becher PF. Toughening behavior in ceramics associated with the transformation of tetragonal ZrO<sub>2</sub>. *Acta Metal* 1996; **34**:1885 - 91.
- [5] Davidowitz G, Kotick PG. The Use of CAD/CAM. *Dent Clin North Am* 2011; **55**:559 - 70.
- [6] Mizuno M, Obata S, Takayama S, Ito S, Kato N, Hirai T, et al. Sintering of alumina by 2.45 GHz microwave heating. *J Eur Ceram Soc* 2004; **24**:387 - 91.
- [7] Cheng J, Agrawal D, Zhang Y, Roy R. Microwave sintering of transparent alumina. *Mater Lett* 2002; **56**:587 - 92.
- [8] Menezes RR, Kiminami RG. Microwave sintering of alumina–zirconia nanocomposites. *J Mater Proc Tech* 2008; **203**:513 - 17.
- [9] Travitzky NA, Goldstein A, Avsian O, Singurindi A. Microwave sintering and mechanical properties of Y-TZP/20 wt.% Al<sub>2</sub>O<sub>3</sub> composites. *Mate Sci Eng A* 2000; **286**:225-29.
- [10] Upadhyaya DD, Ghosh A, Gurumurthy KR, Prasad R. Microwave sintering of cubic 3131zirconia. *Ceram Intern* 2001; **27**:415 - 18.
- [11] Binner J, Annapoorani K, Paul A, Santacruz I, Vaidhyanathan B. Dense nanostructured zirconia by two stage conventional/hybrid microwave sintering. *J Eur Ceram Soc* 2008; **28**:973 - 7.
- [12] Garcia GC, Meléndez MJ, Gómez GD, Domínguez MA. Microwave sintering of nanocrystalline Y-TZP (3mol.%), *J Mat Sci* 2006; **41**:5231 - 4.
- [13] Reidy CJ, Fleming TJ, Hampshire S, Towler MR. Comparison of microwave and conventional sintered Ytria-doped Zirconia ceramics. *Intern J Appl Ceram Tech* 2011; **8**:1475 - 85.
- [14] Oghbaei M, Mirzaee O. Microwave versus conventional sintering: A review of fundamentals, advantages and applications. *J All Comp* 2010; **494**:175 - 89.
- [15] Clark DE, Sutton WH, Microwave processing of materials. *Ann Rev Mater Scie* 1996; **26**: 299 - 331.
- [16] Lewis D, Rayne RJ, Bender BA, Kufihara LK, Chow GM, Fliflet A. Conventional and

high frequency microwave processing of nanophase ceramic materials. *Nanostr Mater* 1997;**9**:97 - 100.

[17] Thostenson ET, Chou TW. Microwave processing: fundamentals and applications. *Composites: Part A* 1999;**30**:1055 - 71.

[18] Clark DE, Folz DC, West JK. 2000. Processing materials with microwave energy. *Mater Sci Eng A* 2000;**287**:153-8.

[19] Yasuoka M, Nishimura Y, Nagaoka T, Watari K. Influence of different methods of controlling microwave sintering: the characteristics of oxide ceramics. *J Therm Anal Calor* 2006;**83**:407 - 410.

[20] European Standard EN 623-2, 1993. Advanced technical ceramics - monolithic ceramics - general and textural properties - Part 2: Determination of density and porosity. Geneva: ISO; 1995. Available at: <http://www.iso.org/iso/store.htm>

[21] Garvie RC, Nicholson PS. Phase analysis in zirconia systems. *J Am Ceram Soc* 1972; **55**:302 - 5.

***CHAPTER 4***

**Bonding effectiveness of zirconia after different sandblasting procedures.**

## 4.1 Abstract

**Objectives.** To determine the effect of sandblasting before and after sintering on the surface roughness of zirconia and the microtensile bond strength of a pressable veneering ceramic to zirconia.

**Materials and Methods.** Pre-sintered zirconia blocks (ZirCAD Ivoclar Vivadent, Shaan, Liechtenstein, Ivoclar-Vivadent) were cut into specimens and randomly divided into five groups of three specimens each: four test groups (B-E) and one control group (A). Any surface treatment was performed in the control group (A). Groups B, C and D were sandblasted with 30 $\mu$ m SiO<sub>2</sub> (CoJet), 50 $\mu$ m Al<sub>2</sub>O<sub>3</sub>, and 110 $\mu$ m Al<sub>2</sub>O<sub>3</sub>, respectively, before sintering. Group E was sandblasted with 30 $\mu$ m SiO<sub>2</sub> after sintering. After sintering of zirconia blocks, a liner and a pressable ceramic were fired. Sixteen micro bars were obtained from each block and submitted to the microtensile bond strength test. Data were analyzed with one-way ANOVA and Tukey-Kramer *post hoc* tests for comparisons.

**Results.** Regarding surface roughness, sandblasting with 110 $\mu$ m, 50 $\mu$ m, and 30 $\mu$ m particles resulted in significantly higher values than the control group and the group sandblasted with 30 $\mu$ m particles before sintering. Ra values for the specimens sandblasted with 110 $\mu$ m ( $3.436 \pm 0.441 \mu\text{m}$ ), 50 $\mu$ m ( $2.325 \pm 0.465\mu\text{m}$ ), and 30 $\mu$ m ( $1.217 \pm 0.217\mu\text{m}$ ) particles and the control value ( $0.464 \pm 0.107 \mu\text{m}$ ). The highest  $\mu$ TBS were observed when sandblasting the sintered zirconia with 30 $\mu$ m particles ( $26.793 \pm 14.802 \text{ MPa}$ ) obtain by;  $\mu$ TBS values for the specimens sandblasted were  $23.991 \pm 16.834$ ,  $21.276 \pm 15.189$  and  $20.899 \pm 11.704 \text{ MPa}$  for the 110-, 50-, and 30- $\mu$ m particles, respectively;  $\mu$ TBS control value was ( $17.437 \pm 14.035 \text{ MPa}$ ). Ra values for the. Finally, we obtained the percentage of interfacial failures: groups A to E was 77, 73, 67, 71, and 88%, respectively. The percentage of mixed failures in groups A to E was 60, 70, 65, 46 and 52%, respectively; percentage of cohesive failure was 13, 23, 27, 33 and 29% and percentage of adhesive failure was 27, 7, 8, 21, 19%.

**Significance.** Sandblasting the zirconia surface before sintering enhances the surface roughness in direct proportion to the size of the sand used. The Co-Jet treatment of zirconia after sintering appears to enhance the adhesion between the veneering ceramic and zirconia.

bond strength test.

## 4.2 Introduction

Porcelain-fused to metal prosthesis (PFM) are routinely used in dental practice thanks to the well known technical procedures, good aesthetics and reliability over years [1]. Despite the survival rate of PFMs range from 74 to 85% at 15 years, discolorations may occur at the metallic margin and some alloy's components may generate allergic reactions [2-3].

Therefore, replacement of PFMs by all-ceramic restorations has been driven by the improved aesthetics and lower allergenic potential achieved using ceramic materials as core frameworks. All-ceramic single crowns and anterior fixed partial dentures (FPD) have been used successfully since nineties. Afterwards, due to the development of high-strength ceramic frameworks, such as tetragonal zirconia polycrystals (TZP), missing teeth in the posterior regions have also been replaced by all-ceramic FPDs. The superior mechanical properties of zirconia combined with state-of-the-art computer-aided design and machining (CAD/CAM) fabrication procedures have allowed large and complex restorations with high accuracy and success rates [4]. To achieve better aesthetics, zirconia frameworks can be veneered with a ceramic material, which is built in successive layers, giving the final restoration individual optical characteristics that can barely be distinguished from the surrounding natural dentition. Alternatively, ceramic can be pressed on zirconia frameworks for veneering. The main advantage of the heat pressing technique is that it allows pores due to the lost-wax technique to be avoided and one-step layering procedures [5].

However, establishing a strong and stable bond between yttrium, partially stabilized tetragonal zirconia polycrystal materials (Y-TZP) and veneering ceramics has been proven to be cumbersome [6]. Bonding mechanisms between veneering ceramics and zirconia frameworks are currently subject of comprehensive investigations [7].

It has been reported that the zirconia-veneer bond is weaker than that of other all-ceramic systems, which suggests that layered zirconia frameworks are more susceptible to delamination and chipping during function [8].

Clinical studies have reported a failure rate of 13.0% after three years and 15.2% after five years for veneered yttrium-TZP (YTZP) frameworks due to chipping of the ceramic veneer [9]. This fracture pattern is associated with a thin layer of glass-ceramic that remains on the zirconia framework [10]. This finding supports the hypothesis of a reliable bonding of veneering ceramics to zirconia frameworks, but also reveals the brittleness weakness of the veneering ceramic. Moreover, it is difficult to determine the point of initial fracture. As already explained by Aboushelib *et al.*, a crack initiated at the ceramic-zirconia interface can propagate through the weakest layer due to the asymmetric stress distribution in the specimen. As a

consequence, traces of elements may be left attached to the interface. When analyzing, this will be incorrectly classified as cohesive failure [6-7].

Silica coating has been proved to improve bonding of zirconia to luting agents, particularly when using the Co-Jet system (3M ESPE, St. Paul, MN, USA) [11]. This system uses silicate-coated alumina particles for sandblasting, thereby welding a silicate layer onto the surface by means of the high spot heat produced by the blasting pressure followed by silanization. The effects of CoJet system are related to the high kinetic energy of the  $Al_2O_3$  particles modified with  $SiO_2$  at impact and the fusion of the silica to the substrate surface.

Since silicate-based veneering porcelains are often used to bond to zirconia frameworks, silica coating of zirconia might enhance the bond strength of the veneering ceramics as well. However, any other studies have previously been carried out to support this hypothesis [12].

In general, shear tests or microtensile tests are used to measure the bond strength of an all-ceramic system, but using shear bond test may lead to undesired stress pattern distribution, causing cohesive failures and erroneous interpretation of the data, and to evaluate the influence of the substrate surface on bond quality. In particular the microtensile bond strength test ( $\mu$ TBS) has been proven to be a reliable test for evaluating the bond strength of composite materials to a variety of substrates [13]. To evaluate bond quality is preferable to use SEM analysis.

Aim of this study was to determine the effect of different sandblasting procedures on the surface roughness of zirconia and the microtensile bond strength of a veneering ceramic to zirconia. The hypotheses tested were that sandblasting before sintering enhances the surface roughness of zirconia (hypothesis 1) and the  $\mu$ TBS of a pressable veneering ceramic to zirconia (hypothesis 2).

### **4.3 Materials and Methods**

Three zirconia ZirCAD C15L (Ivoclar Vivadent, Schaan, Liechtenstein) specimens were cut using a low-speed diamond disc (MDS100, Norton, USA) in a special device to obtain 15 blocks of zirconia of 7.2 mm height, 9.2 mm width, and 9.2 mm length.

The surface of each test block was sandblasted before or after sintering. Then, ZirLiner (Ivoclar Vivadent, Schaan, Liechtenstein) was applied and veneered with the pressable ceramic ZirPress (Ivoclar Vivadent, Schaan, Liechtenstein). Finally, the specimens were cut into micro-bars to measure the core-veneer microtensile bond strength.

The materials tested and their properties are summarized in Table 1. Pre-sintered zirconia blocks (ZirCAD C15L, Ivoclar Vivadent, Schaan, Liechtenstein) were cut into specimens and

divided randomly into five groups of three specimens each. Groups B to E were the test groups and group A was the control. The following surface treatments were applied. Groups B to D were sandblasted before sintering with 30- $\mu\text{m}$   $\text{SiO}_2$  (CoJet, 3M ESPE), 50- $\mu\text{m}$   $\text{Al}_2\text{O}_3$ , and 110- $\mu\text{m}$   $\text{Al}_2\text{O}_3$  particles, respectively. Group E was sandblasted after sintering with 30- $\mu\text{m}$   $\text{SiO}_2$  (CoJet, 3M ESPE). Group A was sintered without any surface treatment. The sandblasting was performed at the same pressure of 2 bars for 15 seconds. The distance between the nozzle and the surface differed; it was 1 cm for the 30- $\mu\text{m}$   $\text{Al}_2\text{O}_3/\text{SiO}_2$  (CoJet, 3M ESPE) and 1.5 cm for the 50- $\mu\text{m}$  and 110- $\mu\text{m}$   $\text{Al}_2\text{O}_3$ . The treatments are summarized in Table 2. The zirconia blocks (20% ca. contraction) were sintered in a Sintramat (Ivoclar Vivadent, Shaan, Liechtenstein) oven according to the manufacturer's instructions. The surface roughness (Perthometer M4P, Mahr Perthen) of the polished, sandblasted, and silica-coated specimens was measured for each treatment. The surface for each treatment was scanned two times by five parallel tracings with 1.0-mm intervals and the Ra values were registered.

After the preliminary measurements, a layer of ZirLiner (IPS e.max, Ivoclar Vivadent, Shaan, Liechtenstein) was applied to the zirconia blocks and fired at a temperature of 960°C. Then, wax-up onto the coping was performed in order to obtain an equivalent veneering structure for the corresponding ZirCAD specimen. The wax surface was smoothed, finished, and invested in a special investing material (IPS PressVEST, Ivoclar Vivadent, Shaan, Liechtenstein) in a size two muffle according to the manufacturer's instructions. The wax was burnt out and the muffle was heated. The copings were over-pressed using special porcelain (IPS e.max ZirPress, Ivoclar Vivadent, Shaan, Liechtenstein) with the appropriate coefficient of thermal expansion with respect to zirconia. After cooling, the investment was removed in the sandblasting unit (Eurosab, Tissi, San Donato Milan, Italy) using 50- $\mu\text{m}$  glass beads at 2 bars pressure. The reaction layer formed during the pressing procedure was removed by immersing the crowns in HF solution (IPS e.max Press Invex Liquid, Ivoclar Vivadent, Shaan, Liechtenstein) in an ultrasonic cleaner (Sonorex, Bandelin, Berlin, Germany) for 5 min. Subsequently, the blocks were cleaned under running water for 3 min and dried. The pressing sprue and extrusion flashes were removed using a water-cooled air-turbine without pressure to protect the porcelain from heat damage.

The 15 blocks ZirCAD-ZirPress were stored in distilled water at 37°C for at least 1 week. Then, they were cutted using a diamond-coated blade (Acutom-40, Automatic Blade) for sintered zirconia, under water cooling, to obtain 20 micro bars from each block ZirCAD-ZirPress. Each micro bar had a vertical dimension of 10 mm (5 mm of ZirCAD and 5 mm of ZirPress) and a

horizontal cross-section of 1 mm<sup>2</sup>. Randomly, 16 sound micro bars were selected from each group. Using reported methods, the micro bars were attached to the attachment unit using an adhesive resin (Model Repair II Blue, Dentsply-Sankin, Ohtawara, Japan), taking care to centre the zirconia veneer interface at the free space of the attachment unit, and were loaded to failure at a crosshead speed of 1 mm/min (LRX, Lloyd, Hampshire, UK). The maximum load at failure [N and MPa] was extracted from computer-generated files.

The surface roughness measurements and microtensile values were analyzed statistically using one-way analysis of variance (ANOVA), follow by a *post hoc* Tukey-Kramer test (Jmp7 ver. 7.0, Chicago, USA).

#### 4.4 Results

The morphology of sintered zirconia surfaces was observed by using a scanning electron microscope (SEM, Zeiss EVO 40, D) equipped with an energy-dispersive X-ray analyzer (EDS, Inca, Oxford Instruments, UK), after gold sputtering.

The mode of failure was analyzed by using a stereomicroscope at 50× (Wild M5A, Heerbrugg, Switzerland) at 25× magnification. Failures fractures were classified into three groups: cohesive (within the veneer ceramic), mixed, and adhesive (within the interface between veneer and zirconia ceramics). In addition, the lateral side of some of the tested micro-bars were cleaned ultrasonically and analyzed by SEM and EDS. Regarding surface roughness (Ra), the values for the specimens sandblasted with 110µm were  $3.4 \pm 0.4\mu\text{m}$ , with 50µm were  $2.3 \pm 0.4\mu\text{m}$ , with 30µm were  $1.2 \pm 0.2\mu\text{m}$  for the control group were  $0.4 \pm 0.1$ , (Figure 1).

The highest value of the micro-tensile bond strength was obtain by Group E sandblasting the already sintered zirconia with a µTBS of  $26.793 \pm 14.802$  MPa. The µTBS values for the specimens sandblasted were  $23.9 \pm 16.8$ ,  $21.2 \pm 15.1$  and  $20.8 \pm 11.7$  MPa for the 110-, 50-, and 30-µm particles, respectively; the µTBS of the control group (A) was ( $17.4 \pm 14.0$  MPa). The results are shown in Figure 2. The mean microtensile bond strength, standard deviation and failure pattern are summarized in Table 3.

The statistical analysis showed that sandblasting the zirconia surface before sintering enhanced the roughness values in direct proportion to the dimensions of the sand used. There was a significant difference between group D and the control group, whereas the results for the other test groups were intermediate between these two groups. Finally, we determined the percentages of failures involving defects that crossed the interface with the porcelain veneer (mixed), at the interface (adhesive), and within the veneering porcelain itself (cohesive). The

term “interfacial failure” was used for both mixed and adhesive failures. Regarding the type of failure, the percentage of mixed failures in groups A to E was 60, 70, 65, 46 and 52%, respectively; percentage of cohesive failure was 13, 23, 27, 33 and 29% and percentage of adhesive failure was 27, 7, 8, 21, 19%. The results are shown in Figure 3.

#### 4.5 Discussion

Clinical recommendations on materials and procedures are often based on mechanical laboratory tests. Most common tests used for evaluating the bond strength are the shear bond test and microtensile bond strength test. These tests are also used to evaluate the bond strength between core and veneer in different all-ceramic systems. Al-Dohan et al. reported for commercially available core veneered all-ceramic systems shear bond strength in the range of 22-31 MPa [14].

Unfortunately, using shear bond test may lead to undesired stress pattern distribution, causing cohesive failures and erroneous interpretation of the data.

Application of the microtensile bond strength test for measuring the tensile strength of the core and veneer components of all-ceramic restorations allowed direct evaluation of their tensile strength. However, using the microtensile bond strength to measure the core veneer bond strength this test requires careful attention while cutting the brittle specimens in order to avoid creating cutting defects or unexpected cracking of the microbars. Using sharp new cutting discs at high cutting speeds and low loads reduces vibration and ensures fine cutting of the specimens.

The data of surface roughness and microtensile tests did not show a direct correlation between the Ra values and the strength of adhesion obtained in the different test groups. The **Ra parameter**, the most common one reported in the dental literature [15], represent the average roughness as measured by the profilometer, and as lower is its value, smoother is the surfaces [16]. Relative to the roughness values, the data are shown in Figure 1. The statistical analysis showed that sandblasting the zirconia surface before sintering enhanced the roughness values in direct proportion to the dimensions of the sand used.

The SEM analysis of the same samples allowed to have a more deep sight of the real surfaces morphology. The sand blasted surfaces drastically change the surface microstructure of the zirconia samples, increasing the roughness according to the dimensions of the impacting particles [17].

The worn surfaces present detachments and plastic deformation of the material, Fig. **A**. The sand-blasting operation causes also changes from a chemical point of view, the EDS analysis allowed to recognize the presence of small fragments of alumina and silica. In particular, for the samples of the groups CB and DC, alumina particles appear to be well immersed the zirconia matrix, and co-sintered (Fig. **B**). While for the samples of the group ED, several fine silica particles, coming from the CoJet abrasive, are smeared on the zirconia surface (Fig. **C**).

The best adhesion was obtain by sandblasting the already sintered zirconia with the smallest sand particles (30  $\mu\text{m}$ ) ( $R_a = 0.546 \pm 0.099 \mu\text{m}$ ;  $\mu\text{TBS} = 26.793 \pm 14.802 \text{ MPa}$ ). There was a significant difference between group D and the control group, whereas the results for the other test groups were intermediate between these two groups. Therefore, the surface treatment with CoJet after sintering is a good way to enhance the adhesion between zirconia and the veneering porcelain.

In addition, the bond strength of the samples sandblasted before sintering was increased relative to the control group. The values were  $23.991 \pm 16.834$ ,  $21.276 \pm 15.189$ , and  $20.899 \pm 11.704 \text{ MPa}$  for the 110-, 50-, and 30- $\mu\text{m}$  particles, respectively, and all were better than the control value ( $17.437 \pm 14.035 \text{ MPa}$ ), although the differences were not significant. By contrast the  $R_a$  values for the specimens sandblasted with 110- $\mu\text{m}$  ( $3.436 \pm 0.441 \mu\text{m}$ ), 50- $\mu\text{m}$  ( $2.325 \pm 0.465 \mu\text{m}$ ), and 30- $\mu\text{m}$  ( $1.217 \pm 0.217 \mu\text{m}$ ) particles were significantly different from the control value ( $0.464 \pm 0.107 \mu\text{m}$ ).

The results obtained for the specimens sandblasted before sintering were likely dependent on the roughness produced by sandblasting, whereas the significant improvement obtained with sandblasting after sintering was likely associated with the CoJet treatment.

We determined the percentages of failures involving defects that crossed the interface with the porcelain veneer (mixed), at the interface (adhesive), and within the veneering porcelain itself (cohesive). (Fig. 3).

The failure analysis showed a high percentage of mixed interfacial failures with all treatments; the percentage of mixed interfacial failures in groups A to E was 60, 70%, 65%, 46%, 52%, respectively. These values depend on the correct execution of the microtensile test and the distribution of forces at the interface are due to the brittleness of veneer ceramics [18]. Figure D shows an example of mixed failure with exposed zirconia crystals.

Different punctual micro-analysis, conducted in the contact area zirconia-veneering ceramic, on the cross section of the sample (Fig. **D**), pointed out the presence of a certain reaction area at

the interface of the two materials. The EDS spectrum corresponding to the contact area, shows the presence of large amount both of zirconia and the elements, characteristics of the veneering layer. It is to underline as the sandblasting, after the sintering step, as in the samples of group ED, not only causes a widespread silica particles smearing on the surface, but it is also responsible of a partial zirconia phase transformation, from tetragonal to monoclinic, and a lattice distortion, as indicated by the hump at the left shoulder of (111) peak, for the presence of residual stresses (Fig. E). **(il centro ceramico ci deve dare questa Figura)** Even if additional crystallographic study is necessary, it is rather clear as these phenomena give a higher reactivity to the zirconia surface, that results to be more prone to react with the veneering ceramic.

To prevent the delamination or chipping of a restoration, it is necessary to select the appropriate ceramic materials. Surface treatments are used to enhance the bonding of the ceramic.

Different treatments can be used to color the zirconia framework for aesthetic purposes. As our results showed, the best way to enhance the bonding between zirconia and ceramic is post-sintering sandblasting with 30- $\mu\text{m}$  sand (CoJet, 3M ESPE). Tribochemical silica coating also deposited a silica layer on the ceramic surface, due to the high-pressure impaction of alumina particles modified by silica on the conditioned substrate. Unfortunately, less information is available regarding the effect of tribochemical silica coating in zirconia–resin bonds. Such a technique is supposed to provide ultra fine mechanical retention embedding treated surfaces with silica particles [19].

The addition of pigments to the zirconia framework could alter its structure, necessitating a different surface treatment before veneering. To prevent delamination and chipping failure of zirconia veneered restorations, careful selection of both the framework and veneer ceramic materials, in addition to proper surface treatment, are essential for maintaining good bond strength.

In Aboushelib *et al.*, the liner was applied over a sandblasted surface. Although it increased the bond strength of colored zirconia frameworks, it also increased the percentage of interfacial failures. Further study is needed to understand this phenomena.

#### **4.6 Conclusions**

Within the limitations of this study, the following conclusions were drawn:

1. Sandblasting the zirconia surface before sintering enhances the surface roughness in direct proportion to the size of the sand used;
1. Increasing the surface roughness of the zirconia enhance its microtensile strength, although the differences were not significant;
2. Evaluating microtensile bond strength we can say that using the CoJet treatment after sintering is recommended for clinical situations where it is important improve the adhesion of ceramic veneer to zirconia;
3. Improving the strength of veneering ceramics is necessary to realize the benefits of the high strength of zirconia frameworks.
4. High percentage of mixed failures are due to the brittleness of veneer ceramics.

## 4.7 Tables.

Material	Batch	Numbers	Composition	Coefficient of thermal expansion (ppm/°C)
ZirCAD	K30504	K54201	yttrium oxide (4–6% vol) hafnium oxide (1–5% vol) and alumina and silica (<1% vol)	10.75 (0.25)
ZirPress	H26883	H20589	SiO <sub>2</sub> primarily, with Li <sub>2</sub> O, Na <sub>2</sub> O, K <sub>2</sub> O, MgO, Al <sub>2</sub> O <sub>3</sub> , CaO, ZrO <sub>2</sub> , P <sub>2</sub> O <sub>5</sub>	10 to 10.5

**Table 1:** Properties of the materials according to the manufacturer's data used in this study

Group	Abrasive	Working distance	Working time
A	No sandblasting	-	-
B	Al <sub>2</sub> O <sub>3</sub> , SiO <sub>2</sub> 30 µm Co-Jet pre-sintered treatment	1 cm	15 sec
C	Al <sub>2</sub> O <sub>3</sub> 50 µm pre-sintered treatment	1,5 cm	15 sec
D	Al <sub>2</sub> O <sub>3</sub> 110 µm pre-sintered treatment	1,5 cm	15 sec
E	Al <sub>2</sub> O <sub>3</sub> , SiO <sub>2</sub> 30 µm Co-Jet post-sintered treatment	1 cm	15 sec

**Table 2:** Different treatment of the groups A to E.

Group	Abrasive	MTBS (MPa)	Failure Pattern
A	-	17,44 (14,03)	Cohesive 13% Mixed 60% Adhesive 27%
B	Al <sub>2</sub> O <sub>3</sub> , SiO <sub>2</sub> 30 µm Co-Jet pre-sintered treatment	20,9 (11,7)	Cohesive 23% Mixed 70% Adhesive 7%
C	Al <sub>2</sub> O <sub>3</sub> 50 µm pre-sintered treatment	21,28 (15,19)	Cohesive 27% Mixed 65% Adhesive 8%
D	Al <sub>2</sub> O <sub>3</sub> 110 µm pre-sintered treatment	23,99 (16,83)	Cohesive 33% Mixed 46% Adhesive 21%
E	Al <sub>2</sub> O <sub>3</sub> , SiO <sub>2</sub> 30 µm Co-Jet post-sintered treatment	26,79 (14,8)	Cohesive 29% Mixed 52% Adhesive 19%

**Table 3:** Micro tensile bond strength ( $\mu$ TBS) and percentage of failure mode of the different groups.

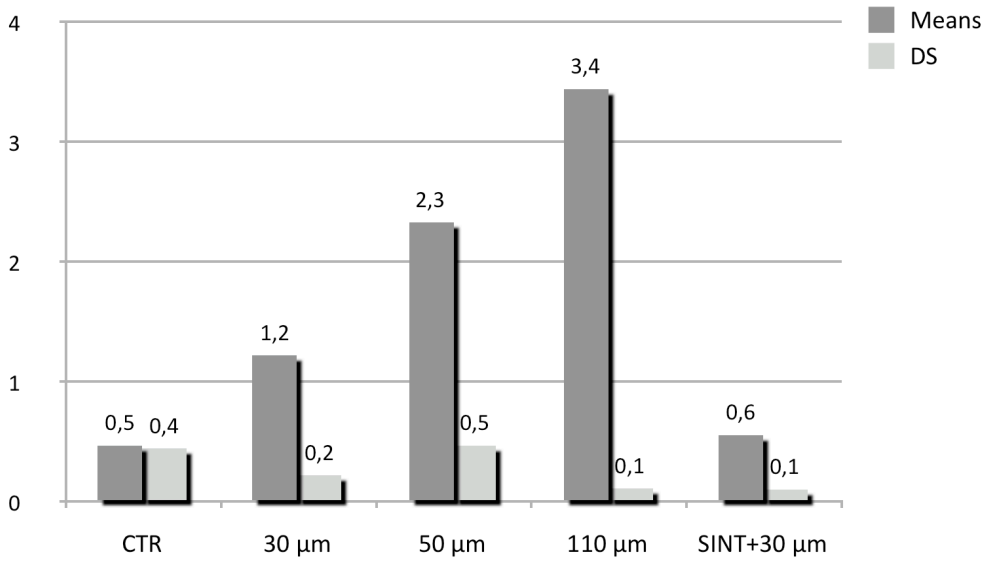


**Figure 1.** Surface roughness (Ra) expressed in micron.

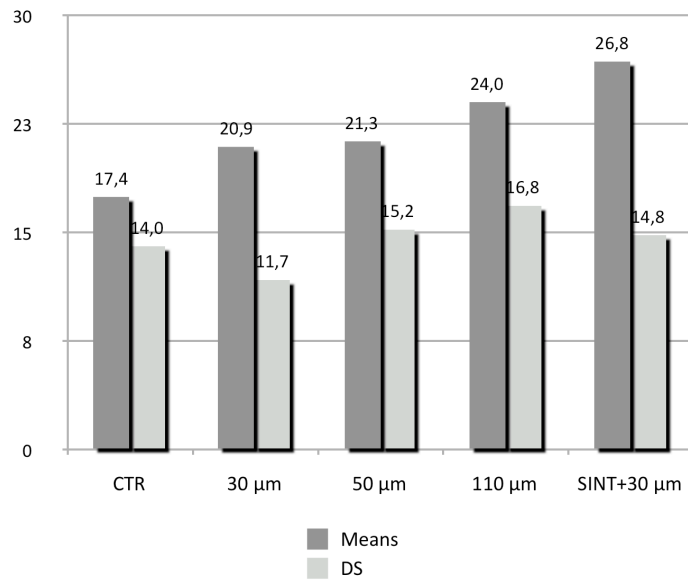
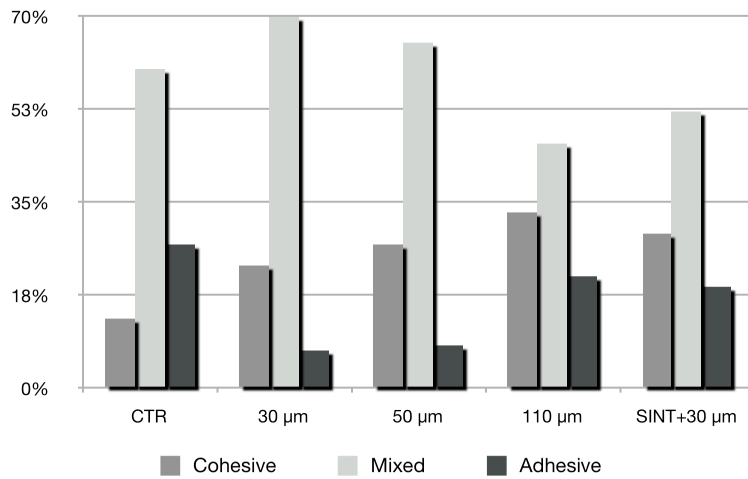


**Figure 2.** Micro tensile bond strength ( $\mu$ TBS) expressed in



MPa.

**Figure 3.** Percentage of failure mode of the different groups.

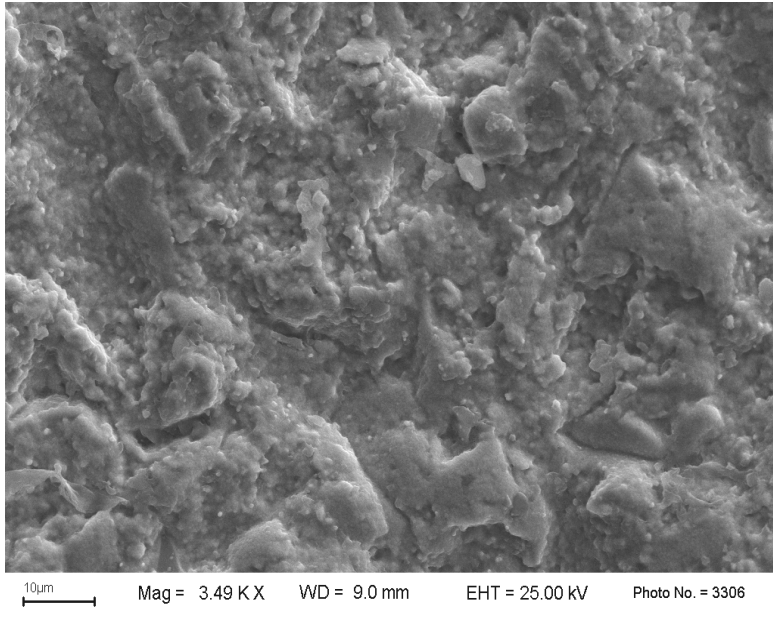


**Figure A.** SEM micrograph of the zirconia surface, group B.

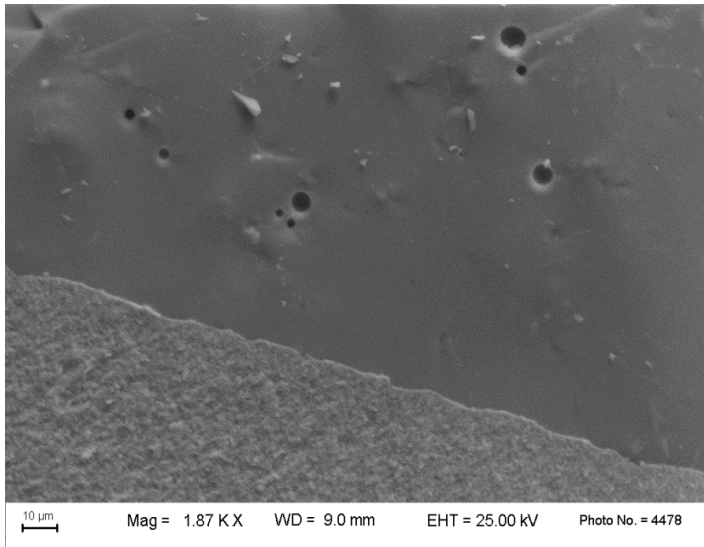


**Figure B.** SEM micrograph of the zirconia surface, group C. The darker particles, arrowed, is alumina.

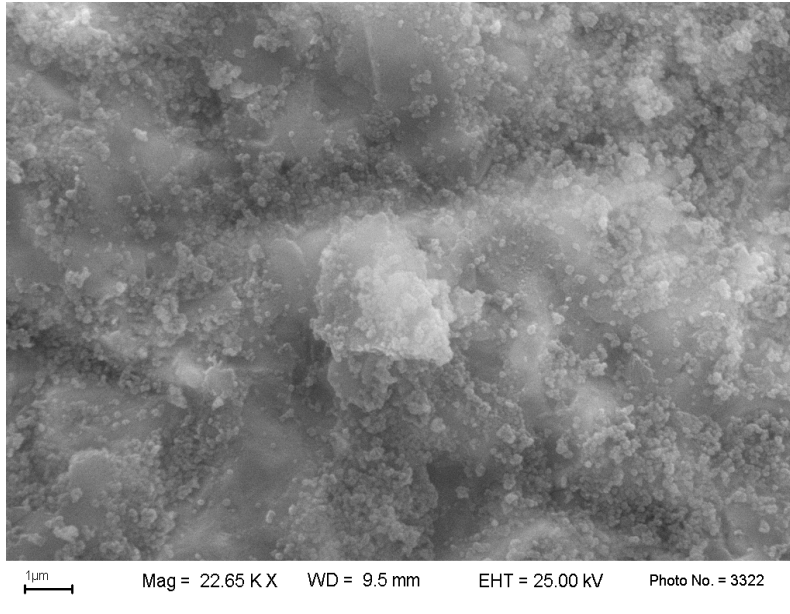


**Figure C.** SEM micrograph of the zirconia surface, group D. The several light particles are rich in silicon.

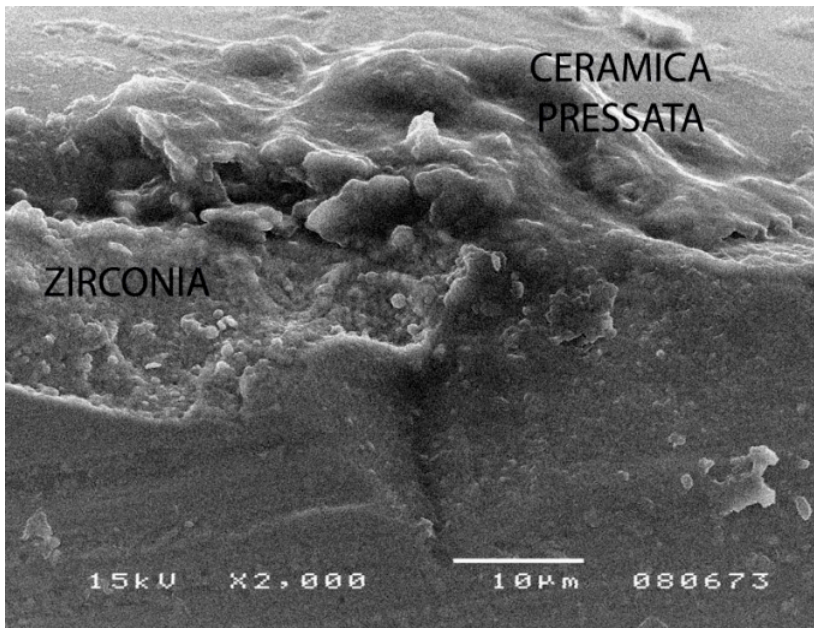


**Figure D.** A fractured microbar showing exposed zirconia crystal

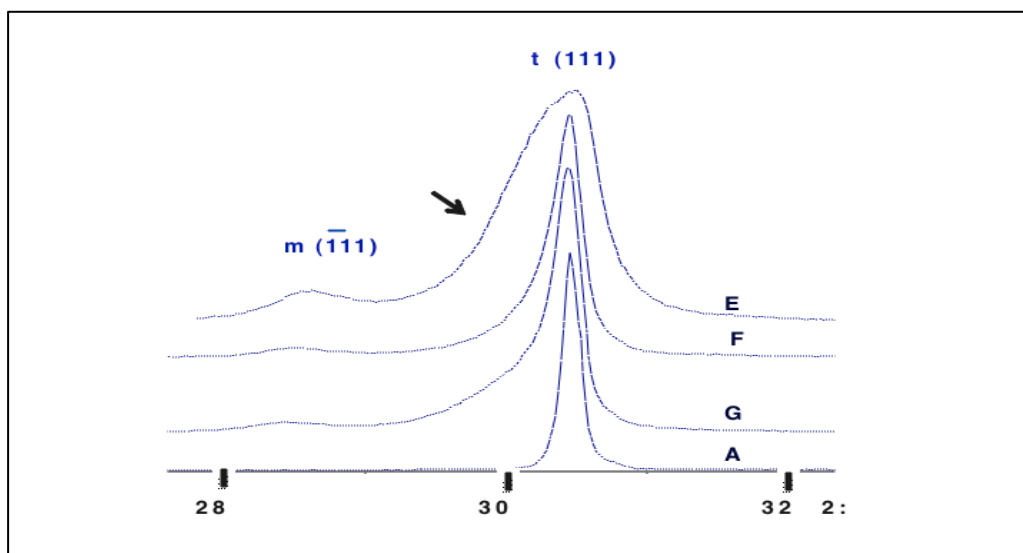


**Figure E** – X-ray diffraction patterns of the control sample (A) and samples E–G, the surfaces of which were treated with 110-, 50-, and 30- $\mu\text{m}$  abrasive particles, respectively. Arrow indicates the hump.

## References

- [1] Raigrodski AJ. Contemporary materials and technologies for all-ceramic fixed partial dentures: A review of the literature. *J Prosthet Dent* 2004;**92**:557 - 562.
- [2] Kansu G, Aydin AK. Evaluation of the biocompatibility of various dental alloys: Part I—Toxic potentials. *Eur J Prosthodont Restor* 1996;**4**:129 - 136.
- [3] Kansu G, Aydin AK. Evaluation of the biocompatibility of various dental alloys: Part 2—Allergenic potentials. *Eur J Prosthodont Restor Dent*. 1996;**4**:155 - 161.
- [4] Blatz MB. Long-term clinical success of all-ceramic posterior restorations. *Quintessence Int*. 2002;**33**:415–426.
- [5] Oguri T, Tamaki Y, Hotta Y, Miyazaki T. Effect of a convenient silica-coating treatment on shear bond strengths of porcelain veneers on zirconia-based ceramics. *Dent Mater J*;**31**:788 - 96.
- [6] Aboushelib MN, de Jager N, Kleverlaan CJ, Feilzer AJ. Microtensile bond strength of different components of core veneered all-ceramic restorations. *Dent Mater* 2005;**21**:984 - 91.

- [7] Aboushelib MN, DDS, Cornelis J, Kleverlaan, Feilzer AJ. Microtensile Bond Strength of Different Components of Core Veneered All-Ceramic Restorations. Part 3: Double Veneer Technique. *J Prosthodont*; 2008;**17**: 9 - 13.
- [8] Isgro G, Feilzer AJ. The influence of the veneering porcelain and difference surface treatments on the biaxial flexural strength of a heat-pressed ceramic. *J Prosthet Dent* 2004;**90**: 465 - 73.
- [9] Sailer I, Fehér A, Filser F, Gauckler LJ, Lüthy H, Hämmerle CHF. Five-year clinical results of zirconia frameworks for posterior fixed partial dentures. *Int J Prosthodont* 2007;**20**: 383 - 8.
- [10] Sailer I, Fehér A, Filser F, Lüthy H, Gauckler LJ, Schärer P, Hämmerle CHF. Prospective clinical study of zirconia posterior fixed partial dentures: 3-year follow-up. *Quintessence Int* 2006; **37**: 41 - 49.
- [11] Kim BK, Bae HE, Shim JS, Lee KW. The influence of ceramic surface treatments on the tensile bond strength of composite resin to all-ceramic coping materials. *J Prosthet Dent* 2005;**4**:357 - 62.
- [12] Fischer J, Stawarczyk B. Effect of zirconia surface treatments in the shear strength of zirconia/veneering ceramic composites. *Dent Mater* 2008;**3**:448 - 54.
- [13] El Zohairy AA, De Gee AJ, de Jager N, Ruijven LJ, Feilzer AJ. The influence of specimen attachment and dimension on the microtensile strength. *J Dent Res* 2004; **83**:420-4.
- [14] Al-Dohan HM, Yaman P, Dennison JB, Razzoog ME, Lang BR. Shear strength of core-veneer interface in bi-layered ceramics. *J Prosthet Dent* 2004; **91**:349-55
- [15] Ayad MF, Fahmy NZ and Rosenstiel SF. Effect of surface treatment on roughness and bond strength of a heat-pressed ceramic. *J Prosthet Dent* 2008;**2**:123-130.
- [16] Advanced technical ceramics. Monolithic ceramics. General and textures properties. Part 4: Determination of surface roughness. The European Standard EN 623-4:2004.
- [17] Aboushelib MN, Kleverlaan CJ, Feilzer AJ. Effect of Zirconia Type on Its Bond Strength with Different Veneer Ceramics. *J Prosthodont* 2008;**17**:401 - 408.
- [7] Burke FJ, Flemming GI, Nathanson D, Marquis PM. Are adhesive technologies needed to support ceramics? An assessment of the current evidence. *J Aesthet Dent* 2002;**4**:7 - 22.
- [18] Valandro LF, Della Bona A, Bottino MA, Neisser MP. The effect of ceramic surface treatment on bonding to densely sintered alumina ceramic. *J Prosthet Dent* 2005;**93**:253 - 9.
- [19] Sun R, Suansuwan N, Kilpatrick N, Swain M. Characterisation of tribochemically assisted bonding of composite resin to porcelain and metal. *J Dent* 2000;**28**:441-5.
- [20] De Oyahue RC, Monticelli F, Toledano M, Osorio E, Ferrari, Osorio R. Influence of surface treatments and resin cement selection on bonding to densely-sintered zirconium-oxide

ceramic. *Dent Mater* 2009;**2**:172 - 9.



**CHAPTER 5**

**Adhesion mechanisms at the interfaces between Y-TZP and veneering ceramics**

## **5.1 Introduction**

Due to better mechanical properties of Yttria-stabilized tetragonal zirconia (Y-TZP) compared with other polycrystalline ceramics such as alumina; the use of this framework material has been increasingly on dental practice. The most important characteristics of this material are high flexural strength and fracture toughness, and the capacity of phase transformation from tetragonal to monoclinic ( $t \rightarrow m$ ), which results in a volumetric increase preventing crack propagation [1-3].

Despite all qualities of this material, several authors have been reported clinical failures mainly because chipping of the veneering porcelain [4]. A recently literature review, which evaluated the clinical studies published between 1999 and 2009 and with 330 fixed partial dentures or crowns made with zirconia framework, revealed that in 41 cases was detected chipping of veneered ceramics, being the most frequently complication type occurred and reflecting as a 5 year-complication-free rate of 79.44% [5].

Several authors attempt to explain the causes of these failures and many hypotheses are raised, such as different thermal-expansion coefficients of zirconia and veneering ceramics [6-7] or the problem of residual stress that may occur during preparation procedures combined with contact-induced cracking [8-9].

In order to enhance the bond strength between zirconia and veneering porcelain and, consequently, reduce the incidence of chipping during the life of prostheses, various procedures have been proposed. The surface treatment of zirconia before veneering process is one of the means to increase bonding area and, thereby, increase the bond strength between the two materials. Another tested procedure is the tribochemical silica coating and silanization, where the zirconia is sandblasted with silica modified aluminum oxide particles causing

the incorporation of silica on the ceramic surface and, then a silane is applied linking the silica of the zirconia surface with veneer porcelain [10].

There are also works that proposed the use of a liner between zirconia and veneering porcelain. Aboushelib et al. conducted a study comparing the aluminum oxide sandblasting of zirconia combined or not with the application of liner and their results showed that, independent of veneering porcelain type, this layer can promote delamination of the porcelain, principally when press-on ceramic is used [11].

Furthermore, most of studies tested the adhesive strength of veneered zirconia by means of microtensile or shear. But is also important analyze the phase transition ( $t \rightarrow m$ ) of zirconia, since it can be stimulated by the mechanical treatment of zirconia or even because the technical application of veneer ceramics [12].

Based on the literature and seeking a way to reduce the chipping occurrence of veneered zirconia, the objective of this study was to evaluate the use of a liner combined or not with the silica coating sandblasting of zirconia, assessing the fracture resistance, phase composition and SEM observation. The objective of this study was to evaluate the Adhesion mechanisms at the interfaces between Y-TZP and veneering ceramics.

## **5.2 Material and Methods**

Thirty-two specimens of a commercial zirconia (Y-TZP) (Lava Frame 61mm blocks; 3M ESPE, Seefeld, Germany) were cut from presintered blocks with a low speed diamond blade (MDS100, Norton, USA) connected to a special device; the dimensions of the resulting presintered specimens were 7.2 mm height, 9.2 mm width, and 9.2 mm length. In order to assure the same starting roughness, a surface treatment with 3 steps of polishing paper (600-800-1000grit) was performed for all the specimens. Before sintering, the specimens of each group were divided between the ones that had to be tested after fracture (-F specimens) and the ones that has to be observed after mirror finishing (-M specimens). For these latter, with the aims to easily induce crack, two wedge-shaped incisions were performed on the surfaces, one obtained in the zirconia surface before sintering and the opposing one obtained in the veneering ceramic, after its application. At the end, the first sintering were performed (Lava Therm, 3M ESPE) following manufacturer's instructions. After randomly dividing into 4 groups, the zirconia specimens were veneered with a layerable ceramic (Lava Ceram Overlay Porcelain, 3M ESPE), with different intermediate steps, as reported in Table I. For the specimens of group A, the zirconia base was directly veneered, without the application of framework modifier. The zirconia samples of the group B were coated with the framework modifier provided by the manufacturer (Framework Modifier, 3M ESPE) and fired as manufacturer's recommendation before the final veneering. The zirconia samples of the group C were sandblasted with 30 $\mu$ m SiO<sub>2</sub>-coated Al<sub>2</sub>O<sub>3</sub> (Cojet, 3M ESPE) with a pressure of 2 bars, at a distance of 15mm for 15 seconds; subsequently they were veneered without the application of modifier layer. Group D specimens were both sandblasted and layered with the framework modifier before veneering. The final veneering sintering, for all the

samples, followed the manufacturer's instructions, that foresee a firing at 850°C for 1 minute.

In Figure 1, the -F and -M specimens, as appeared after the final sintering step, are shown.

The analysis of the interface were conducted both on polished and fractured samples, after the final sintering. The first ones were obtained by embedding in a polyester resin the -M subgroup specimens; then the sides with the interface were mirror finished in a bench grinder polisher machine (LECO Co., VP-150, USA). For the second ones, the -F subgroup specimens were easily fractured, with the aid of the two wedge-shaped incisions.

The average roughness values,  $R_a$ , of the zirconia surfaces, in both the as fired and after the Coject treatment, were measured by using a roughnessmeter (Hommel Tester, T2000, Germany), according to the test method recommended in the standard EN 623-4 (European Standard EN 623-4, Advanced technical ceramics - monolithic ceramics-general and textural properties - Part 4: Determination of surface roughness, 1993).

The phase fraction amounts of zirconia were evaluated by X-rays diffraction technique (XRD), with the use of a diffractometer (Philips PW 3830; Netherlands), with  $CuK\alpha$  radiation (0.02° step-scan, 10s per step). Zirconia diffraction peaks were deconvoluted by using a Lorentz function in order to obtain the integral breadth. The monoclinic phase fraction of the zirconia was calculated using the Garvie and Nicholson method [13].

The microstructure of the surface and the interfaces between the two ceramics was analysed by using a scanning electron microscope (SEM, Zeiss EVO 40, Germany) equipped with an energy-dispersive X-ray analyser (EDS, Inca, Oxford Instruments, UK), after gold sputtering. The EDS spectra at the interface were acquired by using an acceleration voltage of 10kV with an acquisition time of 150 of live second per point. The observations have been

repeated on at least for 10 times, the more meaningful micrographs are reported in the present study.

Table I – Grouping and treatments characteristics for the tested samples.

Group	Zirconia	Surface condition before veneering		Veneering
A	Lava	--	--	Lava Ceram
B	Lava	--	framework modifier	Lava Ceram
C	Lava	Cojet pretreatment	--	Lava Ceram

### 5.3 Results

The microstructural changes, induced on the zirconia surface by the Coject treatment, were assessed by means of both the techniques XRD and SEM. The zirconia crystalline phases, existing in the pre-sintered condition, are tetragonal and monoclinic (3 wt%) phases, as detected by the XRD analysis. After the first sintering step, in the untreated zirconia surfaces, samples of groups A and B before the veneering step, only peaks of the high temperature phases (tetragonal and cubic) were detected without any diffraction peaks of monoclinic phase. After the impact with the erosive particles of the Coject treatment, monoclinic phase is present in an amount of 5 wt%.

The surface average roughness value, for the differently treated zirconia surfaces, presents only a slight increase after the Coject treatment, passing from the  $0.36\pm 0.14$   $\mu\text{m}$  of the as fired condition to  $0.42\pm 0.05$   $\mu\text{m}$  after the erosive treatment. The morphological features variations induced by the erosive treatment were also analysed. The sintered zirconia surface, corresponding to the substrates for samples A and B (Fig. 2a), before the application of the veneering ceramic, even if rough, does not present cracks. After the Coject treatment, the zirconia surface, corresponding to the substrates of samples C and D (Fig. 2b, c), is characterised by the presence of some cracks of reduced dimension. In addition, the surface is covered by very small loose particles, well adhering at the surface (Fig. 2c), they correspond to residues of the impacting erosive particles, because the EDS analyses revealed in them the presence of silicon and aluminium.

The morphological analysis of the polished cross sections of the samples after the final sintering step, belonging to all the groups samples, clearly shows a well defined interface zirconia-veneering ceramic (Fig. 3). The interfaces in the samples of the A and C groups, without the application of the framework modifier, are characterized by the presence of round porosities opening in the

ceramic layer and micro detachments (Fig. 4a, c). Differently, the zirconia-veneering ceramic interfaces in the samples of the B and D groups, with the framework modifier layer, present a rather well continuous contact between the two different materials (Fig. 4b, d). No detachments were observed, only rather small pores in the ceramic layer, essentially far from the interface.

Different punctual micro-analysis were performed in the contact areas zirconia-veneering ceramic, on the cross section of the samples of all groups. In particular, many EDS spectra were collected starting from the interfaces and moving toward the inner part both of zirconia and ceramic veneer layers, at distances of about 500nm, 1 $\mu$ m and 5 $\mu$ m. These analysis were repeated almost 3 times in different parts of the interfaces to have sound results. In addition, the chemical analysis were performed, by EDS, on the surface of the ceramic veneer, to assess the possible presence of zirconium that could affect the analysis at the interface. The result, reported in Table II, shows the absence of this element in the bulk of the ceramic veneer layer.

Table II - Chemical analysis of the ceramic veneer

Oxides	Na <sub>2</sub> O	Al <sub>2</sub> O <sub>3</sub>	SiO <sub>2</sub>	K <sub>2</sub> O	CaO	TiO <sub>2</sub>	BaO
Wt%	10.51	12.10	65.62	6.46	2.43	0.65	2.23

For all the four samples groups, the elemental analysis showed the presence of zirconium in the ceramic veneer layer and the elements characteristics of the veneering layer (silicon as main element) in the zirconia layer, till a distance of about 1 $\mu$ m from the interface. At 5 $\mu$ m from the interface both in the zirconia and in the veneering ceramic layers, zirconia and silicon, respectively, amounts were not detectable. In Figure 5, a representative sequence of EDS spectra performed at 500nm and 1 $\mu$ m from the interface both in the ceramic veneering and in the zirconia layers are reported for sample A and D.

To be sure that no elemental interchange due to the polishing operation had affected the results, the interface of fresh fractured surfaces, sample type-F, were analysed, and the results were identical to the previous ones.

## **5.4 Discussion**

In order to clarify the effect of the Coject treatment on the zirconia surface, a preliminary microstructural analysis was carried out on some specimens of sintered zirconia before the veneering step. This kind of erosion treatment does not usually change in a dramatic way the surface roughness [14] and for the present study too, only a slight increase in the average roughness value has been detected, while a more meaningful morphological features and crystalline phases variation was observed.

As detected by the XRD analysis, the first sintering step, the sintering of the zirconia alone, allowed to transform the small amount of residual monoclinic phase, still existing in the presintered (as received) material, in a such way that only the high temperature phases (tetragonal-cubic) are present. The impact with the erosive particles of the Coject treatment causes a certain amount of stress induced tetragonal to monoclinic phase transformation, in fact about 5wt% of monoclinic phase has been detected. The erosion action of the ceramic particles, constituted by silica coated alumina, this latter a harder material than zirconia [15], causes a mechanical stress able to induce the phase transformation of the metastable tetragonal phase into the monoclinic one [16]. This phase transformation is associated to an increase of volume, about 4%, and a shear strain, about 7% both ones develop a compressive residual stress on the zirconia surface, often associated to widespread cracks network, if the intrinsic strength of the material is overcome, as here observed on the zirconia surfaces[17], corresponding to the substrates of samples C and D (Fig. 2b, c). Without the Coject treatment, cracks are not present on the zirconia surface, substrates for samples A and B (Fig. 2a).

From the morphological analysis of the cross sections of the zirconia-veneering ceramic, it is evident the effect of the presence of the framework modifier layer, that, changing the chemical surface conditions at the interface, allow to obtain

interfaces characterized by a rather well continuous contact between zirconia and veneering ceramic, samples of the B and D groups (Fig. 4b, d). Where it has not been applied, samples of the A and C groups, the adhesion is poor, micro detachments and several round porosities, opening in the ceramic layer, are observed (Fig. 4a, c). The present results testify as the application of the modifier layer is able to better decrease the wettability of the zirconia surfaces, differently by the use of the ceramic veneer alone, so to allow a continuous contact between the two layer and strength their adhesion.

The pore formation, in samples belonging to groups A and C, is due to the evolution of bubbles of gas during the final thermal step. This phenomenon can be due both to the presence of gas trapped among the ceramic particles, that have not the possibility to escape for the viscosity of the viscous mass, and to devitrification phenomena. During the sintering step, in the veneering ceramic the amount of glassy phase decreases and the concentration of the dissolved gas in the decreased glassy phase increases, if the solubility limits are overcome, bubbles of gas can nucleate and grow [18-19]. The presence of the framework modifier layer could be able locally to decrease the viscosity of the viscous mass, favouring the escape of the gas and not allowing the formation of larger pores

Moreover, the formation of large closed pores at the interface is expected to result in weakening of the mechanical strength of the end product.

The several punctual micro-analysis, performed in the contact areas zirconia-veneering ceramic, on the cross section of the samples of all groups, underline as a certain diffusion of the different elements through the interfaces from both the two different layers happened during the firing, for a length of about 500nm.

Theoretical calculations for  $ZrO_2/SiO_2$  interface show as bulk  $ZrO_2$  in contact with bulk  $SiO_2$  and silicon are both interfaces thermodynamically slightly

unstable, with the formation of  $ZrSiO_4$ , with a small negative enthalpy [20-21], even if kinetic effects limit this reaction and the real solubility between the two oxides is low. Despite this low solubility, when glass ceramics are used a good bonding results with a  $ZrO_2$  film, for an effective wetting of the zirconia surface [22]. It is reported that when a glassy phase becomes viscous or liquid at high temperatures, the adhesion and chemical compatibility between glassy phases and base ceramics are generally good [23]. In the present case, during the second firing step, the increase of the temperature causes the glassy silicate phase, existing in the veneering ceramic layer, to become viscous. That is sufficient to promote a strong bonding, as a result from the wetting and dissolution of zirconia along the grain boundaries. Depending from the chemistry of the veneering ceramic layer and the thermal cycle, the thickness of the reaction layer at the interface can be variable. It is to underline as the formation of a glassy phase along grain boundary may destabilize the tetragonal phase, because these sites are yttria segregation points, with a spontaneous phase transformation into the monoclinic phase [24], but also a thermal expansion coefficients difference mismatch could affect the tetragonal stability, which could cause local mechanical stress and decrease the reliability of the final product.

## 5.5 References

- [1] Christel P, Meunier A, Heller M, Torre JP, Peille CN. Mechanical properties and short-term in vivo evaluation of Yttrium-oxide-partially-stabilized zirconia. *J Biomed Mater Res* 1989;**23**:45-61.
- [2] Conrad HJ, Seong WJ, Pesun IJ. Current ceramic materials and systems with clinical recommendations: a systematic review. *J Prosthet Dent* 2007;**98**:389–404.
- [3] Denry I, Kelly JR. State of the art of zirconia for dental applications. *Dent Mater* 2008;**24**:299–307
- [4] Wittneben JG, Wright RF, Weber HP, Gallucci GO. A systematic review of the clinical performance of CAD/CAM single-tooth restorations. *Int J Prosthodont* 2009;**22**:466-71.
- [5] Sailer I, Gottnerb J, Kanelb S, Hammerle CH. Randomized controlled clinical trial of zirconia-ceramic and metal-ceramic posterior fixed dental prostheses: a 3-year follow-up. *Int J Prosthodont* 2009;**22**:553-60.
- [6] Saito A, Komine F, Blatz MB, Matsumura H. A comparison of bond strength of layered veneering porcelains to zirconia and metal. *J Prosthet Dent* 2010;**104**:247-57.
- [7] Ozkurt Z, Kazazoglu E, Unal A. In vitro evaluation of shear bond strength of veneering ceramics to zirconia. *Dent Mater J* 2010;**29**:138-46.
- [6] Schley J-S, Heussen N, Reich S, Fisher J, Haselhuhn K, Wolfart S. Survival probability of zirconia-based fixed prostheses up to 5 yr: a systematic review of the literature. *Eur J Oral Sci* 2010;**118**: 443-450.
- [7] Saito A, Komine F, Blatz M B, Matsumura H. A comparison of bond strength of layered veneering porcelains to zirconia and metal. *J Prosthet Dent* 2010; **104**:247-257.

- [8] Ozkurt Z, Kazazoglu E, Unal A. In vitro evaluation of shear bond strength of veneering ceramics to zirconia. *Dental Materials Journal*, 2010; 29(2): 138-146.
- [9] Wittneben JG, Wright RF, Weber HP, Gallucci GO. A systematic review of the clinical performance of CAD/CAM single-tooth restorations. *Int J Prosthodont*. 2009 Sep-Oct;22(5):466-71.
- [10] Fischer J, Stawarczyk B, Tomic M, Strub J, Hammerle C. Effect of thermal misfit between different veneering ceramics and zirconia frameworks on in vitro fracture load of single crowns. *Dent Mater J* 2007;26:766-772.
- [11] Aboushelib Moustafa N, Cornelia J Kleverlaan, Albert J. Feilzer. Effect of Zirconia Type on Its Bond Strength with Different Veneer Ceramics. *Journal Prosthodontics* 2008;17:401–408.
- [12] Tholey M J, Berthold C, Swain M V, Tiel N. XRD2 micro-diffraction analysis of the interface between Y-TZP and veneering porcelain: Role of application methods. *Dental Materials* (26) 2010:545-552.
- [13] Garvie R.C., Nicholson P.S. Phase analysis in Zirconia systems. *J Am Ceram Soc* 1984;67:119-121.
- [14] Scherrer SS, Cattani-Lorente M, Vittecoq E, de Mestral F, Griggs JA, Wiskott HW. Fatigue behavior in water of Y-TZP zirconia ceramics after abrasion with 30µm silica-coated alumina particles. *Dent Mater* 2011;27:e28-42.
- [15] Chevalier J, Gremillard L. Ceramics for medical applications: A picture for the next 20 years *J Eur Ceram Soc* 2009;29:1245–1255.
- [16] Monaco C, Tucci A, Esposito L, Scotti R. Microstructural changes produced by abrading Y-TZP in presintered and sintered conditions. *J Dent* 2013;41:121-6.

[17] Swain M.V. Limitation of maximum strength of zirconia-toughened ceramics by transformation toughening increment. *J Am Ceram Soc* 1985;**68**: C97-C99.

[18] Boffè M, Pecriaux G, Plumet E. Formation of Bubbles During Devitrification and Remelting of Crystals in Glass. In Symposium on Nucleation and Crystallization in Glasses and Melts, ed. M. K. Reser, G. Smith, H. Insley, American Ceramic Society, 1962, Columbus, Ohio, pp. 47-48.

[19] Davis MJ, Ihinger PD. Heterogeneous crystal nucleation on bubbles in silicate melt, *Am. Mineral.* 1998;**83**:1008-15.

[20] Gutowski M, Jaffe JE, Liu CL, Stoker M, Hegde RI, Rai RS, Tobin PJ. Thermodynamic Stability of High-K Dielectric Metal Oxides ZrO<sub>2</sub> and HfO<sub>2</sub> in Contact with Si and SiO<sub>2</sub>. *Appl Phys Lett* 2002;**80**:1897–99.

[21] Jarvis EAA, Carter EA. Exploiting Covalency to Enhance Metal–Oxide and Oxide–Oxide Adhesion at Heterogeneous Interfaces *J Am Ceram Soc* 2002;**86**:373–86.

[22] Zeng L, Case ED, Crimp MA. The Interfacial Microstructure of Zirconia and MaCor™ Joined Using Spin-On Layers. *Mater Sci Eng* 2001;**307**:74-79.

[23] Santella ML. A Review of techniques for Joining Advanced Ceramics *Am Ceram Soc Bull.* 1992;**71**: 947-54.

[24] Budan J, Matsunaga K, Yamamoto T, Ikuhana Y. Systematic study of grain boundary structure and chemical Analysis of [100] and [111] tilt grain boundaries in yttria-stabilized zirconia. *Microsc Microanal* 2004;**10**:304-5.

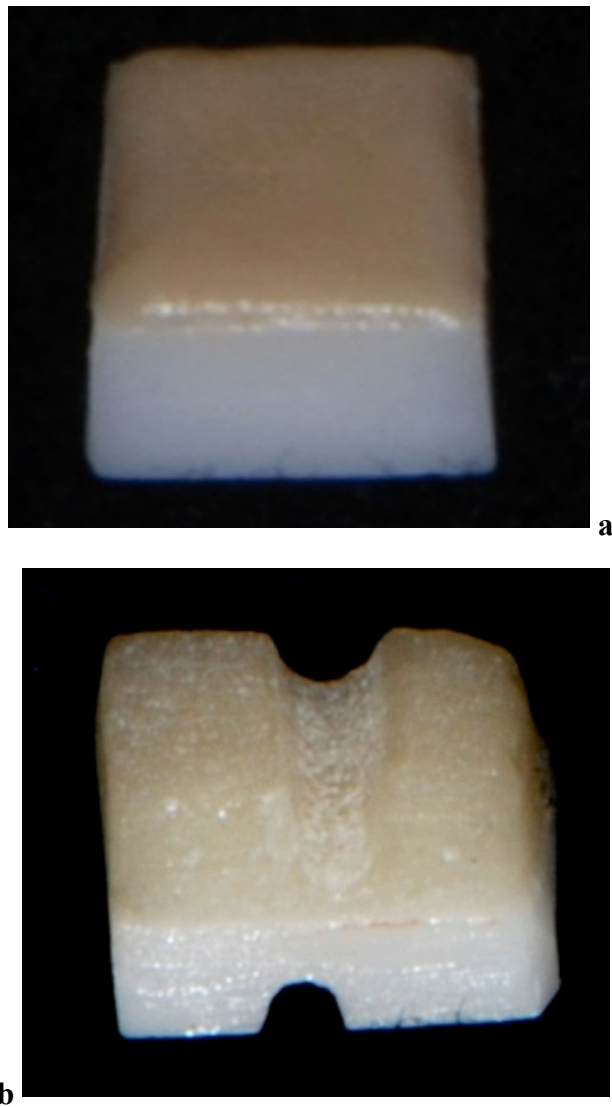
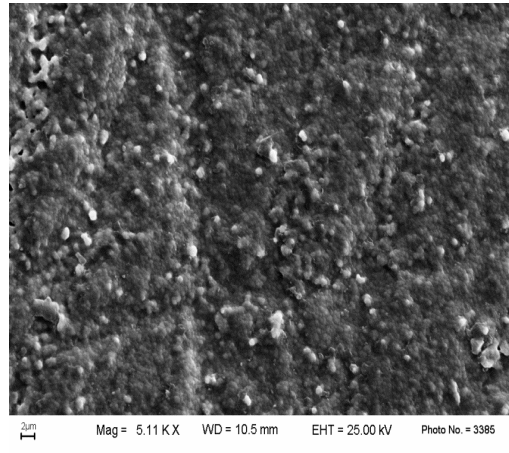
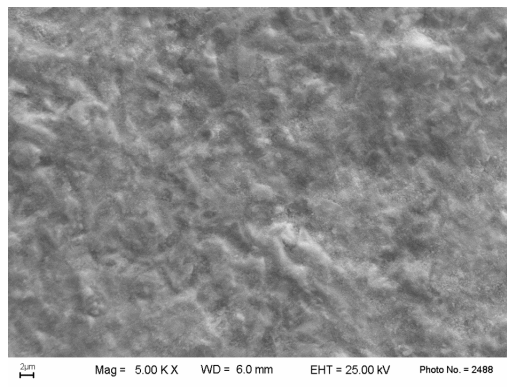


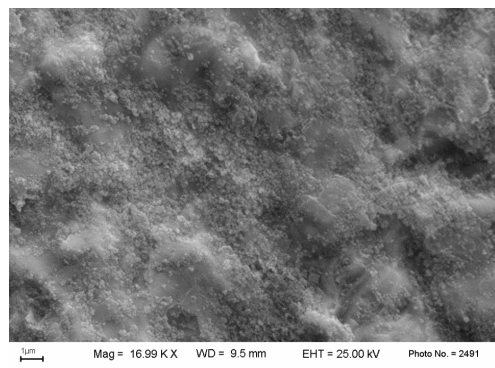
Figure 1 – M-type (a) and F-type (b) specimens after sintering. The veneer layer is at the top.



a)

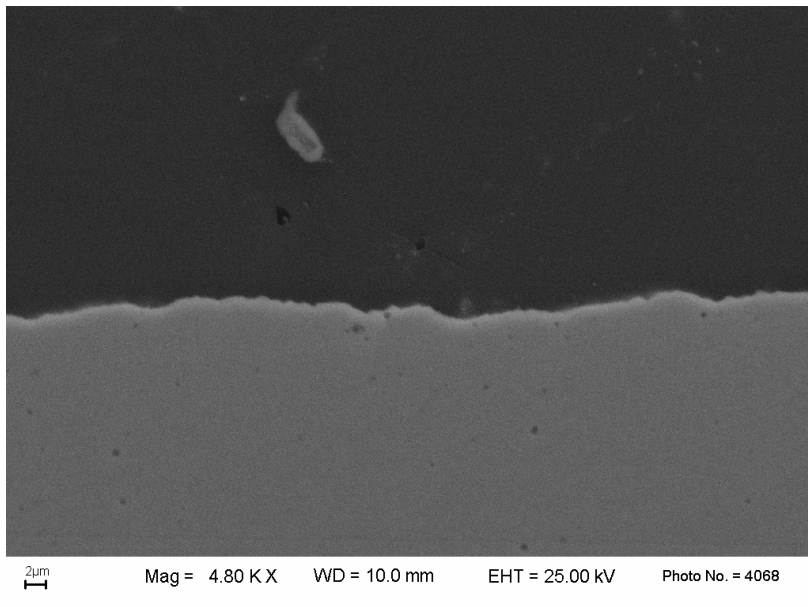


b)

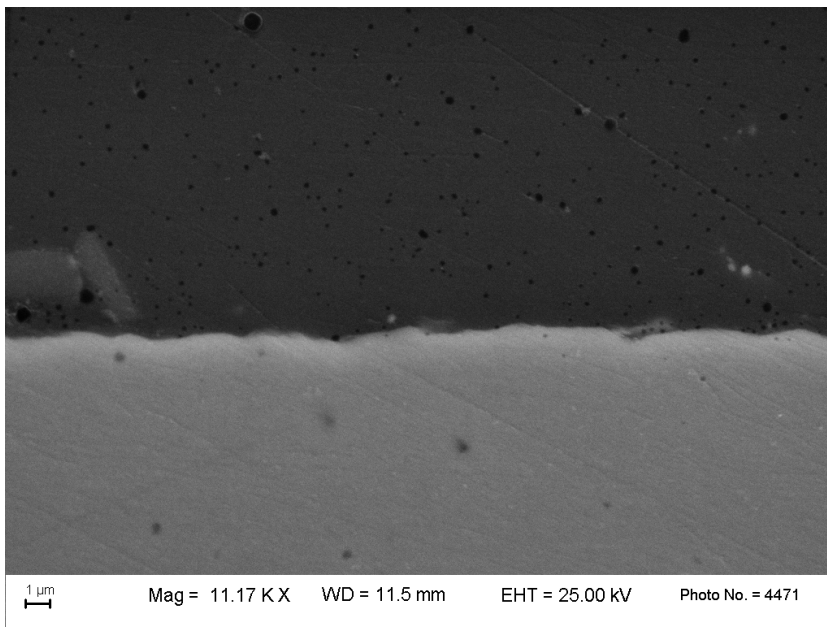


c)

Figure 2 - SEM-SEI micrographs of the surface of the sintered zirconia a) without the Coject treatment, b) and c) after the Coject treatment. In c) the EDS analysis of the fine loose particles adhering onto the zirconia surface report the presence of silicon and aluminum.

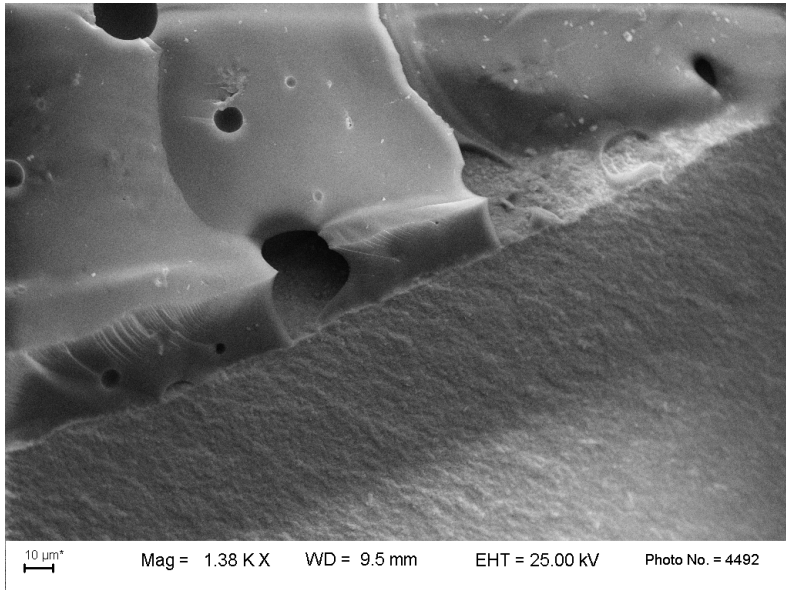


a)

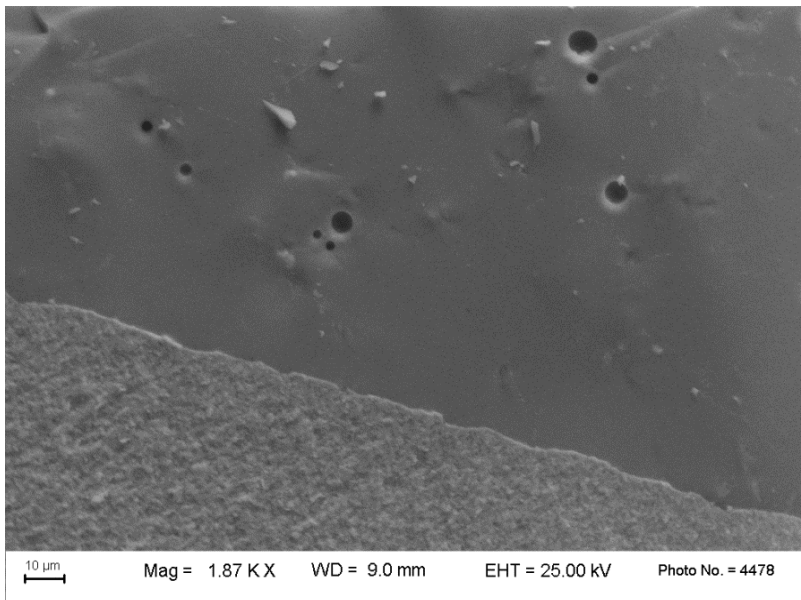


b)

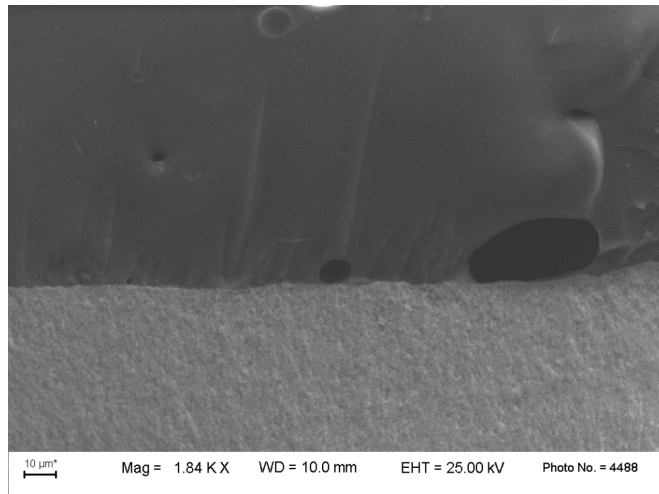
Figure 3 - SEM-SEI micrographs of the cross section of the polished samples of a) A group, b) C group. The zirconia layer is at the bottom, the veneering ceramic at the top of the micrographs.



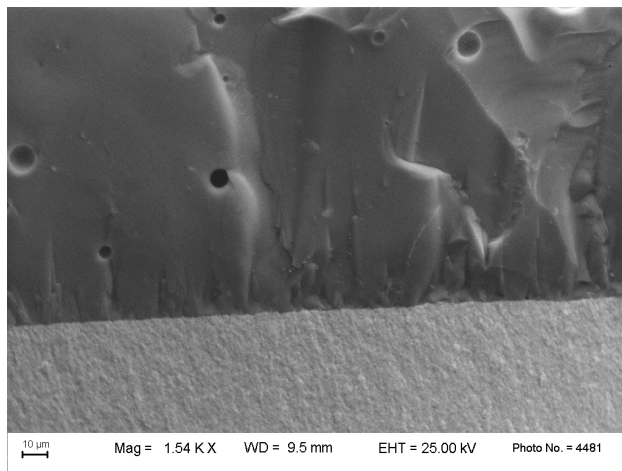
a)



b)

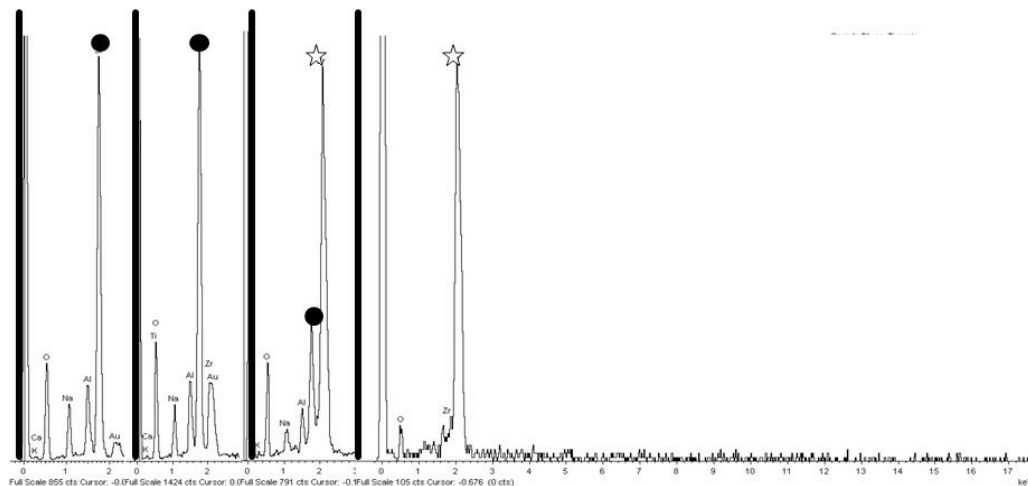
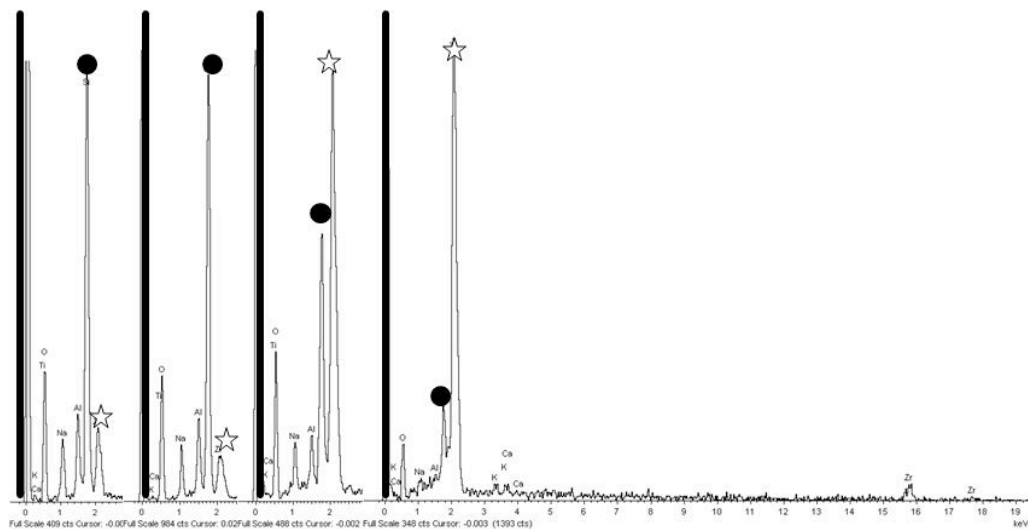


c)



d)

Figure 4 - SEM-SEI micrographs of the cross section of the fractured samples of a) A group, b) B group, c) C group and d) D group. The zirconia layer is at the bottom, the veneering ceramic at the top of the micrographs.



a) b) c) d)

Figure 5 - EDS spectra performed at the interface of sample A (at the top) and sample D (at the bottom). In the ceramic veneer a) at 500nm and b) at 200nm

from the interface. In the zirconia layer c) at 200nm and d) at 500nm from the interface. The peaks are labeled with a black circle for the silicon, with a star for the zirconium.

**CHAPTER 6**

**Marginal adaptation, gap width, and fracture strength of teeth restored with different all-ceramic vs metal ceramic crown systems: an in vitro study.**

## **6.1 Abstract**

**Aims:** This study evaluated marginal adaptation before and after thermomechanical loading, gap width and fracture strength of all-ceramic single crowns, as compared to porcelain-fused-to-metal (PFM).

**Materials and Methods:** Twenty-four extracted premolars were prepared with a round shoulder of 1.0 mm depth. Specimens were restored with zirconia–ceramic (Group 1), lithium disilicate (Group 2) and metal–ceramic single crowns (Group 3). All crowns were luted with a self-adhesive luting agent. Thermal cycling and mechanical loading (TCML) was performed to simulate a 5-year period of oral service. The replica of each sample was observed with a scanning electron microscope (SEM) to evaluate the crown–cement (c–c) and tooth–cement interface (t–c). After TCML, the restorations were loaded with an universal testing machine ( $v = 1 \text{ mm/min}$ , Zwick 1446, Germany,) in the axial direction at an angle of  $135^\circ$ . Medians and 25<sup>th</sup>/75<sup>th</sup> percentiles were calculated and statistical analyses were performed using the Mann–Whitney and Tukey–Kramer tests, at a significance level of  $\alpha = 0.05$ .

**Results:** Before TCML, 100% perfect margins were observed in Groups 1 and 2 at both interfaces. The proportions of perfect margins for Group 3 were 81.6% (c–c) and 69.8% (t–c). After TCML, perfect margins decreased to 91.3% (c–c) and 93.9% (t–c) in Group 1, 94.6% (c–c) and 96.0% (t–c) in Group 2 and 73.5% (c–c) and 53.1% (t–c) in Group 3. The differences among the groups were not significant before ( $P < 0.001$ ) or after TCML ( $P < 0.019$ ). The mean of the gap, measured as arithmetic mean, width between Group 1 ( $165 \mu\text{m} \pm 21$ ), Group 2 ( $97 \mu\text{m} \pm 14$ ) and Group 3 ( $124 \mu\text{m} \pm 24$ ) was significantly different ( $P < 0.001$ ), while that between Groups 2 and 3 was not ( $P = 0.144$ ). The mean fracture strengths were  $654.8 \pm 98.1 \text{ N}$  for Group 1,  $551.3 \pm 127 \text{ N}$  for Group 2 and  $501.43 \pm 110.1 \text{ N}$  for Group 3. During the TCML, four fractures occurred in Group 1, and one each in Groups 2 and 3. The median (25<sup>th</sup>/75<sup>th</sup> percentile) fracture strengths were 643 N (608 N/682 N) for Group 1, 556 N (444 N/651 N) for Group 2, and 496 N (418 N/580 N) for Group 3; Tukey–Kramer analysis showed no significant difference among the groups.

**Conclusions:** Although metal–ceramic crowns showed a tendency towards lower marginal adaption, no statistically significant difference was observed with the all-ceramic systems under the conditions of this experiment. Zirconia restorations showed the highest value of fracture strength than the others two groups. All-ceramic systems could substitute for metal–ceramic crowns, but chipping of veneering ceramics, especially in zirconia-based crowns, should be investigated.

## 6.2 Introduction

Conventional metal–ceramic crowns (MCC) still represent the gold standard for the rehabilitation of endodontically treated teeth. However, the metal framework reduces the translucency, tends to cause a graying of the free gingival margin and may give rise to allergic or toxic reactions [1-2]. The need for aesthetic enhancement and the desire to use metal-free restorative materials have increased the demand for all-ceramic systems, in both the anterior and posterior areas [3]. The rapid improvement of these intrinsically brittle materials, combined with the use of CAD/CAM, has made all-ceramic systems increasingly popular over the past decade. All-ceramic materials show advantageous characteristics, such as translucency, color stability, biocompatibility, low thermal conductivity, high wear resistance, and greater effectiveness of diagnostic radiographs [4].

Among ceramic materials, excellent aesthetic results have been obtained with the introduction of densely sintered aluminum oxide ceramic (Procera AllCeram, NobelBiocare, USA) and lithium disilicate material (IPS Empress II, Ivoclar Vivadent, Liechtenstein); the latter is a thermopressed glass ceramic in which the inclusion of fluoroapatite crystals causes the enhancement of translucency, brightness and light diffusion within the material [5]. Nevertheless, the flexural strength of these materials is 500–650 MPa for alumina [6] and 350–400 MPa for lithium disilicate [7], limiting their application to single crowns or fixed partial dentures (FPDs) in the anterior and premolar regions [8].

CAD/CAM systems have been continuously developed and upgraded in prosthetic dentistry; zirconium oxide, is commonly used for single crowns and FPDs in both the anterior and posterior areas. Zirconia seems to satisfy both aesthetic [9-10] and mechanical needs [11-12] as a core material for all-ceramic restorations. *In vitro* studies of Y-TZP samples have shown values of 900–1200 MPa for flexural strength and values of 9–10 MPa·m<sup>3/2</sup> for fracture toughness [13]. In production, different types of zirconium oxide are used, differing in the concentration of zirconium and yttrium oxide, grain size of the matrix, sintering technique [14], compounds and methods used for coloration [15] and surface treatment [16].

After aesthetic and mechanical properties, marginal adaptation is considered to be one of the most important criteria in clinical success [17]. A high marginal discrepancy leads to cement dissolution and microleakage, which can lead to plaque retention, recurrent caries and periodontal disease [18].

For monolithic lithium disilicate glass, leucite glass, and feldspathic restorations, the adhesive technique is key for successful bonding and reduced marginal discrepancies. Adhesive

cementation has been shown to increase fracture loading and to improve clinical performance [19]. However, no significant difference exists between conventional and adhesive luting with zirconia restorations in terms of retention [20]. The strength of an all-ceramic restoration depends on the characteristics of the material used, thickness of the crown, design of the restoration, core-veneer bond strength and cementation [21]. An *in vitro* study showed that among different zirconia veneering porcelains, the highest microtensile strength was obtained with pressable veneering ceramics [22].

Several *in vivo* studies were conducted with zirconia FPDs demonstrating good clinical performance, but the most commonly reported clinical complication was chipping of the veneering porcelain [23] [24] [25]. The causes of this phenomenon are supposedly insufficient support of the veneering material by the framework design, changes in the ceramic composition versus conventional feldspathic ceramics, mismatch of the coefficient of thermal expansion (CTE), unfavorable surface and heat treatments, and thermal conductivity of the Y-TZP (12 times lower than  $Al_2O_3$ , 99%) [26]. Short-term *in vivo* studies have demonstrated that survival rates for all-ceramic restorations are in the range 88-100% [27]. A recent systematic review [28] of the survival and complication rates of all-ceramic and metal–ceramic single crowns after an observation period of at least 3 years reported that all-ceramic crowns, when used for anterior teeth, showed survival rates of 5 years, comparable with those seen for metal–ceramic crowns. When used for posterior teeth, only the survival rates of densely sintered alumina crowns (Procera technique; 94.9%) and reinforced glass–ceramic crowns (Empress technique; 93.7%) were similar to those obtained for metal–ceramic crowns (95.6%). Furthermore, the survival of InCeram- (90.4%) and glass ceramic-crowns (84.4%) was lower than that of MCC. Based on *in vivo* studies, the choice of material for rehabilitation in the posterior area was difficult because only limited clinical information is available for zirconia–ceramic or lithium disilicate single crowns [29].

The aim of this *in vitro* study was to evaluate marginal adaptation before and after thermomechanical loading, gap width, chipping during loading and fracture strength of all-ceramic single crowns compared with metal–ceramic crowns.

### **6.3 Materials and Methods**

In total, 24 caries-free extracted premolars with completed root growth and nearly identical size were selected for the study. The size was measured at the cement–enamel junction (CEJ) using a digital caliper (Tresna Instruments, USA). First, for all teeth, the points of the maximum

equator on the vestibular and buccal sides were signed. Then, the equidistant point from the previous markers in the mesial and distal sides was individuated. The measurements of the mesio–distal and vestibular–buccal sides were performed using these four points. The inclusion criterion was that the difference of width measured as mesio–distal and vestibular–buccal distance was in the range of 1 mm. The teeth were stored in 0.02% thymol solution for at least 3 months at 4°C before the start of the experiment. All teeth were endodontically treated and the root canal preparations were performed using NiTi rotary instruments (Protaper, Denstply Maillefer, Switzerland) in a low-speed handpiece (Tecnika, Denstply Maillefer) under intermittent rinsing with 5% NaOCl (Nicolor 5, Ogna, Italy). An epoxy sealer (Pulp Canal Sealer, Kerr, USA) and warm gutta percha (Denstply Maillefer) associated with a vertical condensation technique (System B, Sybron Dental, USA) were used as the three-dimensional canal filling system. Provisional restorations of the pulp chamber were made with Cavit (3M ESPE, Germany) before cavity preparations.

The crowns of the endodontically treated teeth were cut off 2 mm coronal to the CEJ. All teeth were restored with fiber posts (FRC Postec, Ivoclar Vivadent), luted using a dual curing composite resin cement (Multilink Automix, Ivoclar Vivadent). A composite build-up was conducted using a bonding system (Adhese, Ivoclar Vivadent) and a dual curing composite (MultiCore HB, Ivoclar Vivadent). The decision to devitalize the samples cut off at the coronal portion at 2 mm to obtain the ferrule effect and reconstruct them with post and resin composite was clinically driven. Based on a minimal intervention approach, all vital teeth are commonly treated with adhesive partial restorations, not complete crowns. All teeth were prepared in a standardized manner: 2 mm of occlusal reduction, 1.5 mm of axial reduction and a round shoulder of 1.0 mm depth with  $\sim 8^\circ$  convergence, placed coronal to the cement–enamel junction. Teeth preparations and finishing were made using diamond burs (881, 8881, 881EF, 8379 Komet, USA), Dura White stones (CN1  $4^\circ$  convergence) and silicon points (Shofu, Japan) under profuse water-spray cooling. Impressions were made with polyester material (Permadyne Penta H + Permadyne Garant; 3M ESPE) with a simultaneous mixing technique, according the manufacturer’s instructions. The teeth were randomly divided into three equal groups for the material and system applied for the restoration using the Random Allocation Software 1.0

### **Laboratory manufacturing process**

Group 1 teeth were restored with all-ceramic crowns, fabricated with a zirconia core and pressable veneering ceramic with specific CTE for zirconia (ZirCad/Zirpress, Ivoclar

Vivadent). The CEREC II CAD/CAM system was used for scanning the gypsum models, designing the framework and milling the e.max ZirCad blocks. The thickness of the core was 0.5 mm according to the manufacturer. For Group 1 specimens, zirconium was prepared and veneered with Zirliner (Ivoclar Vivadent) and placed in brass dies for the veneering process. Glass–ceramic ingots (IPS e.max ZirPress, Ivoclar Vivadent) were heat-pressed according to the manufacturer's recommended parameters (pressing temperature 910°C, pressing time 15 min, pressure 5 bar). After cooling, the crowns were cleaned under running water for 2 min and dried.

Group 2 was restored with a monolithic lithium disilicate glass ceramic material (IPS e.max press, Ivoclar Vivadent). This material was processed in a dental laboratory with Empress pressing equipment. A wax-up of the restoration was made before pressing the ingot of the precrystallized ceramic in the refractory mound created with the final anatomy of the restorations according to the (pressing temperature 910/850°C, pressing time 15 min, pressure 5 bar). Group 3, as a control group, used a conventional metal alloy framework (IPS D.sign 91, Ivoclar Vivadent) and a pressable veneering ceramic specific for metal (IPS In Line PoM, press on metal, Ivoclar Vivadent). The pressing technique of the veneering ceramic was the same as for Groups 1 and 2. The choice of pressable ceramic on metal was made to standardise the application of the veneering ceramic to the other two groups.

### **Luting procedure**

All teeth were cleaned with a polishing brush and a fluoride-free cleaning paste (Nupro, Dentsply, USA), then rinsed with a water spray and dried. Luting was effected with a self-adhesive, dual-curing composite cement (Multilink Sprint, Ivoclar Vivadent). No particle air-abrasion was performed on the inner side of the crowns. The debridements were cleaned with a gentle spray using a small steam-cleaning unit for dental laboratories (Mini Vapor ceramic, Brega). Luting was effected with a self-adhesive, dual-curing composite cement (Multilink Sprint, Ivoclar Vivadent). Cement from the automix syringe was applied into the restoration and then the crown was seated in place and held with a steady pressure. Excess material was removed with a scaler and microbrush and after the setting time, the marginal area of the restoration was finished with silicone polishers (Astropol, Ivoclar Vivadent).

## **Evaluation**

### **Semi-quantitative investigation of marginal adaptation**

The samples were cleaned with rotating nylon brushes (Hawe Neos) and toothpaste (Signal Anti Caries) before making impressions for the replicas. Impressions of the samples were taken using polyvinylsiloxane impressions (President Plus Light-body, Coltène AG, Altstätten, Switzerland), and replicas in epoxy resin (Epoxy VP 1031, Ivoclar Vivadent) were made before and after the artificial aging. The replicated specimens were subjected to a semi-quantitative evaluation of marginal adaptation at a standard 200× magnification with a scanning electron microscope (SEM; Cambridge S240 Leica, Nußloch G, Germany) before and after thermal cycling and mechanical loading (TCML) with a Regensburg device. Analysis of SEM images for the complete circumference was carried out with the Optimas 6.2 system (Optimas Inc., USA). TCML was performed to simulate a 5-year period of oral service with a Regensburg machine (Fig. 1) [parameters: 6000 thermal cycles (5°C/55°C) 2 min each cycle,  $1.2 \times 10^6$  mastication cycles at 50 N with a vertical loading] using an artificial oral environment [30] [31].

The interface between crown and cement and the interface between cement and dentine were examined. The assessment criteria were as follows:

1. Perfect margin (PM): the two adjoining surfaces showed no interruption of the continuous margin and merged into each other, with no difference in level.
1. Marginal gap (MG): the two adjoining surfaces showed slight imperfections with interruptions in continuity, and the formation of gaps or cracks due to loss of cohesion or adhesion.
3. Non-assessable areas (NA): all adjoining areas that did not fit criteria 1 or 2. Overhangs, underfilled margins or dusty part of the sample in which is impossible see PM or MG.

The distance between tooth and restoration ('gap width') was measured only before TCML to control the thickness of the luting composite. The mean of the gap width was randomly measured every 100 micron of the perimeter for a total of approximately 200 site for each of the restoration.

### **Fracture resistance testing after TCML**

After TCML, the restorations were loaded to evaluate the fracture resistance. Each sample was tilted at an angle of 135° with respect to the axial direction of the punch testing in a universal testing machine ( $v = 1$  mm/min, Zwick 1446, Germany) until fracture occurred. To distribute the force evenly and to avoid peaks, a 0.3-mm-thick tin foil was placed between the sample and

the loading die. The failure procedures were evaluated using a stereomicroscope (Olympus SV8, Japan). Types of failure for the restorations were divided into four groups: root fracture, crown fracture, cracking of the veneering ceramic, and chipping of the veneering ceramic.

From all results, means, medians, and 25<sup>th</sup>/75<sup>th</sup> percentiles were calculated and statistical analyses were performed using the Mann–Whitney and Tukey–Kramer tests, at a significance level of  $\alpha = 0.05$ .

## **6.5 Results**

### **SEM marginal adaptation**

The marginal adaptation for all groups is described in Table 1. Before TCML, 100.0% perfect margins were observed in Groups 1 and 2 at both interfaces, crown–cement and tooth–cement. In Group 3, the proportion of perfect margins was 81.6% at the crown–cement interface and 69.8% at the tooth–cement interface.

After TCML, perfect margins in Group 1 decreased to 91.3% (crown–cement interface) and 93.9% (tooth–cement). For Group 2, values of 94.6% (crown–cement) and 96.0% (tooth–cement) were found. Group 3 revealed results of 73.5% (crown–cement) and 53.1% (tooth–cement). The percentage of non-assessable areas before and after TCML were 0%. The influence of TCML on marginal adaptation was not significant ( $P > 0.28$ ). Although the results of Group 3 showed a tendency towards lower marginal adaptation, high variation in the results meant that there was no statistically significant difference among the groups before or after TCML ( $P < 0.019$ ). The mean of the gap width among Group 1 ( $165 \mu\text{m} \pm 21$ ), Group 2 ( $97 \mu\text{m} \pm 14$ ) and Group 3 ( $124 \mu\text{m} \pm 24$ ) was significantly different ( $P < 0.001$ ), while that between Groups 2 and 3 was not ( $P = 0.144$ ). During TCML, four fractures occurred in Group 1, three of them were chipping of the ceramic veneering and one was a delamination of the veneering from the zirconia, and respectively one chipping each for Groups 2 and 3 (Fig. 2; 3a–c). No fractographic but only visual analysis was done after TCML and fracture test.

### **Fracture results**

The mean fracture strengths (Table 2) were  $654.8 \pm 98.1$  N for Group 1,  $551.3 \pm 127$ . N for Group 2, and  $501.4 \pm 110.1$  N for Group 3; The zirconia restorations showed the highest value of the fracture strength respect the metal-ceramic and lithium disilicate crowns. Moreover Tukey–Kramer analysis showed no significant difference among the groups. The median (25<sup>th</sup>/75<sup>th</sup> percentile) fracture strengths were 643 N (608 N/682 N) for Group 1, 556 N (444 N/651 N) for Group 2, and 496 N (418 N/580 N) for Group 3.

## 6.6 Discussion

An *in vitro* study was conducted to examine marginal adaptation and fracture strength of single crowns made of different materials. Specimens restored with both ZirCad/ZirPress and e.max Press materials showed greater marginal adaptation, with a proportion of perfect margins greater than 90%, suggesting adequate clinical performance. No significant difference was seen between Groups 1 and 2 in marginal adaptation before or after the thermal cycling and mechanical loading. The highest percentage of perfect margins was at the cement–tooth interface. The results obtained for Groups 1 and 2 may be explained by the strong bonding created between the luting agent (Multilink Sprint, Ivoclar Vivadent) and the core materials. Recent studies have demonstrated the high retentive strength of all-ceramic systems with resin luting agents [32]. Additionally, some treatments, such as air-abrasion with fine particles at low bars of pressure [33], specific primers containing phosphonic acid monomers purposely prepared for zirconia [34] [35], and phosphate ester monomer [36] could increase the bond and, as a consequence, the marginal adaptation of zirconia restorations. Nevertheless, specimens from Group 3 showed a significantly lower percentage of perfect margins, after and before TCML. As expected for metal–ceramic restorations, the lowest values were found for the tooth–cement interface [37] [38]. The results obtained were probably due to weak bonding between the luting agent and the IPS D.sign 91 alloy.

All samples were subjected to TCML to simulate a 5-year period of oral service [39]. After TCML, the restorations were loaded in the axial direction until failure. The mean fracture strengths of Groups 1 and 2 were not statistically different from that of Group 3, which suggests that all-ceramic crowns are comparable to conventional metal–ceramics restorations in terms of resistance. These results may be expected for Group 1, in which the Y-TZP substructure, with high mechanical properties, allows the production of resistant prosthetic restorations. Potiket et al. [40] also concluded that no significant difference of fracture strength existed between metal–ceramic single crowns and those prepared from alumina or zirconia. The results from the second group are interesting; in these specimens, the monolithic lithium disilicate ceramic material showed a high fracture strength value, not significantly different from that of the control group. Lithium disilicate is a monolithic material, as opposed to the other groups, in which the restoration is with a combination of two materials with completely different mechanical properties. Although the mechanical properties of this material, such as the flexural strength, are lower than zirconia and metal, the results of the fracture strength were comparable with those of the other groups.

During TCML, four failures resulted in Group 1, one in Group 2, and another in Group 3. Visual analysis of the failed specimens showed that the mode of fracture was chipping of the veneering ceramic. Cohesive fracture of the veneering ceramic has been reported to be the failure pattern in different *in vivo* studies with Y-TZP all-ceramic FPDs. The causes of this phenomenon are supposedly due to insufficient support of the veneering material by the framework design, changes in the ceramic composition versus conventional feldspathic ceramics, mismatch of the CTE, unfavorable surface and heat treatments and thermal conductivity of the Y-TZP (12 times lower than Al<sub>2</sub>O<sub>3</sub> 99%) [41] [42].

The matching of the thermal expansion between the porcelain and underlying framework, be it metal or ceramic, is critical for the avoidance of cracking after firing. A great difference in the CTE between core and veneering material results in clinical failure; the failure mode, adhesive or cohesive, depends on whether the porcelain has a higher or lower CTE than the framework [43]. If the porcelain has a much higher CTE than the framework, cracks usually initiate from the surface because of the tensile stresses on cooling that result in chipping. If the CTE of the framework is considerably higher, delamination of the porcelain may occur. An important factor in the chipping of layering materials could be the design of the zirconia framework. A simplistic and not anatomical modelling of the zirconium core can result in inappropriate support for the veneering ceramic [44]. In our study, the high number of chippings in Group 1 may have been due to insufficient support of the veneering ceramic. Currently upgraded software for the design of the zirconia substructure could allow a framework derived from a virtual diagnostic wax-up with a digital cutback procedure. In this way, the thickness of the veneering ceramic could be equally distributed and supported [45]. However, a fractographic analysis is necessary to better evaluate causes and modes of fracture.

Various values have been reported as the maximally acceptable marginal gap width, depending on the type of restoration. Some authors define clinically acceptable values for the marginal gap after cementation to be smaller than 150 µm. Others consider only marginal gap values of less than 120 µm to be within the clinically acceptable limit. Moreover, it has been demonstrated that marginal discrepancies can be affected by the type of finish line, the firing procedure of the veneering porcelain and cement, and the cementation technique. Additionally, it must be underscored that the marginal fit changes before and after luting procedures, as demonstrated by Kern et al. In our study, although the marginal adaptation after loading and thermocycling of two ceramic systems was greater than 90%, the gap width of zirconia-based crowns (165 µm±21) was statistically different from the other groups. This value may have been due to

the CAD/CAM system used (Cerec II). The milling machine has been upgraded to a more precise system (Cerec III). The gap width of lithium disilicate (97  $\mu\text{m}$ ) and metal–ceramic crowns (124  $\mu\text{m}$ ) was similar to the value reported in the previous literature.

### 6.7 Conclusions

Within the limits of this type of *in vitro* study, no significant difference was found in terms of fracture strength between teeth restored with all-ceramic and metal–ceramic single crowns. Although the control group showed a tendency toward lower marginal adaption, no significant difference was detected between all-ceramic and metal–ceramic single crowns. Pressable monolithic lithium disilicate ceramic, in combination with a resin luting agent, can act as a biomimetic of enamel, optimizing the distribution of occlusal stresses at the margin and showing the same value in fracture strength in restorations.

### 6.8 Tables

Crown–cement interface	Group 1 (ZirCad/ZirPress)	Group 2 (IPS e.max press)	Group 3 (IPS D.sign91/PoM)
Before loading	100%	100%	81,6%
After loading	91,3%	94,6%	73,5%
Tooth–cement interface			
Before loading	100%	100%	69,8%
After loading	93,9%	96%	53,1%

**Table 1.** Percentage of perfect margin of the marginal adaptation before and after loading at the crown–cement and tooth–cement interfaces.

	Group 1 (ZirCad/ZirPress)	Group 2 (IPS e.max press)	Group 3 (IPS D.sign91/PoM)
<b>Mean fracture strength</b>	654.8 $\pm$ 98.1 N	551.3 $\pm$ 127. N	501.4 $\pm$ 110.1 N
<b>Median (25<sup>th</sup>/75<sup>th</sup> percentile)</b>	643N (608 N/682 N)	556N (444 N/651 N)	496N (418 N/580 N)

**Tables 2.** Percentage of perfect margin of the marginal adaptation before and after loading at

the crown–cement and tooth–cement interfaces.

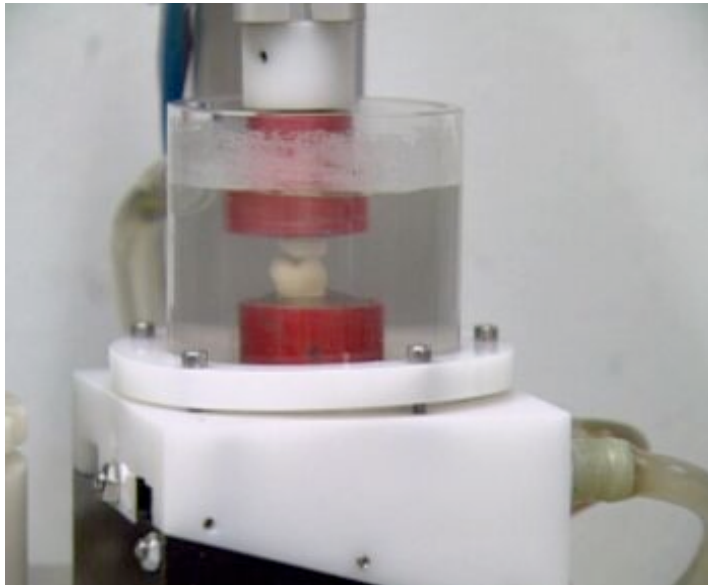
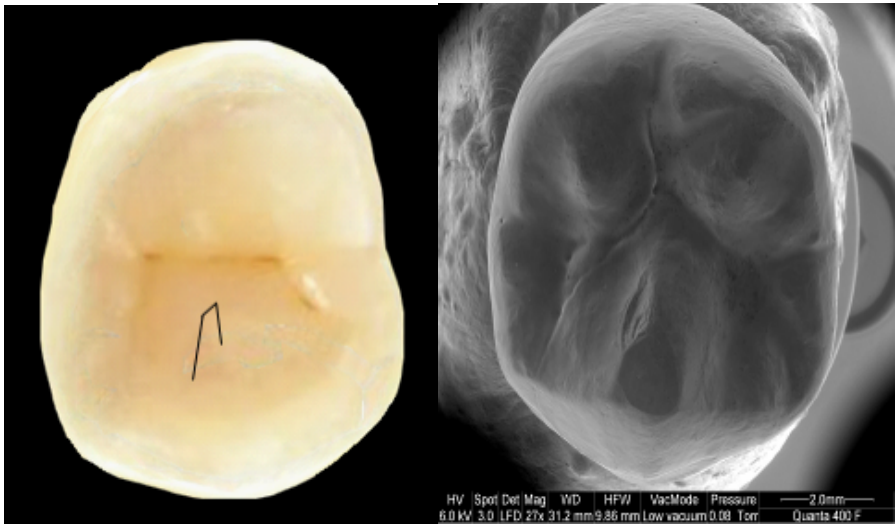


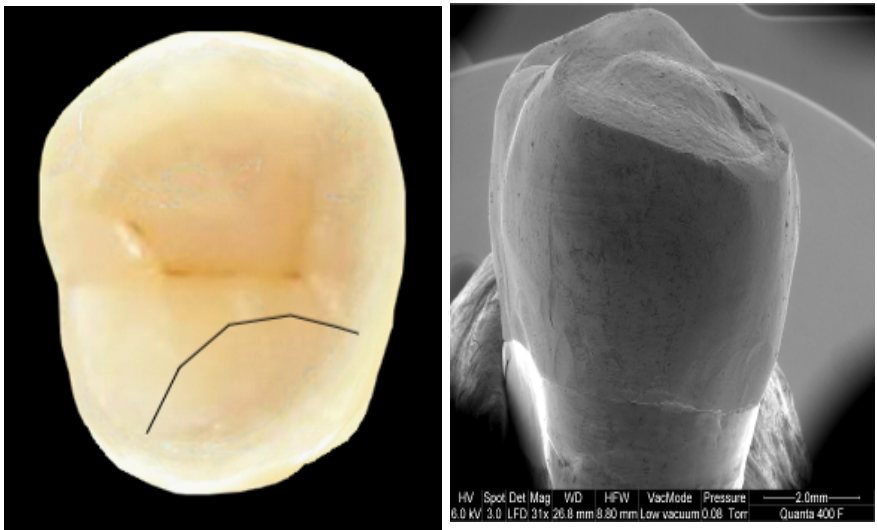
**Figure 1.** A sample in the Regensburg device for a thermal cycling and mechanical loading (TCML) to simulate a 5-year period of oral service.



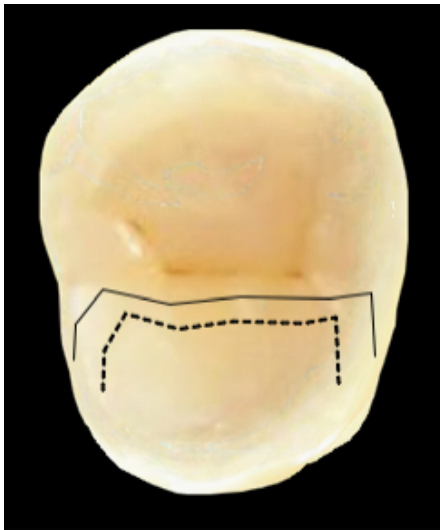
**Figure 2.** Chipping of the veneering of the zirconia/ ceramic during TCML but no zirconia exposition was visible.



A: Small chipping



B: Large chipping



C: Delamination

**Figure 3a-c:** Main fracture patterns. Dotted line: delamination of the veneering ceramic with exposed zirconia; Continuous line: chipping of the veneering ceramic without exposed zirconia.

## 6.9 References

- [1] Kansu G, Aydin AK. Evaluation of the biocompatibility of various dental alloys: Part I—Toxic potentials. *Eur J Prosthodont Restor* 1996;**4**:129–136.
- [2] Kansu G, Aydin AK. Evaluation of the biocompatibility of various dental alloys: Part 2—Allergenic potentials. *Eur J Prosthodont Restor Dent* 1996;**4**:155–161.
- [3] Blatz MB. Long-term clinical success of all-ceramic posterior restorations. *Quintessence Int.* 2002;**33**:415–426.
- [4] Raigrodski AJ. Contemporary materials and technologies for all-ceramic fixed partial dentures: A review of the literature. *J Prosthet Dent* 2004;**92**:557–562.
- [5] Della Bona A., Mecholsky JJ Jr, Anusavice KJ. Fracture behavior of lithia disilicate- and

leucite-based ceramics. *Dent Mater* 2004;**20**:956–962.

[6] Zeng K, Oden A, Rowcliffé D. Flexure tests on dental ceramics. *Int J Prosthodont* 1996;**9**:434–439.

[7] Sorensen JA. The Empress 2 system: Defining the possibilities. *Quintessence Dent Technol* 1999;**22**:153–163.

[8] Zawta C. Fixed partial dentures with an all-ceramic system: A case report. *Quintessence Int* 2001;**32**:351–358.

[9] Toksavul S, Türkün M, Toman M. Esthetic enhancement of ceramic crown with zirconia dowel and cores: A clinical report. *J Prosthet Dent* 2004;**92**:116–119.

[10] Raigrodski AJ. All-ceramic full-coverage restorations: Concepts and guidelines for material selection. *Pract Proc Aesthet Dent* 2005;**17**:249–256.

[11] Coli P, Karlsson S. Precision of a CAD/CAM technique for the production of zirconium dioxide copings. *Int J Prosthodont* 2004;**17**:577–580.

[12] Coelho PG, Silva NR, Bonfante EA, Guess PC, Rekow ED, Thompson VP. Fatigue testing of two porcelain–zirconia all-ceramic crown systems. *Dent Mater* 2009 ;**25**:1122–1127.

[13] Denry I, Kelly JR. State of the art of zirconia for dental applications. *Dent Mater*. 2008;**24**:299–307.

[12] Blatz MB, Sadan A, Kern M. Ceramic restorations. *Compend Contin Educ Dent* 2004;**25**:412-416

[14] Lee YK, Cha HS, Ahn JS. Layered color of all-ceramic core and veneer ceramics. *J Prosthet Dent* 2007;**97**:279–286.

[15] Guazzato M, Quach L, Albakry M, Swain MV. Influence of surface and heat treatments on the flexural strength of Y-TZP dental ceramic. *J Dent* 2005;**33**:9–18.

[16] Rinke S, Hüls A, Jahn L. Marginal accuracy and fracture strength of conventional and copy-milled all-ceramic crowns. *Int J Prosthodont* 1995;**8**:303–310.

[172] Jacobs MS, Windeler AS. An investigation of dental luting cements solubility as a function of a marginal gap. *J Prosthet Dent* 1991;**65**:436–442.

[18] Bindl A, Lüthy H, Mörmann WH. Strength and fracture pattern of monolithic CAD/CAM-generated posterior crowns. *Dent Mater* 2006;**22**:29–36.

[19] Ernst CP, Cohnen U, Stender E, Willershausen B. In vitro retentive strength of zirconium oxide ceramic crowns using different luting agents. *J Prosthet Dent* 2005;**93**:551–558.

Aboushelib MN, de Jager N, Kleverlaan CJ, Feilzer AJ. Microtensile bond strength of different components of core veneered all-ceramic restorations. *Dent Mater* 2005;**21**:984–991.

[20] Aboushelib MN, Kleverlaan CJ, Feilzer AJ. Microtensile bond strength of different components of core veneered all-ceramic restorations. Part II: Zirconia veneering ceramics. *Dent Mater* 2006;**22**:857–863.

[21] Raigrodski AJ, Chiche GJ, Potiket N, Hochstedler JL, Mohamed SE, Billiot S. The efficacy of posterior three-unit zirconium-oxide-based ceramic fixed partial dental prostheses: a prospective clinical pilot study. *J Prosthet Dent* 2006;**96**:237–244.

[22] Sailer I, Fehér A, Filser F, Gauckler LJ, Lüthy H, Hämmerle CH. Five-year clinical results of zirconia frameworks for posterior fixed partial dentures. *Int J Prosthodont* 2007;**20**:383–388.

[23] Vult von Steyern P, Carlson P, Nilner K. All-ceramic fixed partial dentures designed according to the DC-Zirkon technique. A 2-year clinical study. *J Oral Rehabil* 2005;**32**:180–187.

[24] Edelhoff D, Florian B, Florian W, Johnen C. HIP zirconia fixed partial dentures--clinical results after 3 years of clinical service. *Quintessence Int* 2008;**39**:459–471.

Conrad HJ, Seong WJ, Pesun IJ. Current ceramic materials and systems with clinical

recommendations: A systematic review. *J Prosthet Dent* 2007;**98**:389–404.

[25] Pjetursson BE, Sailer I, Zwahlen M, Hämmerle CH. A systematic review of the survival and complication rates of all-ceramic and metal-ceramic reconstructions after an observation period of at least 3 years. Part I: Single crowns. *Clin Oral Implants Res.* 2007;**18** Suppl 3:73–85.

[26] Al-amleh B, Lyons K, Swain M. Clinical trials in zirconia: a systematic review. *J Oral Rehabil.* 2010;**37**:641-652.

[27] Ernst CP, Cohnen U, Stender E, Willershausen B. In vitro retentive strength of zirconium oxide ceramic crowns using different luting agents. *J Prosthet Dent* 2005;**93**:551–558.

[28] Phark JH, Duarte S Jr, Blatz M, Sadan A. An in vitro evaluation of the long-term resin bond to a new densely sintered high-purity zirconium-oxide ceramic surface. *J Prosthet Dent* 2009;**101**:29–38.

[29] Kitayama S, Nikaido T, Takahashi R, Zhu L, Ikeda M, Foxton RM, Sadr A, Tagami J. Effect of primer treatment on bonding of resin cements to zirconia ceramic. *Dent Mater* 2010;**26**:426-432.

[30] Magne P, Paranhos MP, Burnett LH Jr. New zirconia primer improves bond strength of resin-based cements. *Dent Mater* 2010;**26**:345–352.

[31] Mirmohammadi H, Aboushelib MN, Salameh Z, Feilzer AJ, Kleverlaan CJ. Innovations in bonding to zirconia based ceramics: Part III. Phosphate monomer resin cements. *Dent Mater* 2010;**26**:786-792.

[32] White SN, Sorensen JA, Kang SK, Caputo A.A. Microleakage of new crown and fixed partial denture luting agents. *J Prosthet Dent* 1992;**67**:156–161.

[33] White SN, Zhaokun Y, Tom JF, Sangsurasak S. In vivo microleakage of luting cements for cast crowns. *J Prosthet Dent* 1994;**74**:333–338.

[34] Rosentritt M, Behr M, van der Zel JM, Feilzer AJ. Approach for valuating the influence of laboratory simulation. *Dent Mater* 2009;**25**:348–352.

[35] Potiket N, Chiche G, Finger I.M. In vitro fracture strength of teeth restored with different all-ceramic crown systems. *J Prosthet Dent* 2004;**92**:491–495.

[36] Swain MV. Unstable cracking (chipping) of veneering porcelain on all-ceramic dental crowns and fixed partial dentures. *Acta Biomater* 2009;**5**:1668–1677.

[37] Edelhoff D, Florian B, Florian W, Johnen C. HIP zirconia fixed partial dentures--clinical results after 3 years of clinical service. *Quintessence Int* 2008;**39**:459–71.

[38] Anusavice KJ, Dehoff PH, Hojjatie B, Gray A. Influence of tempering and contraction mismatch on crack development in ceramic surfaces. *J Dent Res*.1989;**68**:1182–1187.

[39] Rosentritt M, Behr M, Thaller C, Rudolph H, Feilzer A. -Fracture performance of computer-aided manufactured zirconia and alloy crowns. *Quintessence Int* 2009;**40**:655–662.

[12] Rosentritt M, Steiger D, Behr M, Handel G, Kolbeck C. Influence of substructure design and spacer settings on the in vitro performance of molar zirconia crowns. *J Dent* 2009;**37**:978–983.

[40] Fransson B, Oilo G, Gjeitanger R. The fit of metal-ceramic crowns, a clinical study. *Dent Mater* 1985;**1**:197–199.

[41] Tinschert J, Natt G, Mautsch W, Spiekermann H, Anusavice KJ. Marginal fit of alumina- and zirconia-based fixed partial dentures produced by a CAD/CAM system. *Oper Dent* 2001;**26**:367–74.

[42] Att W, Komine F, Gerds T, Strub JR. Marginal adaptation of three different zirconium dioxide three-unit fixed dental prostheses. *J Prosthet Dent* 2009;**101**:239–247.

[43] Kokubo Y, Ohkubo C, Tsumita M, Miyashita A, Vult von Steyern P, Fukushima S.

Clinical marginal and internal gaps of Procera AllCeram crowns. *J Oral Rehabil* 2005;**32**:526–30.

[44] Bindl A, Mörmann WH. Fit of all-ceramic posterior fixed partial denture frameworks in vitro. *Int J Periodontics Restorative Dent* 2007;**27**:567–75.

[45] Kern M, Schaller HG, Strub JR. Marginal fit of restorations before and after cementation in vivo. *Int J Prosthodont* 1993;**6**:585–591.



**CHAPTER 7**

**Marginal and internal fitting of zirconia-based single crowns made after intraoral digital impression.**

## **7.1 Abstract**

**Objectives:** The aim of this clinical trial was to test the accuracy of single all-ceramic zirconia crowns resulting from digital intraoral impressions with active wavefront sampling technology by measuring the marginal and internal fits of the crowns.

**Materials and Methods:** Thirty-seven teeth (24 anterior, 13 posterior) in fifteen patients were restored with single zirconia-ceramic crowns (Lava/Lava Ceram; 3M ESPE) generated from a digital intraoral scanner (Lava Chairside Oral Scanner; 3M ESPE). Before definitive insertion, silicone replicas were produced for all 37 crowns. The sample was cut in four sections; each section was evaluated in four points: marginal gap, mid-axial wall, axio-occlusal edge and centro-occlusal. A total of 592 measurements (148 for each evaluation point) was examined using stereomicroscopy with a magnification of x50. The Wilcoxon signed rank test was used to evaluate whether there were differences between anterior and posterior values ( $p \leq 0.05$ ).

**Results:** The mean values for each point were: 48.65  $\mu\text{m}$  for the marginal gap, 112.25  $\mu\text{m}$  at the mid-axial wall, 138.25  $\mu\text{m}$  at the axio-occlusal edge of the abutments, and 159.22  $\mu\text{m}$  at the centro-occlusal location. No statistical differences were found between the anterior and posterior group.

**Conclusions:** The marginal and internal fitting values were clinically satisfactory for both anterior and posterior teeth.

**Clinical Relevance:** Zirconia–ceramic crowns obtained from digital intraoral impressions using active wavefront sampling technology could be used single crown restorations with a clinically acceptable fit.

## 7.2 Introduction

All-ceramic restorations are a metal-free alternative with excellent aesthetic and biocompatibility properties [1].

These systems often use the concept of computer-aided design/computer-aided manufacturing (CAD/CAM) for the fabrication of ceramic crowns and fixed dental prostheses (FDPs). This technology has been largely limited to the dental laboratory; today, various systems are available for taking digital intraoral impressions.

The CEREC system (Sirona, Bensheim, Germany) is based on the ‘triangulation of light’ concept, in which the intersection of three linear light beams is used to locate a given point in three-dimensional (3D) space [2]. An opaque powder coating (titanium dioxide) is used to provide uniform light dispersion and enhance the accuracy of the scan [3].

Another available digital-impression technology is based on parallel confocal imaging; it utilises laser and optical scanning to capture the surfaces and contours of the teeth and gingival structures. A commercially available system (iTero; Cadent) can capture 100 000 points of laser light at 300 focal depths of the tooth structure. These focal depth images are spaced approximately 50  $\mu\text{m}$  apart [4-5]. Another currently used digital-impression system was developed around a laser acquisition technology (E4D; D4D Technologies, LLC); it is also capable of model scanning and conventional impression scanning [6].

A digital-impression system based on the principle of active (optical) wavefront sampling was recently introduced (Lava™ Chairside Oral Scanner; 3M ESPE, Seefeld, Germany) [7]. Active wavefront sampling refers to obtaining 3D information from a single-lens imaging system. Three sensors simultaneously capture the clinical situation from different perspectives; 3D surface patches are generated in real time by means of proprietary image processing algorithms using in-focus and out-of-focus information [8]. This should enhance the accuracy of the impression and thus promote an accurate fit of the restoration.

Regarding ceramic restorations, the marginal and internal fits are two of the most important criteria for the long-term success of ceramic restorations, in addition to fracture resistance and aesthetics. A significant space between the tooth and the restoration exposes the luting material to the oral environment, resulting in a more aggressive rate of cement dissolution caused by oral fluids and chemomechanical forces [9]. The consequent micro-leakage may result in inflammation of the periodontal tissues, secondary caries, and subsequent failure of the prosthesis [10-11]. McLean and von Fraunhofer [12] concluded that 120  $\mu\text{m}$  was the maximum tolerable marginal opening [13-14-15]; however, there is no consensus on what constitutes a clinically acceptable maximum marginal gap width. The values reported in the literature have a wide range (50–200  $\mu\text{m}$ ) [16-17-18]. Moreover, there is no standardisation in the methodology used, which makes data comparison difficult [19-20-21-22-23]. Marginal gaps of 1 to 161  $\mu\text{m}$  have been reported in the literature for conventionally fabricated ceramic crowns [24-25]. In contrast, marginal gaps of 17 to 118  $\mu\text{m}$  have been reported for CAD/CAM-fabricated ceramic crowns [26-27-28-29-30-31-32-33-34-35-36]. Larger internal discrepancies may have weakening effects on the ceramic [37]. Even for zirconia core materials, an influence of the cement thickness on radial crack growth has been demonstrated [38-39].

According to the manufacturer of the active wavefront scanner cited above, the high data redundancy resulting from many overlapping pictures together with special image-processing algorithms ensures excellent image quality and, consequently, high accuracy. However, there are few clinical studies on the *in vivo* performance of this intraoral scanner, especially on clinical fitting of the copings [40].

The aim of this clinical trial was to test the accuracy of a digital intraoral impression system with active wavefront-sampling technology by measuring the marginal and internal fits of the zirconia-ceramic crowns that have been generated.

### 7.3 Materials and methods

Fifteen patients with indications for full-coverage restorations were provided with thirty-seven zirconia–ceramic single crown (24 anterior, 13 posterior). The preparation of the abutment teeth for the all-ceramic FDPs was similar to that for metal–ceramic crowns. A distinct chamfer finish line was prepared. The circumferential reduction of the tooth substance was between 1.2 and 1.5 mm, in accordance with the remaining hard tissue. Occlusal reduction was approximately 1.5 mm. All internal edges were rounded to an estimated radius of 0.6 mm. After preliminary preparation, temporary restorations of polymethyl methacrylate (PMMA) resin were placed. The patients were then scheduled for refining of the preparation with small grain-sized diamond burs and Arkansas stone, followed by polishing with a brown amalgam rubber point.

After this stage, two retraction cords of different sizes (Ultrapack, Ultradent Products, South Jordan, Utah, USA) were placed for the final impression. The correct cord sizes were chosen according to each patient’s gingival biotype and sulcus depth; the coronal cord was placed slightly apical to the margin of the preparation. A waiting time of 5 minutes allowed for adequate sulcus expansion; meanwhile, a disposable soft tissue retractor (Optragate; Ivoclar Vivadent, Schaan, Liechtenstein) was placed to retract the cheeks and lips.

The mouth was then rinsed with water and air dried, and a light dusting of the teeth and gingival tissues was performed by a dedicated powder for optical scanning (Lava™ Powder for Chairside Oral Scanner, 3M ESPE) with its own device (Lava™ Sprayer, 3M ESPE). Eventual powdering excess was removed by air spraying.

The coronal cord was then delicately removed, avoiding contact with the abutment; a second small powdering was performed to cover the area of the removed cord. The digital intraoral impression of the quadrant hosting the preparation (Lava™ Chairside Oral Scanner, 3M ESPE) was immediately begun. The preparation area was then marked on a 3D simplified view of the

scan to allow the system to show the 3D high-resolution images of the preparation. The evaluation of these images was necessary to verify the correctness of the impression: total abutment visibility, beyond-preparation scanning, impression of the inter-proximal areas of the adjacent teeth, absence of oral fluids and/or powder excess, etc. If the impression revealed any of these problems, the scan was repeated.

Following the scan approval of the prepared tooth and adjacent teeth, the next step was to powder and scan the opposing arch. The system then required the bite scan, which was acquired by vestibularly scanning the opposing quadrants with the arches in maximum inter-cuspitation. A digital Rx was compiled in a dedicated interface of the scanner in which the restoration type (Lava™ Framework, 3M ESPE) was chosen; the colour indication was given after checking with a colour scale (Vita Classical Shade; Vita Zahnfabrik, Bad Säckingen, Germany). After signing, the scans were immediately sent via the Internet to the dental laboratory, where a technician marked the margins. The file was then sent to the United States, where a dedicated structure performed the digital ditching. The file was then returned for framework designing by the technician and stereolithographic (SLA) model construction in a dedicated manufacturer's structure.

Whereas the preparation margins were detected automatically, the shape of the frameworks could be designed individually. An internal marginal area of at least 0.8 mm was not affected by the spacer setting. The cement gap thickness was set at 30 µm for 0.7 mm; the subsequent value for the residual coronal area of the abutment was 50 µm. The virtual framework was then transformed into machine-readable codes, taking into account the sintering shrinkage. Because semi-sintered zirconia blanks were used, it was possible to mill the frameworks by the use of simple hard metal burs in the milling unit (Lava Form; 3M ESPE). The frameworks could have been coloured in one of seven shades to correspond to each patient's natural tooth colour before the sintering process, which lasted for approximately 7 h, was begun (Lava Therm; 3M ESPE).

The densely sintered frameworks were tried in, and a fit check (Fit Checker Black 1-1 PKG; GC Corporation, Tokyo, Japan) was made. If necessary, the abutment was corrected with a red ring handpiece and a fine cylindrical bur under water-cooling. The final wall thicknesses were checked using a calliper so that the recommended framework dimensions of at least 0.5 mm were retained. The frameworks were then veneered with Lava Ceram by an experienced ceramist. Before glazing, the veneered framework was tried in to check both the proximal contacts and the static and dynamic occlusions, and to adjust them if necessary. After glazing, the crowns and the FPD were luted with a resin-based luting agent (RelyX Unicem Applicap, 3M ESPE).

*-FIT RECORDING-*

Before definitive insertion, silicone replicas were produced for all 37 crowns. To document the internal space of the retainers, a technique similar to that described by Boening et al. [31] and Molin & Karlsson [41] was applied: coping was filled with a light-body silicone (Express II; 3M ESPE, Seefeld, Germany) and placed on the abutment tooth. A cotton roll was placed between the opposing arch and the occlusal surface. The thin silicone layer represented the gap width between the inner surface (inclusively, the crown margin) of the crown and the surface of the abutment tooth. After setting the light-body silicone and removing the coping, the thin silicone film contained in it was stabilised by injecting a more viscous silicone into the retainers, that mimicked the abutment tooth [43]. The replicas could then be removed from the copings. The replicas were cut once along the abutment axis in the mesio–distal direction and once in the bucco–oral direction using a razor blade so that four fragments per abutment were produced.

*-MEASUREMENT PROCEDURE -*

The thickness of the low-viscosity silicone was measured using a microscope (Stemi 2000C; Carl Zeiss, Oberkochen, Germany) at a magnification of  $\times 50$ . The cross-sections were adjusted horizontally on modelling clay to obtain a parallel orientation to the microscope's plate and to achieve a vertical observation angle. The distance was counted in  $\mu\text{m}$  using a digital measuring device (AxioVision LE, Carl Zeiss), which was checked and calibrated at regular intervals. The procedure was carried out by one trained investigator who was not involved in clinical treatment. At each cross-section, the following four points were measured:

- Marginal gap (P1): the marginal discrepancy, which represented the marginal gap according to Holmes et al. [19]. The width was measured as the perpendicular distance from the internal surface at the margin of the restoration to the preparation [17].
- Axial wall (P2): the mid-axial discrepancy, which represented the distance between the die and the inner surface of the crown at the mid-axial wall.
- Axio – Occlusal edge (P3): the axio-occlusal transition discrepancy, which was defined as the bisector of the angle between the straight line attached to the incisal plateau and the straight line applied to the axial wall
- Centro-occlusal area (P4): centro-occlusal discrepancy (Fig. 1)

Owing to the availability of four fragments per abutment, four locations per landmark and crown were present.

*-STATISTICAL PROCEDURES-*

The statistical analysis was carried out using JMP, v.9 (SAS Institute, Inc., Cary, NC, USA). Descriptive statistics included the calculation of the mean, standard deviation (SD), median, minimum, maximum, and confidence interval of all available measurements for each landmark the statistical calculation was adapted if the measuring point could not be interpreted. The Wilcoxon signed rank test was used to evaluate whether there were differences between anterior and posterior values ( $p \leq 0.05$ ).

#### **7.4 Results**

The single crowns revealed a mean gap width of 48.65  $\mu\text{m}$  (SD 29.45  $\mu\text{m}$ ) at point P1. The median was 38,81  $\mu\text{m}$ . At point P2, a mean discrepancy of 112.25  $\mu\text{m}$  (SD 55.54  $\mu\text{m}$ ) and a median of 103,03  $\mu\text{m}$  were measured. For point P3, a mean of 137.81  $\mu\text{m}$  (71.31  $\mu\text{m}$ ) and a median of 118,56  $\mu\text{m}$  were obtained. At point P4, mean and median values of 157.25  $\mu\text{m}$  (75.51  $\mu\text{m}$ ) and 141.48  $\mu\text{m}$  were found, respectively. There was no significant difference between anterior and posterior gap widths, either considering marginal or internal measurement points. The overall values and anterior and posterior results are displayed in Tables 1–3, respectively. Graph 1 shows a comparison between anterior and posterior results.

#### **7.5 Discussion**

The aim of this study was to examine the placement accuracy of zirconia–ceramic crowns under clinical conditions after a digital intraoral impression. As a result of the study design, only intraoral data were recorded; thus, it was not possible to evaluate differences between the model and the *in vivo* situation. As recent publications have shown, the clinical marginal and

internal fit of prosthetic restorations is still an important topic [42,43]. A mean marginal gap of 100 to 120  $\mu\text{m}$  is deemed to be clinically acceptable. It has been reported that for single telescopic crowns, median values of 23  $\mu\text{m}$  before cementation and 63  $\mu\text{m}$  after cementation could be achieved [44]. A further report discussed single-cast crowns in which 50% of the marginal values obtained were greater than 150  $\mu\text{m}$  [45]. Single metal-alloy crowns fabricated using computer-supported laser-melting technology revealed mean marginal openings from 74 to 99  $\mu\text{m}$  [46]. With respect to all-ceramic restorations for Procera crowns, which are clinically established restorations [47], median values between 80 and 95  $\mu\text{m}$  for anterior restorations and between 90 and 145  $\mu\text{m}$  for posterior indications were measured. The two latter investigations used a replica technique similar to that applied in this study.

A clinical study analysed the marginal fit of 20 zirconia crowns from digital intraoral impressions with active wavefront sampling and reported a mean marginal gap of 49  $\mu\text{m}$ ; this value can be considered comparable to the value obtained in the present investigation.

Despite some extreme values measured, the overall marginal 95% confidence interval showed a narrow range between 43.59 and 53.43  $\mu\text{m}$ . The study revealed that it is possible to fabricate accurate zirconia-ceramic crowns by the use of digital intraoral impressions with active wavefront sampling technology. These results also showed that it is possible to accurately reproduce the clinical situation by means of scanning, even in a sub-gingival location if the soft tissues are retracted.

In a study of the marginal accuracy of a laboratory-processed glass-ceramic crown, Wolfart et al. [48] determined a random error of 4.9% between different examiners. In the present study, the random error among measurements by a single investigator was 7.3%. This relatively higher deviation might be explained by the different replica methods and different finish lines. Wolfart et al. applied a shoulder preparation with a 1.2-mm width, which did not exceed a sub-gingival depth of 0.5 mm. The authors took external impressions from the marginal gaps and

used casts to determine the marginal-gap width. As a result of the mostly sub-gingival locations of the finish lines in the present study, experience was required to define the marginal gaps on the cross-sections and these measurements might be more prone to variability; this experience has been confirmed by other publications. However, despite some shortcomings, the replica method is a commonly accepted evaluation method for clinical accuracy [49]. The internal gap widths are also regarded as important. Large discrepancies at the axio-occlusal transition and centro-occlusally reduce the inter-occlusal distance between the occlusal surface of the framework and the antagonists. This limits the space available for the layering ceramic and may lead to functional drawbacks due to the limitation of the anatomical design of the occlusal surfaces. On the other hand, greater reduction in the occlusal plateau compromises the vitality of the abutment tooth and therefore must be avoided. It has also been described that large internal-gap widths and variations in internal discrepancies may affect the stability of ceramic restorations. The internal gaps revealed in the present study were smaller than those found in other studies. Clinical long-term observations will show whether these internal discrepancies have a clinical impact.

## **7.6 Conclusion**

This clinical study demonstrated that it was possible to fabricate CAD-CAM zirconia-ceramic single crowns with satisfactory accuracy following a digital-impression technique based on active wavefront sampling.

## **7.7 References**

- 
- [1] Conrad HJ, Seong WJ and Pesun IJ. Current ceramic materials and systems with clinical recommendations: a systematic review. *Journal of Prosthetic Dentistry*, 2007; **98**:389-404.
- [2] Mormann WH. The evolution of the CEREC system. *Journal of the American Dental Association*, 2006; **137**(Suppl.)7S-13S.
- [3] Cerec 3. *Operating instructions for the acquisition unit*. Sirona The Dental Company. 2004.
- [4] iTero Cadent *Technical Datasheet*; 2011.
- [5] Kachalia PR and Geissberger MJ. Dentistry a la carte: in-office CAD/CAM technology. *Journal of the California Dental Association*, 2010 May; **38**(5):323-330.
- [6] E4D D4D *Technical Datasheet*; 2011
- [7] Rohaly J, inventor. Three-channel camera systems with non-collinear apertures. *United States Patent 7,372,642*; 2006.
- [8] Lava Chairside Oral Scanner C.O.S. *3M ESPE Technical Datasheet*; 2009.
- [9] Jacobs MS and Windeler AS. An investigation of dental luting cement solubility as a function of the marginal gap. *Journal of Prosthetic Dentistry*, 1991; **65**:436-442.
- [10] Knoernschild KL and Campbell SD. Periodontal tissue responses after insertion of artificial crowns and fixed partial dentures. *Journal of Prosthetic Dentistry*, 2000; **84**:492-498.
- [11] Sailer I, Fehér A, Filser F, Gauckler LJ, Lüthy H and Hämmerle CH. Five-year clinical results of zirconia frameworks for posterior fixed partial dentures. *International Journal of Prosthodontics*, 2007; **20**:383-388.
- [12] McLean JW and von Fraunhofer JA. The estimation of cement film thickness by an in vivo technique. *British Dental Journal*, 1971; **131**:107-111.

- [13] Belser UC, MacEntee MI and Richter WA. Fit of three porcelain-fused-to-metal marginal designs in vivo: a scanning electron microscope study. *Journal of Prosthetic Dentistry*, 1985; **53**:24-29.
- [14] Yeo IS, Yang JH and Lee JB. In vitro marginal fit of three all-ceramic crown systems. *Journal of Prosthetic Dentistry*, 2003; **90**:459-464.
- [15] Goldin EB, Boyd NW 3rd, Goldstein GR, Hittelman EL and Thompson VP. Marginal fit of leucite-glass pressable ceramic restorations and ceramic-pressed-to-metal restorations. *Journal of Prosthetic Dentistry*, 2005; **93**:143-147.
- [16] Christensen GJ. Marginal fit of gold inlay castings. *Journal of Prosthetic Dentistry*, 1966; **16**:297-305.
- [17] Björn AL, Björn H and Grkovic B. Marginal fit of restorations and its relation to periodontal bone level. II. Crowns. *Odontologisk Revy*, 1970; **21**:337-346.
- [18] Mitchell CA, Pintado MR and Douglas WH. Nondestructive, in vitro quantification of crown margins. *Journal of Prosthetic Dentistry* 2001; **85**:575-584.
- [19] Holmes JR, Bayne SC, Holland GA, Sulik WD. Considerations in measurement of marginal fit. *Journal of Prosthetic Dentistry*, 1989; **62**:405-408.
- [20] Groten M, Axmann D, Pröbster L and Weber H. Determination of the minimum number of marginal gap measurements required for practical in-vitro testing. *Journal of Prosthetic Dentistry*, 2000; **83**:40-49.
- [21] Gassino G, Barone Monfrin S, Scanu M, Spina G and Preti G. Marginal adaptation of fixed prosthodontics: a new in vitro 360-degree external examination procedure. *International Journal Prosthodontics*, 2004; **17**:218-223.
- [22] Gonzalo E, Suárez MJ, Serrano B and Lozano JF. Comparative analysis of two measurement methods for marginal fit in metalceramic and zirconia posterior FPDs. *International Journal Prosthodontics*, 2009; **22**:374-377.

- [23] Groten M, Girthofer S and Pröbster L. Weber H. Marginal fit consistency of copy-milled all-ceramic crowns during fabrication by light and scanning electron microscopic analysis in vitro. *Journal of Oral Rehabilitation*, 1997; **24**:871-881.
- [24] Schaerer P, Sato T and Wohlwend A. A comparison of the marginal fit of three cast ceramic crown systems. *Journal of Prosthetic Dentistry*, 1988; **59**:534-542.
- [25] Pera P, Gilodi S, Bassi F and Carossa S. In vitro marginal adaptation of alumina porcelain ceramic crowns. *Journal of Prosthetic Dentistry*, 1994; **72**:585-590.
- [26] Sulaiman F, Chai J, Jameson LM and Wozniak WT. A comparison of the marginal fit of In-Ceram, IPS Empress, and Procera Crowns. *International Journal Prosthodontics*, 1997; **10**:478-484.
- [27] Bindl A and Mörmann WH. Marginal and internal fit of all-ceramic CAD/CAM crown copings on chamfer preparations. *Journal of Oral Rehabilitation*, 2005; **32**:441-447.
- [281] Coli P and Karlsson S. Precision of a CAD/CAM technique for the production of zirconium dioxide copings. *International Journal Prosthodontics*, 2004; **17**:577-580.
- [29] May KB, Russell MM, Razzoog ME and Lang BR. Precision of fit: the Procera AllCeram crown. *Journal of Prosthetic Dentistry*, 1998; **80**:394-404.
- [30] Beschnidt SM and Strub JR. Evaluation of the marginal accuracy of different all-ceramic crown systems after simulation in the artificial mouth. *Journal of Oral Rehabilitation*, 1999; **26**:582-593.
- [31] Boening KW, Wolf BH, Schmidt AE, Kästner K and Walter MH. Clinical fit of Procera AllCeram crowns. *Journal of Prosthetic Dentistry*, 2000; **84**:419-424.
- [32] Suárez MJ, González de Villaumbrosia P, Pradies G and Lozano JF. Comparison of the marginal fit of Procera AllCeram crowns with two finish lines. *International Journal of Prosthodontics*, 2003; **16**:229-232.

[33] Nakamura T, Dei N, Kojima T and Wakabayashi K. Marginal and internal fit of Cerec 3 CAD/CAM all-ceramic crowns. *International Journal of Prosthodontics*, 2003; **16**:244-248.

[34] Balkaya MC, Cinar A and Pamuk S. Influence of firing cycles on the margin distortion of 3 all-ceramic crown systems. *Journal of Prosthetic Dentistry*, 2005; **93**:346-355.

[35] Nakamura T, Tanaka H, Kinuta S, Akao T, Okamoto K, Wakabayashi K, Yatani H. In vitro study on marginal and internal fit of CAD/CAM all-ceramic crowns. *Dental Materials Journal*, 2005; **24**:456-459.

[36] Lee KB, Park CW, Kim KH and Kwon TY. Marginal and internal fit of all-ceramic crowns fabricated with two different CAD/CAM systems. *Dental Materials Journal*, 2008; **27**:422-426.

[37] Tuntiprawon M and Wilson PR. The effect of cement thickness on the fracture strength of all-ceramic crowns. *Australian Dental Journal*, 1995; **40**:17-21.

[38] Lawn BR, Pajares A, Zhang Y, Deng Y, Polack MA, Lloyd IK, Rekow ED and Thompson VP. Materials design in the performance of all-ceramic crowns. *Biomaterials*, 2004; **25**:2885-2892.

[39] Thompson V and Rekow ED. Dental ceramics and the molar crown testing ground. *Journal of Applied Oral Science*, 2004; **12**:26-36.

[40] Syrek A, Reich G, Ranftl D, Klein C, Cerny B and Brodesser J. Clinical evaluation of all ceramic crowns fabricated from intra-oral digital impressions based on the principle of active wavefront sampling. *Journal of Dentistry*, 2010 Jul; **38**(7):553-559.

[41] Molin M and Karlsson S. The fit of gold inlays and three ceramic inlay systems. A clinical and in vitro study. *Acta Odontologica Scandinavica*, 1993; **51**:201-206.

[42] Sailer I, Pjetursson BE, Zwahlen M and Hammerle CH. A systematic review of the survival and complication rates of all-ceramic and metal-ceramic reconstructions after an

observation period of at least 3 years. Part I: Single crowns. *Clinical Oral Implants Research*, 2007 Jun; **18** Suppl 3:73-85. Review. Erratum in: *Clinical Oral Implants Research*, 2008 Mar; **19**(3):326-328.

[43] Wettstein F, Sailer I, Roos M and Hammerle CH. Clinical study of the internal gaps of zirconia and metal frameworks for fixed partial dentures. *European Journal of Oral Sciences*, 2008; **116**:272-279.

[441] Kern M, Schaller HG and Strub JR. Marginal fit of restorations before and after cementation in vivo. *International Journal of Prosthodontics*, 1993; **6**:585-591.

[45] Fransson B, Oilo G and Gjeitanger R. The fit of metal-ceramic crowns, a clinical study. *Dental Materials*, 1985; **1**:197-199.

[46] Quante K, Ludwig K and Kern M. Marginal and internal fit of metal-ceramic crowns fabricated with a new laser melting technology. *Dental Materials*, 2008; **24**:1311-1315.

[47] Odman P and Andersson B. Procera AllCeram crowns followed for 5 to 10.5 years: a prospective clinical study. *International Journal of Prosthodontics*, 2001; **14**:504-509.

[48] Wolfart S, Wegner SM, Al-Halabi A and Kern M. Clinical evaluation of marginal fit of a new experimental all-ceramic system before and after cementation. *International Journal of Prosthodontics*, 2003; **16**:587-592.

[49] Reich S, Wichmann M, Nkenke E and Proeschel P. Clinical fit of all-ceramic three-unit fixed partial dentures, generated with three different CAD/CAM systems. *European Journal of Oral Sciences*, 2005; **113**:174-179.

Figures

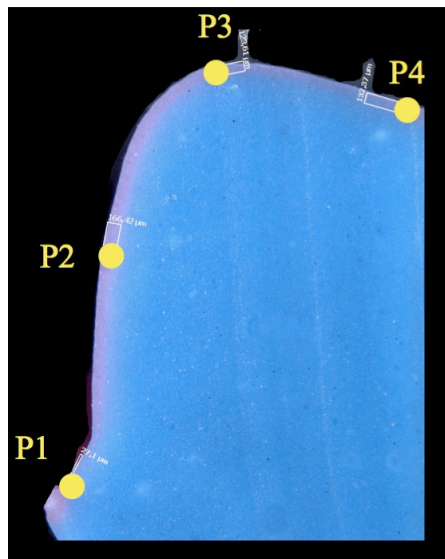
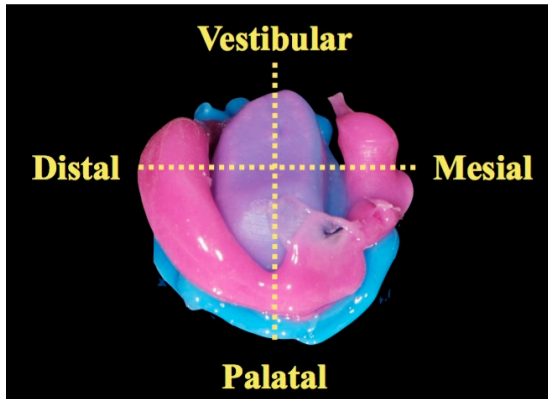


**Figure a-b.** Cross-section of the PVS used to measure the internal fit.

**Tables**

Intraoral scanner	Company	Working principles	Light source	Imaging type	Necessity of coating	In-office milling	Output format
CEREC® AC – Bluecam	Sirona Dental System GmbH (DE)	Active triangulation and optical microscopy	Visible blue light	Multiple images	Yes	Yes	Proprietary
iTero	Cadent Inc (IL)	Parallel confocal microscopy	Red laser	Multiple	None	No	Proprietary or Selective STL
E4D	D4D Technologies, LLC (US)	Optical coherence tomography and confocal microscopy	Laser	Multiple	Occasionally	Yes	Proprietary
Lava™ C.O.S.	3M ESPE (US)	Active wavefront sampling	Pulsating visible blue light	Video	Yes	No	Proprietary
IOS FastScan	IOS Technologies, INC (US)	Active triangulation and Schleimpflug principle	Laser	3 images	Yes	No	STL
MIA3d	Densys LTD (IL)	Active stereophotogrammetry	Visible light	2 images	Yes	No	ASCII
DPI-3D	Dimensional Photonics International, INC (US)	Accordion fringe interferometry (AFI)	Wavelength 350-500 nm	Multiple images	None	No	STL
3D Progress	MHT SpA (IT) – MHT Optic Research AG (CH)	Confocal microscopy and Moiré effect	Not disclosed	3 images	Occasionally	No	STL
directScan	Hint-Els GmbH (DE)	Stereoscopic vision	Not disclosed	Multiple images	Not disclosed	No	Not Disclosed
Trios	3Shape A/S (DK)	Confocal microscopy	Not disclosed	Multiple images	None	No	Proprietary or STL

	Mean	SD	Median	Min.	Max.	95% CI	
						Lower Bound	Upper Bound
P1	48.65	29.25	38.81	5.9	175.86	43.89	53.42
P2	112.03	55.45	103.03	19.61	360.39	102.99	121.07
P3	137.81	71.31	118.56	25.99	413.72	126.18	149.43
P4	157.25	75.51	141.48	32.64	443.09	144.95	169.56

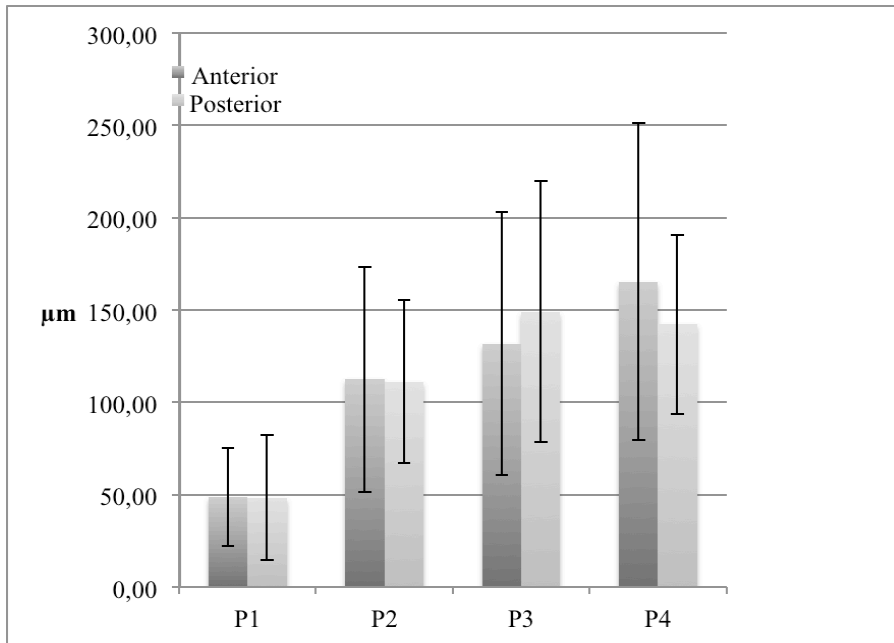
**Table 1.** Means, standard deviation (SD), medians, minima (Min.), maxima (Max.), and confidence intervals of gap width revealed for zirconia all-ceramic single crowns at the landmarks P1, P2, P3, and P4.

	Mean	SD	Median	Min.	Max.	95% CI	
						Lower Bound	Upper Bound
P1	48.81	26.56	38.81	17.14	145.96	43.4	54.22
P2	112.45	61.02	98.66	25.71	360.39	100.02	124.88
P3	131.68	71.23	111.75	25.99	391.88	117.17	146.19
P4	165.47	85.94	150.34	32.64	443.69	147.96	182.97

**Table 2.** Mean, standard deviation (SD), median, minimum (Min.), and maximum (Max.) values of gap width on anterior abutments at the landmarks P1, P2, P3, and P4.

	Mean	SD	Median	Min.	Max.	95% CI	
						Lower Bound	Upper Bound
P1	48.38	33.91	38.33	5.9	175.86	38.94	57.82
P2	111.27	44	106.62	19.61	227.17	99.02	123.52
P3	149	70.79	129.85	59.03	413.72	129.29	168.71
P4	142.25	48.53	134.35	38.81	236.67	128.74	155.76

**Table 3.** Mean, standard deviation (SD), median, minimum (Min.), and maximum (Max.) values of gap width on posterior abutments at the landmarks P1, P2, P3, and P4



	Anterior		Posterior	
	Mean	SD	Mean	SD
<b>P1</b>	48,81	26,56	48,38	33,91
<b>P2</b>	112,45	61,02	111,27	44,00
<b>P3</b>	131,68	71,23	149,00	70,79
<b>P4</b>	165,47	85,94	142,25	48,53

**Graph 1.** Mean comparison between anterior and posterior values for each measurement point, with standard deviation represented.

**CHAPTER 8**

**Clinical evaluation of 1132 zirconia-based single crowns: a retrospective cohort study from the AIOP Clinical Research Group.**

## **8.1 Abstract**

**Aim:** The aim of this retrospective cohort study was to gather the outcomes of zirconia single crowns made by 15 members of the Italian Academy of Prosthetic Dentistry (AIOP) over a time period of up to 5 years.

**Methods:** In total, 398 patients treated in private practices with 1132 zirconia-based single-crown restorations made on natural teeth during the period January, 2005 to July 2010, were included. A total of 343 anterior restorations (30.3%) and 789 posterior crowns (69.7%) were made with 16 types of zirconia, using primarily chamfer or knife-edge tooth preparation, and were examined according to the esthetic, functional, and biological USPHS criteria as modified by the FDI World Dental Federation. To evaluate the relationship of parafunction with mechanical failure, patients with clenching or bruxism were not excluded from the study group.

**Results:** The cumulative survival rate of all restorations was 98.1%, while the cumulative success rate was 94.2%. Functional criteria showed the most failures, with only 1 fractured zirconia core, 13 delaminations, and 46 chippings of the ceramic veneering. The odds ratio (OR) for all restorations was calculated to clarify the relationship between patients who were subject/not subject to parafunctions and technical complications; the OR was 2.60 (95% confidence interval (CI) = 1.60–4.24;  $P < 0.001$ ). An association between parafunction and mechanical failure was found in patients with severe parafunction (OR 3.29 95% CI = 1.62–6.72).

**Conclusions:** Porcelain-veneered zirconia single crowns with chamfer and knife-edged preparations showed good clinical results over a period of up to 5 years. Technical complications were few and were limited primarily to patients with parafunction.

## 8.2 Introduction

Conventional metal–ceramic crowns were the most common restorations for severely compromised, heavily repaired teeth and were used for the replacement of unsuitable prosthetic restorations. Moreover, they still represent the "gold standard" for comparison with newer metal-free materials [1]. However, the metal framework can reduce the translucency, tends to cause a graying of the free gingival margin, and may give rise to allergic or even toxic reactions [2]. Increasing esthetic demands in dentistry have driven the development of many new ceramic materials for their esthetic properties in terms of translucency, biocompatibility, color stability, wear resistance, and low thermal conductivity[3] and the effectiveness of diagnostic radiographs [4]. Densely sintered alumina has been introduced as a favorable material with increased mechanical properties versus feldspathic ceramics for metal-free restorations in the posterior region [5]. Indeed, in the posterior region, the 5-year survival summary estimates of densely sintered alumina crowns (94.9%) and reinforced glass–ceramic crowns (93.7%) were similar to those obtained for metal–ceramic crowns (95.6%). Furthermore, lower survival rates of 90.4% and 84.4% were seen for In-Ceram crowns and glass–ceramic crowns, respectively, when used for posterior teeth [6].

Rapid improvements in the properties of these intrinsically brittle materials, combined with the use of computer-aided design (CAD) / computer-aided manufacturing (CAM), has made all-ceramic systems increasingly popular over the past decade. CAD/CAM systems have been continuously developed and upgraded in prosthetic dentistry in association with zirconium oxide, used primarily for the restoration of single crowns and fixed partial dentures (FPDs) in both the anterior and posterior regions. Zirconia seems to satisfy both esthetic and mechanical needs as a core material for all-ceramic restorations [7]. Its mechanical properties are the highest ever reported for any dental ceramic; indeed, this material can exhibit toughness higher than  $6 \text{ MPa}\sqrt{\text{m}}$  and strength greater than 1000 MPa [8].

Zirconia dioxide in its pure form is a polymorphic material that occurs in three temperature-dependent forms, monoclinic (room temperature to 1170°C), tetragonal (1170–2370°C), and cubic (2370°C up to the melting point) [9]. However, when stabilizing oxides such as ceria or yttria are added to zirconia, the tetragonal phase is retained in a metastable condition at room temperature, enabling a phenomenon called transformation toughening, which increases its crack-propagation resistance. However, mechanical stress can induce phase transformation, leading to metastable tetragonal grains in the monoclinic phase with volume expansion that induces compressive stresses with sequential crack propagation. Another failure mechanism

due to this metastability is low-temperature degradation (LTD, also referred to as aging) in the presence of water that causes the progressive tetragonal to monoclinic transformation at the surface, triggered by water molecules, with surface modifications such as roughening and microcracking. These phenomena can influence the performance and reliability of zirconia restorations and reduce their lifetime [10].

Zirconia dioxide has been used in dentistry during the recent years, but little information on its clinical performance or behavior as a core material in prosthodontic rehabilitation has been reported. A recent systematic review of zirconia restorations and a clinical long-term evaluation of on all-ceramic restorations showed that the most of the studies were performed on FPDs [11-12].

To date, three studies have reported a small number of restorations and short-term results[13-14-15]. These studies demonstrated good clinical performance as a promising prosthodontic alternative in the premolar and molar regions, with a cumulative survival rate that was about 93% after 3 years of clinical service. However, further randomized controlled trials with a larger number of treatments are needed to evaluate the long-term success of the zirconia-based restorations. One of the most commonly reported clinical complications was chipping of the veneering porcelain. Causes of this may include insufficient support of the veneering material by the framework design, changes in the ceramic composition versus conventional feldspathic ceramics, excessive occlusal forces, improper clinical steps/handling, mismatch of the linear coefficient of thermal expansion (CTE), unfavorable surface and heat treatments, and thermal conductivity of the Y-TZP (12 times lower than  $\text{Al}_2\text{O}_3$  99%) [16].

The primary aim of this retrospective cohort study was to evaluate the 1–5 year clinical outcome of a large number of zirconia-based single crowns, performed in general dental practice, in an attempt to establish major risk factors that may contribute to zirconia failure and potential risk indicators associated with zirconia failures.

### **8.3 Materials and Methods**

This retrospective cohort clinical study was conducted in private dental practice in Italy by 15 general dentists who are active members of the Italian Academy of Prosthetic Dentistry (AIOP), with a high level of experience in prosthodontics, in collaboration with 15 dental technicians with a deep knowledge of ceramic restorations.

The study design was organized and conducted by two academic teachers in the Department of the Oral Science of the University of Bologna, Italy who were not involved in the patient

treatment. A specific database created (Access, Office 2003; Microsoft) and used a standardized data-collection form to collect all data recorded for all patients. The two researchers who analyzed all data were blinded with regard to information about the dentist and patient during the period of the analyses.

The dentists recalled all patients who had received zirconia restorations. In total, 398 patients who received one or more single crowns between January 2005 and October, 2009 and who responded to follow up were recruited and examined. Among them, 261 patients were women (65.5%) and 137 were men (34.4%). The mean age was 48.6 years (range, 18–84 years) at the time of crown cementation. In total, 1132 restorations, 343 on anterior teeth (107 patients: 42 men, 65 women) and 789 on posterior teeth (330 patients: 110 men, 220 women), were checked during the last recall. The data collected from patient records are described in tables 1 and 2.

All the patients were treated according to AIOP guidelines. All patients had a moderate-to-good oral hygiene, and low-to-moderate dental caries. All teeth showed an absence of pain and active periodontal or pulpal disease; they had an occlusogingival dimension of at least 3.0 mm from the interdental papilla to the marginal ridge of the abutment teeth and presented at least 1 mm of ferrule effect.

Of the total 1132 tooth elements, 282 restorations were luted on vital teeth while 850 abutments were endodontically treated teeth before prosthetic rehabilitation. Information was also collected regarding the occlusion, and the presence of parafunctions, such as clenching or bruxism was identified. Among all the patients, 273 showed no parafunctions, in combination with the absence of wear facets, whereas 67, 33, and 25 patients showed light, moderate, and severe parafunctional habits, respectively. All patients with parafunction (light to severe; 125) were used as a subgroup for comparison with the other patients (control group). For more than half of the abutments (700), a knife-edge preparation was used. A chamfer design was chosen in 419 treatments, whereas only 13 teeth were prepared with a shoulder. The knife-edge finishing line for complete all-ceramic crowns with a zirconia substructure was prepared with 1.5–2 mm of occlusal clearance and 6° of axial convergence. The chamfer preparation was performed with 1.5–2 mm of occlusal reduction, 0.8–1 mm of marginal depth, and almost 6° of axial convergence. The shoulder design was performed with the same characteristics as the chamfer but with 1–1.2 mm of marginal depth. A gingival displacement procedure was performed, if necessary, by placement of a gingival cord. Polyether or polyvinyl siloxane impression materials in combination with prefabricated or custom-made trays were used to take impressions. Zirconia substructures were fabricated in differing ways, depending on the brand used. In most cases, a gypsum cast of the prepared tooth was scanned with a laser, and the

zirconia core was designed using CAD software. All zirconia substructures were designed anatomically after a traditional or digital wax-up to support each side of the ceramic veneer. The minimum thickness of the core was 0.5 mm. A CAM process was set in relation to the digital information received from the CAD software. The zirconia copings were sintered at different temperatures in the range of 1450–1500°C. Sixteen different types of soft milling zirconia were used in this study and because the distribution was different, five groups of restorations were created, based on the number made with each brand (Table 3). This grouping was performed to allow statistical analyses of the restorations to analyze brands using a large number of restorations and identify within a group of experienced clinicians the major systems of zirconia used. Thirteen ceramic veneering materials (Table 4) were used with the zirconia cores in different combinations. In total, 495 restorations were made with veneering ceramics and zirconia cores produced by the same company. In the other patients, the choice of the ceramic was made independently of the core, but the linear CTE between the two ceramic materials was matched. Particular attention was paid in the analysis of chipping/delamination of the veneering materials, while examining the correlation between zirconia and ceramic veneering of the same versus different brands. Fifteen dental laboratories produced the restorations, according to the recommendations of each manufacturer, but in all crowns, the veneering ceramic was anatomically supported by the zirconia core. In 792 restorations were utilized different resin cement systems for the definitive cementation. Two glass ionomer cements were used for 235 zirconia crowns. Moreover 77 cases were cemented with zinc phosphate cement and 28 zirconia crowns were luted with temporary cement.

## Clinical Evaluation

Bite-wing or periapical radiographs were used in most cases to check the radiographic quality of the interface tooth/zirconia restoration. Most of the restorations were placed in the posterior area (n = 789; 69.7%). Fewer than one-third of the total restorations were in the anterior area (n = 343; 30.3%). Most of the patients who received zirconia single crowns had had the restorations from 1 to 3 years (n = 805; 71%). One-third of the restorations had a short follow-up period of 1 year (n = 388; 34.3%) and a few had a medium/long period observation of 5 years (n = 70; 6.2%).

Esthetic, functional, and biological USPHS parameters modified by the FDI World Dental Federation study design [17] were collected at the final recall: surface luster, framework

fracture, fracture of the ceramic veneering, marginal discrepancy, crown decementation, patient's view, tooth vitality, postoperative hypersensitivity, secondary caries, and periodontal response. Each parameter was ranked in four subclasses, where 1 and 2 indicated excellent and good, respectively, 3 was clinically sufficient or repairable, and 4 was clinically unsatisfactory or not repairable.

In some cases, the same patient reported a score of 4 for two parameters, such as delamination and patient's view. This situation was calculated as a single failure because of the supposition that if the crown were delaminated, the patient would not be satisfied.

### Statistical analysis

The data for the 1132 zirconia single-crown restorations were subjected to a life-table analysis. Cumulative Survival Rate (CSR). This analysis calculated the internal survival rate for each time interval and the cumulative survival rate for the entire 5-year period. Treatment with zirconia restorations was considered a failure when the abutment tooth was extracted or the zirconia crowns were no longer performing, reaching a score of 4 for esthetic, functional, or biological parameters. Fractures of the ceramic veneering (chipping) or decementation were not considered failures because these are at least theoretically repairable.

Cumulative Success Rate (SR). This analysis was stricter than the survival rate analysis because all restorations exhibiting chipping, decementation, or secondary caries of level 3 at the examination were also considered failures. Although the degree of bruxism or clenching was difficult to recognize, the Mantel–Haenszel odds ratios (OR) related to parafunction of all restorations and of the subgroups of patients with light, moderate, and severe parafunctions were also calculated.

## 8.4 Results

The CSR of all zirconia restorations at 1–5 years recall was 98.1%, but if chippings and decementations were considered as failures (not repairable), the SR decreased to 94.2%. Table 5 describes the life-table analysis of the number of failures by year, tooth position and the relative CSR and SR. Results and complications with details regarding esthetic functional and biological USPHS parameters are shown in Table 6. Additional information related to the five groups of zirconia materials is presented in Table 7.

The Odds Ratio for all restorations was 2.60 with a 95% confidence interval (CI) of 1.60–4.24

( $P < 0.001$ ). This result indicates a moderate association between parafunction and failure. The OR of the group with light parafunctions was 0.93 (95% CI, 0.40–2.16), with no statistically significant difference between this group and the patients without parafunction ( $P = 0.863$ ). The groups with moderate and severe parafunctions showed OR of 2.62 (95% CI, 1.38–4.98;  $P = 0.002$ ) and 3.29 (95% CI, 1.62–6.72;  $P = 0.0006$ ), respectively, both statistically significant. The correlation coefficient ( $r^2 = 0.015$ ) showed no strong correlation between failure and parafunction, although a tendency to increase the probability of functional breakdown as chipping or delamination was detected. No correlation in terms of functional failures between the coupling of zirconia with the same/different brand of veneering ceramics was found. Moreover, no correlation was observed between the type of finishing line (chamfer, shoulder, or knife-edge) and any kind of failure. Only two decementations occurring a few weeks after the definitive luting procedure were recorded during the screening of the clinical records. Both of the crowns had knife-edge finishing lines and were luted with resin cements.

## **8.5 Discussion**

In this retrospective cohort study conducted in general dental practice of zirconium oxide-based single crown restorations, the short/medium-term results are promising although some results could be limited scientific value due to the inquiri

The collected data on a large number of the zirconia-based restorations reported a similar survival rate to metal–ceramic restorations over the same period [6], but more observations and randomized clinical studies are need to create a sound basis for the final assessment of the zirconia/ceramic restorations.

The cumulative survival rate of 98.1% and the cumulative success rate of 94.2% after 1–5 years recall reported of the present study were slightly lower than in one recent report of use of a large number of restorations, in which the Kaplan–Meier survival rate was 100% if segregated by tooth number, and ranged from 88% to 99% when failures were analyzed by specific tooth position [18]. Both studies had the same approach to the anatomical design of the framework substructure and had the criterion of not excluding patients with parafunctional habits.

Only one fracture of a zirconia core restored with Procera/Creation and luted with zinc phosphate was found at 3-year follow-up on a posterior endodontically treated tooth. Thirteen delaminations of the veneering ceramic from zirconia core (1 anterior, 12 posterior) occurred during the follow-up period. Of 11 restorations, only two were used zirconia and veneering ceramic of the same brand. No correlation was found between delamination and the finishing

line of the tooth preparation, vitality of the abutment, antagonist tooth, or type of occlusion. Cohesive fracture of the veneering ceramic and delamination from the zirconia core have been reported to be the primary complications in various in vivo studies of Y-TZP single crowns and FPDs [14-15]. One of the causes of this phenomenon could be insufficient support of the veneering material by the framework design. A simplistic and non-anatomical modeling of the zirconium core may result in inappropriate support of the veneering ceramic [11]. Upgraded software for the design of the zirconia substructure facilitates use of a framework derived from a virtual diagnostic wax-up with a digital cutback procedure. With regard to these failures, the results of this study were encouraging. The design of the core zirconia core plays an essential role in preventing crack propagation and fracture of the veneering ceramic. Anatomical support provided by zirconia core results in uniform thickness of the layering material that may better resist the load during the mastication [19].

Chipping occurred in 64 restorations, and was fairly equally distributed in the anterior (3.2%) and posterior (4.4%) regions. Also, the finishing line of the margin did not affect it, with a 4.1% failure rate for knife-edge and 3.8% for chamfer preparation. This phenomenon was more common in endodontically treated teeth with FRC posts (4.8%) than in vital abutments (1.7%). Of a total of 55 patients using a night guard, 23 of them reported delamination or chipping. One might assume that the use of a night guard could limit the nocturnal stress due to the parafunctions, but these habits cannot be completely controlled during the day. However, a fractographic analysis is always necessary to better evaluate the causes and the pattern of fracture.

Chipping could be due to a the mismatch of the CTE, an unfavorable surface, heat treatment, or finally, the thermal conductivity of the Y-TZP being lower than that of gold, which could generate residual stresses within the porcelain during rapid cooling, contributing to chipping-induced fracturing [20]. Matching the thermal expansion between the porcelain and the underlying framework, metal or ceramic, is critical to avoid cracking after firing. A great difference in the CTE between core and veneering materials can result in clinical failure; the failure mode, adhesive or cohesive, depends on whether the porcelain has a higher or lower CTE than the framework [21]. Residual stresses that remain after cooling in the veneering ceramic are one possible explanation for the differences in chipping failures between metal and Y-TZP-based all-ceramic restorations. The markedly different thermal conductivities of the different framework materials may be the origin of this special failure mode. In the present study, no association was found between the zirconia core and ceramic veneering of the same/different brands and mechanical failure. The Lava zirconia in association with Lava

Ceram showed 3.80% mechanical failures versus 3.87% for chippings and delaminations that occurred when sintered with other brands of veneering ceramic.

No secondary caries was detected under the margins of the zirconia restorations and no adverse soft tissue reaction around the crowns was observed. These results could be associated with the excellent quality of the marginal adaptation of the zirconia core in combination with the CAD/CAM system and the reliable sealing of traditional and resin luting cements. Thirty-two cases of postoperative sensitivity for a limited period of time were recorded in this study. In most, the restorations were luted with temporary cement. Gingival blending on probing (level 3 of periodontal response) occurred in only in fourteen restorations. Patient satisfaction with the zirconia-based crowns was very high, and the few completely dissatisfied people or those with minor criticisms about esthetics or function in the most of the cases coincided with the technical failures.

Half of the zirconia crowns were luted with on knife-edge tooth preparations. This type of preparation is supposedly more stressful for all-ceramic restorations, but based on the preliminary results of the present study, the chance to choose the best margin preparation finishing line in relation to the specific clinical situation extends the application of zirconia restorations, especially in esthetically important regions. The historical indication for a knife-edge finishing line is use of fixed prostheses on teeth with periodontal pathology [22]. An *in vitro* test showed a significantly higher mean failure load for cemented zirconia copings with knife-edge margins versus chamfer [23]. In addition, the vertical preparation may be a less invasive alternative and could preserve sound tooth structure more effectively than shoulder or chamfer, not only for periodontally treated teeth, but also for endodontically treated teeth to increase the ferrule effect, teeth affected by caries at the cervical third of the clinical crown and vital teeth in young patients [24]. In addition, a recent clinical study suggests that knife-edge margins in feldspathic porcelain veneered-zirconia crowns do not affect the clinical performance of the restorations during a short-term observation period [25].

## **8.7 Conclusions**

The level of evidence of the retrospective approach of the cohort study has several limitations compared to randomized controlled trials and for this reason the results should be taken with caution. In conclusion, over a period of up to 5 years porcelain-veneered zirconia single

crowns with knife-edge and chamfer preparations showed encouraging clinical results. Technical complications were few and were limited primarily to patients with parafunction although the degree of bruxism or clenching it's a difficult clinical parameter to recognize.

## 8.8 Tables

TOOTH POSITION	MAXILLA	MANDIBLE	TOTAL CROWNS
<b>Incisor</b>	207	40	247 (21.8%)
<b>Canine</b>	69	27	96 (8.4%)
<b>Premolar</b>	246	126	372 (32.9%)
<b>Molar</b>	240	177	417 (36.9%)
Total crowns	762 (67.3%)	370 (32.7%)	1132 (100%)

**Table 1.** Distribution of single crowns by tooth position.

RELATIVE DATA	DETAILS	ANTERIOR	POSTERIOR	TOTAL
<b>Vitality of the abutment and kind of restoration</b>	Yes	115	167	<b>282</b>
	No	228	622	<b>850</b>
<b>Antagonist tooth</b>	un-restored tooth	194	250	<b>444</b>
	Amalgam/composite restoration	3	134	<b>137</b>
	All ceramic or PFM* on natural tooth	138	339	<b>477</b>
	PFM* or gold/resin on the implant	7	67	<b>74</b>
<b>Type of occlusion (patients)</b>	Incisal and canine guidance	55	177	<b>232</b>
	Canine without incisal	14	63	<b>77</b>
	Group function	35	79	<b>114</b>
	other	3	11	<b>14</b>
<b>Type of tooth preparation</b>	Chamfer	153	266	<b>419</b>
	Shoulder	7	6	<b>13</b>
	Knife-edge	183	517	<b>700</b>

RELATIVE DATA	DETAILS	ANTERIOR	POSTERIOR	TOTAL
<b>Clenching and bruxism history (related to patients)</b>	No	56	236	<b>273</b>
	Light	26	51	<b>67</b>
	Moderate	13	27	<b>33</b>
	Severe	12	16	<b>25</b>
<b>Use of a night guard (related to patients)</b>	No	85	286	<b>343</b>
	Yes	22	44	<b>55</b>

**Table 2.** Data at delivery regarding ~~on~~ vitality, antagonist tooth, occlusion, tooth preparation, parafunctions and use of a night guard. \*PFM, porcelain fused to metal.

Table 3. Number of restorations for each zirconia brand divided in five groups.

<b>GROUP (N° OF RESTORATIONS)</b>	<b>NUMBER OF RESTORATIONS (ZIRCONIA BRAND)</b>
Group 1 (1 to 20)	<b>3</b> Everest ZS (Kavo, Germany) <b>9</b> Zirconia dioxide Cara (Heraeus, Germany) <b>19</b> Biotech (Biotech Srl, Italy) <b>19</b> New Ancorvis zirconia (New Ancorvis, Italy) <b>17</b> Echo (Sweden & Martina, Italy) <b>14</b> Kéramo zirconia (Kéramo S.p.A, Italy) <b>11</b> e.max ZirCad (Ivoclar Vivadent, Liechtenstein)
Group 2 (21 to 50)	<b>32</b> Byoziram (Cyrtina), <b>31</b> Zircodent (Orodent Srl, Italy), <b>27</b> Ceramill ZI (Amann Girrbach, Germany), <b>30</b> DD Bio Z (Dental Direkt, Italy), <b>21</b> Diazir (Diadem Srl, Italy), <b>21</b> Zenostar (Wieland Dental, Germany).
Group 3 (51 to 100)	<b>74</b> ICE (Zirkonzhan, Italy).
Group 4 (101 to 500)	<b>180</b> NobelProcera Zirconia (Nobel Biocare, Sweden).
Group 5 (>500)	<b>624</b> Lava (3M ESPE AG, Germany)
<b>TOTAL</b>	<b>1132</b>

Table 4. Veneering materials used in the study.

VENEERING MATERIALS	NUMBER OF RESTORATIONS
Lava Ceram (3M ESPE, Seefeld)	523
Creation (Jensen GmbH, Germany)	211
Initial zr-FS (GC Europe)	119
Triceram (Dentaurum, Germany)	104
Pulse ZR (Ceramay, Germany)	11
NobelRondo (Nobel Biocare, Sweden)	10
CZR press (Noritake, Japan)	9
Duceram (DeguDent GmbH, Germany)	7
Ceramco3 (Densply, Europe)	9
ICE (Zirkonzhan, Italy)	5
Zirox (Wieland, Germany)	8
Natural Zir (Tressis, Italy)	31
e.max ceram (Ivoclar Vivadent, Liechtenstein)	74
not specified	11
<b>TOTAL</b>	<b>1132</b>

Table 5. Life-table analysis of 1132 placed zirconia crowns with success rates (SR) and cumulative survival rates (CSR).

Time	Anterior	Failed and CSR (%)	Failed and SR (%)	Posterior	Failed and CSR (%)	Failed and SR (%)	TOTAL (%)	Failed and CSR (%)	Failed and SR (%)
<b>1 year</b>	<b>105</b>	0 (100)	0 (100)	<b>283</b>	2 (99.3)	7 (97.3)	<b>388 (34.3%)</b>	3 (99.7)	7 (99.7)
<b>2 years</b>	<b>80</b>	0 (100)	0 (100)	<b>192</b>	3 (98.4)	12 (93.7)	<b>272 (24%)</b>	3 (98.9)	12 (95.5)
<b>3 years</b>	<b>90</b>	2 (97.8)	13 (85.6)	<b>160</b>	6 (96.2)	20 (87.5)	<b>250 (22%)</b>	10 (96)	33 (86.8)
<b>4 years</b>	<b>40</b>	0 (100)	0 (100)	<b>112</b>	8 (92.8)	11 (90.1)	<b>152 (13.5%)</b>	11 (92.77)	11 (92.77)
<b>5 years</b>	<b>28</b>	0 (100)	0 (100)	<b>42</b>	0 (100)	2 (95)	<b>70 (6.2%)</b>	0 (100)	2 (97.1)
<b>Total</b>	<b>343</b>	<b>2 (99.4%)</b>	<b>13 (96.2%)</b>	<b>789</b>	<b>19 (96.8%)</b>	<b>52 (93.4%)</b>	<b>1132 (100%)</b>	<b>21 (98.1%)</b>	<b>65 (94.2%)</b>

Table 6. Results and major complications of cemented zirconia crowns in terms of esthetic, functional, and biological properties following the USPHS parameters. The numbers correspond to 1, Clinically excellent/very good; 2, Clinically good; 3, Clinically sufficient/satisfactory; and 4, Clinically unsatisfactory.

PROPERTIES	PARAMETERS	ANTERIOR	POSTERIOR	TOTAL
<b>ESTHETIC PROPERTIES</b>				
<b>Surface luster</b>	1. Surface luster comparable to enamel	305	709	<b>1014</b>
	2. Slightly dull, not noticeable if covered with a film of saliva	38	78	<b>116</b>
	3. Dull, cannot be masked by saliva film	0	1	<b>1</b>
	4. Rough surface, unacceptable plaque-retentive surface	0	1	<b>1</b>
<b>FUNCTIONAL PROPERTIES</b>				
<b>Framework fracture</b>	1. No	343	788	<b>1131</b>
	4. Yes	0	1	<b>1</b>
<b>Fracture of ceramic veneering</b>	1. No	331	739	<b>1070</b>
	2. Yes, hairline crack	0	3	<b>3</b>
	3. Yes, chipping (theoretically "repairable")	11	35	<b>46</b>
	4. Yes, delamination	1	12	<b>13</b>
<b>Marginal discrepancy</b>	1. No gap	342	785	<b>1127</b>
	2. Yes, <50 microns	0	4	<b>4</b>
	3. Yes, >50 but <250 microns	0	0	<b>0</b>
	4. Yes, >250 microns	1	0	<b>1</b>
<b>Crown decementation</b>	1. No	343	787	<b>1130</b>
	4. Yes (re-luted "repairable")	0	2	<b>2</b>
<b>Patient's view</b>	1. Entirely satisfied	292	661	<b>953</b>
	2. Satisfied	44	104	<b>148</b>
	3. Minor criticism of esthetics. No adverse effect.	7	16	<b>23</b>
	4. Completely dissatisfied and/or adverse effect, including pain	0	8	<b>8</b>
<b>BIOLOGICAL PROPERTIES</b>				
<b>Post-op sensitivity; tooth vitality</b>	1. No hypersensitivity, normal vitality	106	151	<b>257</b>
	2. Yes, low hypersensitivity for a limited period of time. Normal vitality	9	14	<b>23</b>
	3. Yes, premature/intense or in response to the stimulus	0	0	<b>0</b>
	4. Yes, very intense. Need for endodontic treatment	0	2	<b>2</b>
<b>Secondary caries</b>	1. No primary or secondary caries	343	788	<b>1131</b>
	2. Yes, very small and localized	0	1	<b>1</b>

PROPERTIES	PARAMETERS	ANTERIOR	POSTERIOR	TOTAL
	3. Yes, large area of demineralization, caries with cavitation, erosion, or abrasion under the margin of the crown	0	0	0
	4. Yes, deep secondary caries or exposed dentine not repairable	0	0	0
<b>Periodontal response</b>	1. No plaque, no inflammation, no pockets	308	669	977
	2. Little plaque, no inflammation (gingivitis), no pocket development	35	105	140
	3. Plaque accumulation not acceptable; gingival bleeding on probe	0	14	14
	4. Severe/acute periodontitis.	0	1	1

Table 7. Cumulative survival rates (CSR) and success rates (SR) of all zirconia restorations divided by group.

Groups	ANTERIOR FAILED AND		POSTERIOR FAILED AND		TOTAL CROWNS FAILED AND	
	CSR (%)	SR (%)	CSR (%)	SR (%)	CSR (%)	SR (%)
<b>All groups (n = 1132; 100%)</b>	<b>2 (99.4%)</b>	<b>13 (96.2%)</b>	<b>19 (96.8%)</b>	<b>52 (93.4%)</b>	<b>21 (98.1%)</b>	<b>65 (94.2%)</b>
<b>Group 5: (anterior = 178 posterior = 446; total n = 624; 55.3%)</b> LAVA	0 (100)	3 (99.5)	10 (98.4)	23 (96.3)	10 (98.4)	26 (95.8)
<b>Group 4: (anterior = 75, posterior = 105, total n = 180; 16%)</b> NobelProcera Zirconia	2 (98.9)	3 (98.3)	6 (96.7)	13 (92.8)	8 (95.6)	16 (91.2)
<b>Group 3: (anterior = 8, posterior = 65, total n = 73; 6.5%)</b> ICE	0 (100)	0 (100)	0 (100)	0 (100)	0 (100)	0 (100)
<b>Group 2: (n = 156; 14%)</b> Byoziram Cyrtina (32), Zircodent (31), Ceramill ZI (27), DD Bio Z (24), Diazir (21), Zenostar (21)	0 (100)	7 (95.5)	0 (100)	9 (94.2)	0 (100)	9 (94.2)
<b>Group 1: (n = 92; 8.2%)</b> Biotech (19), New Ancorvis (19), Echo (17), ZirCad (11), Cara (9), Kéramo (14), Everest (3)	0 (100)	0 (100)	3 (96.7)	7 (92.4)	3 (96.7)	7 (92.4)

## 8.9 References

[1] Walton TR. A 10-year longitudinal study of fixed prosthodontics: clinical characteristics and outcome of single-unit metal–ceramic crowns. *Int J Prosthodont* 1999;12:519–526.

- [2] Kansu G, Aydin AK. Evaluation of the biocompatibility of various dental alloys: Part I—Toxic potentials. *Eur J Prosthodont Restor Dent* 1996;4:129–136.
- [3] Blatz MB. Long-term clinical success of all-ceramic posterior restorations. *Quintessence Int* 2002;33:415–426.
- [4] Raigrodski AJ. Contemporary materials and technologies for all-ceramic fixed partial dentures: A review of the literature. *J Prosthet Dent* 2004;92:557–562.
- [5] Odman P, Andersson B. Procera AllCeram crowns followed for 5-10.5 years: a prospective clinical study. *Int J Prosthodont* 2001;14:504–509.
- [6] Pjetursson BE, Sailer I, Zwahlen M, Hämmerle CH. A systematic review of the survival and complication rates of all-ceramic and metal–ceramic reconstructions after an observation period of at least 3 years. Part I. Single crowns. *Clin Oral Implants Res* 2007;18:73–85.
- [7] Guazzato M, Quach L, Albakry M, Swain MV. Influence of surface and heat treatments on the flexural strength of Y-TZP dental ceramic. *J Dent* 2005;33:9–18.
- [8] Coelho PG, Silva NR, Bonfante EA, Guess PC, Rekow ED, Thompson VP. Fatigue testing of two porcelain–zirconia all-ceramic crown systems. *Dent Mater* 2009;25:1122–1127.
- [9] Manicone PF, Iommetti PR, Raffaelli L. An overview of zirconia ceramics: Basic properties and clinical applications. *J Dent* 2007;35:819–826.
- [10] Chevalier J, Gremillard L, Deville S. Low-temperature degradation of zirconia and implications for biomedical implants. *Annu Rev Mater Res* 2007;37:1–32.
- [11] Raigrodski AJ, Hillstead MB, Meng GK, Chung KH. Survival and complications of zirconia-based fixed dental prostheses: A systematic review. *J Prosthet Dent* 2012;107:170-177.
- [12] Beier US, Kapferer I, Dumfahrt H. Clinical long-term evaluation and failure characteristics of 1,335 all-ceramic restorations. *Int J Prosthodont*. 2012;25:70-78.
- [13] Kollar A, Huber S, Mericske E, Mericske-Stern R. Zirconia for teeth and implants: a case series. *Int J Periodontics Restorative Dent* 2008;28:479-487.
- [14] Cehreli MC, Kökat AM, Akca K. CAD/CAM Zirconia vs. slip-cast glass-infiltrated Alumina/Zirconia all-ceramic crowns: 2-year results of a randomized controlled clinical trial. *J Appl Oral Sci* 2009;17:49–55.
- [15] Ortorp A, Kihl ML, Carlsson GE. A 3-year retrospective and clinical follow-up study of zirconia single crowns performed in a private practice. *J Dent* 2009;37:731-736.
- [16] Edelhoff D, Florian B, Florian W, Johnen C. HIP zirconia fixed partial dentures--clinical results after 3 years of clinical service. *Quintessence Int* 2008;39:459–471.

- [17] Hickel R, Peschke A, Tyas M, Mjör I, Bayne S, Peters M, Hiller KA, Randall R, Vanherle G, Heintze SD. FDI World Dental Federation: clinical criteria for the evaluation of direct and indirect restorations-update and clinical examples. *Clin Oral Investig* 2010;14:349-366.
- [18] Keough BE, Kay HB, Sager RD, Keen E. Clinical performance of scientifically designed, hot isostatic-pressed (HIP'd) zirconia cores in a bilayered all-ceramic system. *Compend Contin Educ Dent* 2011;32:58-68.
- [19] Rosentritt M, Steiger D, Behr M, Handel G, Kolbeck C. Influence of substructure design and spacer settings on the in vitro performance of molar zirconia crowns. *J Dent* 2009;37:978-983.
- [20] Tholey MJ, Swain MV, Thiel N. Thermal gradients and residual stresses in veneered Y-TZP frameworks. *Dent Mater* 2011;27:1102-1110.
- [21] Anusavice KJ, Dehoff PH, Hojjatie B, Gray A. Influence of tempering and contraction mismatch on crack development in ceramic surfaces. *J Dent Res* 1989;68:1182-1187.
- [22] Di Febo G, Carnevale G, Sterrantino SF. Treatment of a case of advanced periodontitis: clinical procedures utilizing the "combined preparation" technique. *Int J Periodontics Restorative Dent* 1985;5:52-62.
- [23] Reich S, Petschelt A, Lohbauer U. The effect of finish line preparation and layer thickness on the failure load and fractography of ZrO<sub>2</sub> copings. *J Prosthet Dent* 2008;99:369-376.
- [24] Schmitt J, Wichmann M, Holst S, Reich S. Restoring severely compromised anterior teeth with zirconia crowns and feather-edged margin preparations: a 3-year follow-up of a prospective clinical trial. *Int J Prosthodont* 2010;23:107-109.
- [25] Poggio CE, Dosoli R, Ercoli C. A retrospective analysis of 102 zirconia single crowns with knife-edge margins. *J Prosthet Dent* 2012;107:316-321.

## ***CHAPTER 9***

### **Conclusions and recommendations**

The following conclusions and recommendations may be drawn from our basic and clinical evaluations on the use of zirconia based restorations applied in dentistry:

1. Abrasion of pre-sintered zirconia specimens resulted in rougher surfaces, and the monoclinic phase associated with the abrasion was completely transformed to the tetragonal state during the subsequent sintering step;
2. Abrasion of sintered zirconia specimens resulted in surfaces with a lower roughness, a monoclinic phase, and compressive surface residual stresses, the degree of which was associated with the abrasive grain size;
3. The phases and microstructural changes induced by abrasion may markedly impact clinical performance, i.e. by increasing the rate of aging.
4. By optimizing the microwaves sintering conditions, it is possible to obtain rather dense specimens strongly reducing both the maximum sintering temperature and the total thermal cycle length, passing from several hundreds of minutes at 1450°C to few minutes at 1200°C.
5. The less drastic sintering conditions, in terms of reduced temperature and thermal cycle length, allowed obtaining a limited grain growth, able to improve the mechanical characteristics of the sintered zirconia components.
6. The dielectric heating method produces specific advantages in terms of energy efficiency, process simplicity, saving costs of equipment maintenance and operator.
7. Sandblasting the zirconia surface before sintering enhances the surface roughness in direct proportion to the size of the sand used;
8. Increasing the surface roughness of the zirconia enhance its microtensile strength, although the differences were not significant;
9. Evaluating microtensile bond strength we can say that using the CoJet treatment after sintering is recommended for clinical situations where it is important improve the

adhesion of ceramic veneer to zirconia;

10. Improving the strength of veneering ceramics is necessary to realize the benefits of the high strength of zirconia frameworks.
11. High percentage of mixed failures are due to the brittleness of veneer ceramics.
12. Pressable monolithic lithium disilicate ceramic, in combination with a resin luting agent, can act as a biomimetic of enamel, optimizing the distribution of occlusal stresses at the margin and showing the same value in fracture strength in restorations.
13. Over a period of up to 5 years porcelain-veneered zirconia single crowns with knife-edge and chamfer preparations showed encouraging clinical results. Technical complications were few and were limited primarily to patients with parafunction although the degree of bruxism or clenching it's a difficult clinical parameter to recognize.

## **Acknowledgements**

I'd like to thank everyone who has been involved in this thesis.

I want to express my thanks to my promoter Prof. Giorgio Timellini and my co-promoter Dr. Eng. Arturo Salomoni. They gave me the possibility to start my adventure in the Ceramic Center in Bologna.

I really don't know how to thank my co-promoter Prof. Roberto Scotti He is for me like a father that provided guidance, scientific advice and continued encouragement throughout this project and without whose help, this work would not have come to fulfilment. Thank you for being a great teacher and a point of reference every day.

My deepest thank to Antonella Tucci and Leonardo Esposito. During my Ph.D program they "switched on the light" of the research. They represented a lighthouse and never I forgot the helpfulness at any time. The research meetings with Antonella and Leonardo represent for me the best lesson of chemistry, engineering and humaneness. They opened my way to the research and always supported my troubles.

I would like to thank my mother Michela that supported me during this busy period. I'll love her forever.

Finally, the biggest kiss to my wife Francesca and my babies Camilla and Ludovico. "All the things they are!!". They represent the milestones of my life.